RESULTS AND DISCUSSION

4.1 Introduction

The Polymer- silane composite films were coated on glass substrates by Spin-coating and sol-gel techniques and they were annealed at various temperatures. These films exhibited hydrophobic properties as ensured by Cassie-Baxter and Wenzel theories. The prepared films were proved for non-wettable character, has application as self cleaning coatings and also in oil-water separation.

4.2 Characterization Technique

The polymer-silane coated films were characterized for its vibrational analysis using FTIR, optical analysis with UV-Visible spectroscopy, structural and morphological analysis with FE-SEM. In order to prove the non-wettable nature of the films, contact angle measurement and surface analysis were done. The thermal stability of the films were studied using TG-DTA. In this chapter, characterization techniques, principles and interpretation of the results of all the samples have been explained.

4.2.1 Thickness Measurement

The thickness of the films were computed with Gravimetric method. Digitalized and quantified methods are being used to find the thickness. Gravimetric method has been chosen for its simple approach in the current work. Thickness of the film is calculated as follows,

$$t = \frac{w}{\rho A}$$

Where, t = Thickness of the film, w = Weight of the film on the substrate (Weight of the substrate after coating – Weight of the substrate before coating), ρ – Density of the film and A – Area of the substrate used.

4.2.2 FTIR

FTIR (Fourier Transform Infra-red Spectroscopy) technique has been used to examine the molecular vibrations of the prepared Polymer-silane films. The molecules intrigue the light in the infra-red region of the electromagnetic spectrum. These absorptions signifies to the bonds present in the molecule. The FTIR spectra was recorded using **JASCO – 4600 type A (Fig. 4.1)** with the scan speed of 2 mm/sec in the range of 4000- 600 cm^{-1} .

Figure. 4.1 FTIR Spectrometer

4.2.3 Contact Angle

One of the primitive methods to identify the hydrophobic properties of any solid surface is to compute contact angle measurement. It is the measure of wetting character of any liquid on the solid surface, which is directly associated to the interfacial energies of the system. Several theories have been derived and equated by Young, Wenzel and Cassie-Baxter. The surface energy is associated with the interface. When the energy of solid-vapour interface, is greater than that of solid-liquid interface, the liquid flows over the surface. Complete wetting occurs when θ = 0 and non-wetting occurs at θ is obtuse. The contact angle for all the coated substrates were measured using **HOLMARC INC- A**, which is shown in the **Fig.4.2**

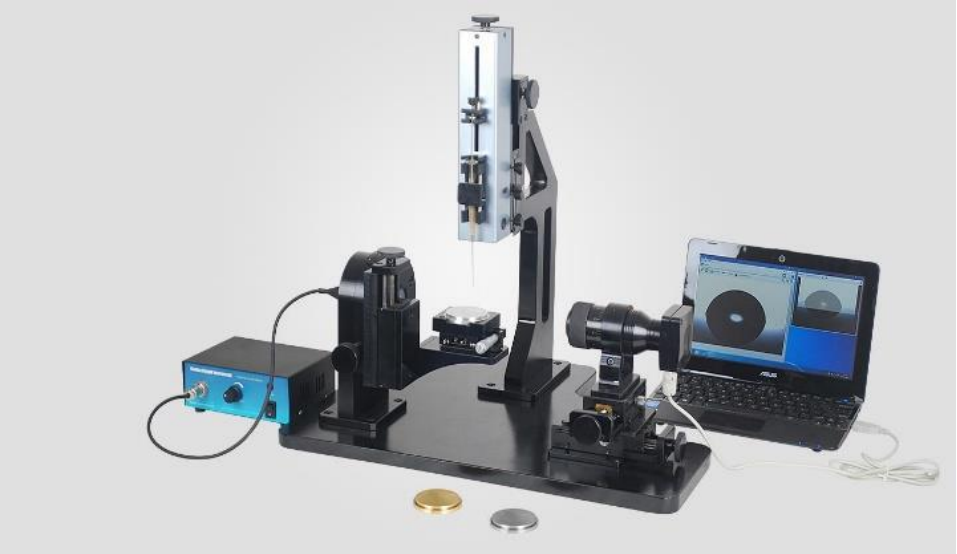

Fig. 4.2 Contact Angle Measurement (Holmarc Inc)

The contact angle, θ is calculated between the solid-liquid interface. The different surfaces based on the contact angles are classified into Superhydrophobic, Hydrophobic and Hydrophilic surfaces as shown in the Fig. 4.3.

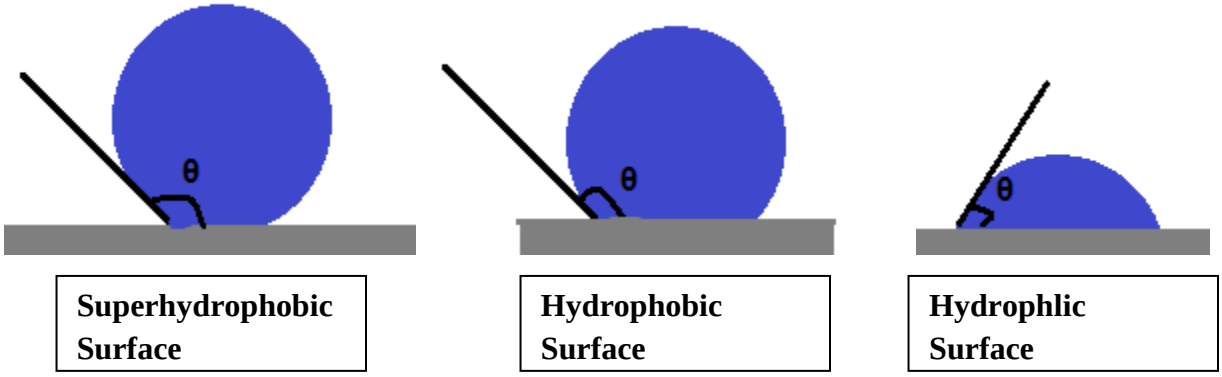

Fig. 4.3 Surfaces

4.2.4 Surface Roughness and Surface Energy

The surface roughness and energy are inter-related. To depict surface wettability nature, both roughness and energy has crucial role. Surface Roughness and Surface energy are inversely proportional. The components Ra, Rp, Rrms, Rpv were calculated from **3D Optical Profilometer (Zeta- 20)** as in the Fig.4.4 and the surface energy was computed as below, $\Upsilon = A_n / 24\pi D^2$, An – Hamaker's Constant, D – intermolecular distance between the molecules.

Fig. 4.4 3D Laser Profilometer (Zeta - 20)

4.2.5 UV-Visible spectroscopy

UV-Visible spectroscopy was used to compute the amount of light absorbed or transmitted by the sample. It is the interaction of electromagnetic radiation with the chemical compound or the sample, which imparts absorption, transmission and reflection of the light over a certain range of wavelength. The optical properties for all the polymer-silane films were interpreted using UV-Vis-NIR spectrophotometer (**JASCO V-670**) as shown in the **Fig.4.5** . It is a double-beam spectrophotometer with a photomultiplier tube detector. The transmittance spectra was recorded between the wavelength region of 200 nm to 1000 nm.

Fig 4.5 UV-Visible Spectrophotometer (JASCO V-670)

4.2.6 FE-SEM

The Field Emission Scanning Electron Microscope works with electrons emitted by field emission source instead of light. Has reduced penetration of low-kinetic energy electrons probes closer to the immediate material surface. All the films are characterized with **BRUKER** model. The surface morphology of the films were studied. E-DAX was taken to study the purity of the prepared film.

4.2.7 Thermal analysis

Materials sometime lose its performance due to thermal, chemical, or mechanical degradation. It has become necessary to understand the environmental impact of its degradation and also its effect on material properties. If the rate of degradation can be accurately measured, then it becomes possible to predict the material properties. In general, thermal analysis can provide important information on the temperature dependent properties of material and on

thermally induced processes (phase transition, decomposition, etc.). The Polymer-silane coatings were analyzed for TG-DTA using **Perkin Elmer (Fig.4.6).**

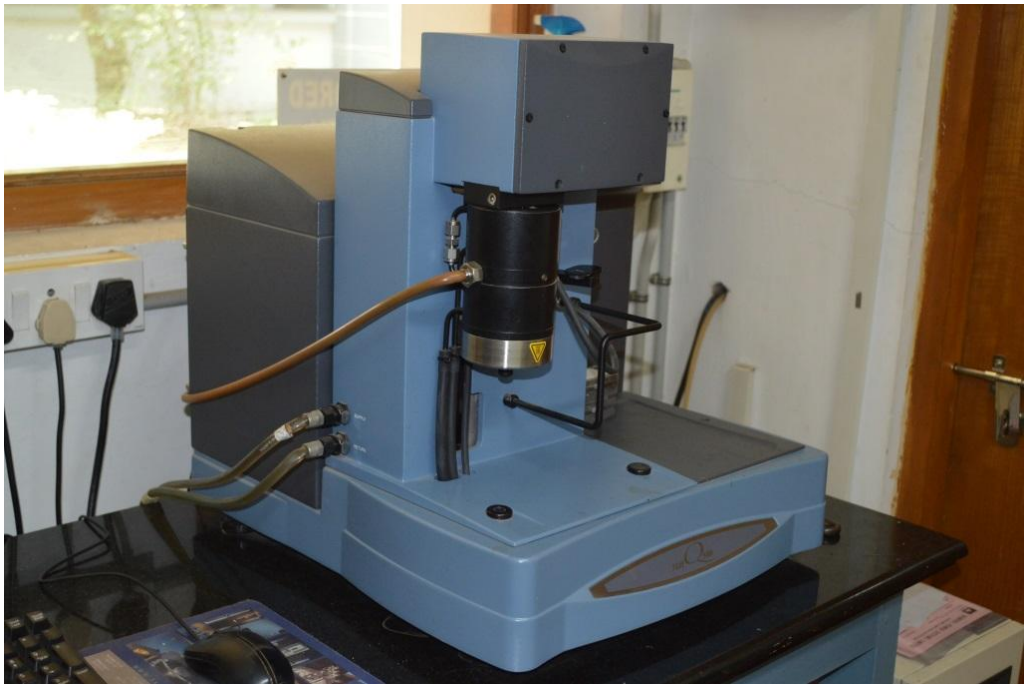

Figure.4.6 Thermal Analysis

4.3 Interpretation of Results

4.3.1 SET – I [TEOS + Polymer]

4.3.1.1 FTIR

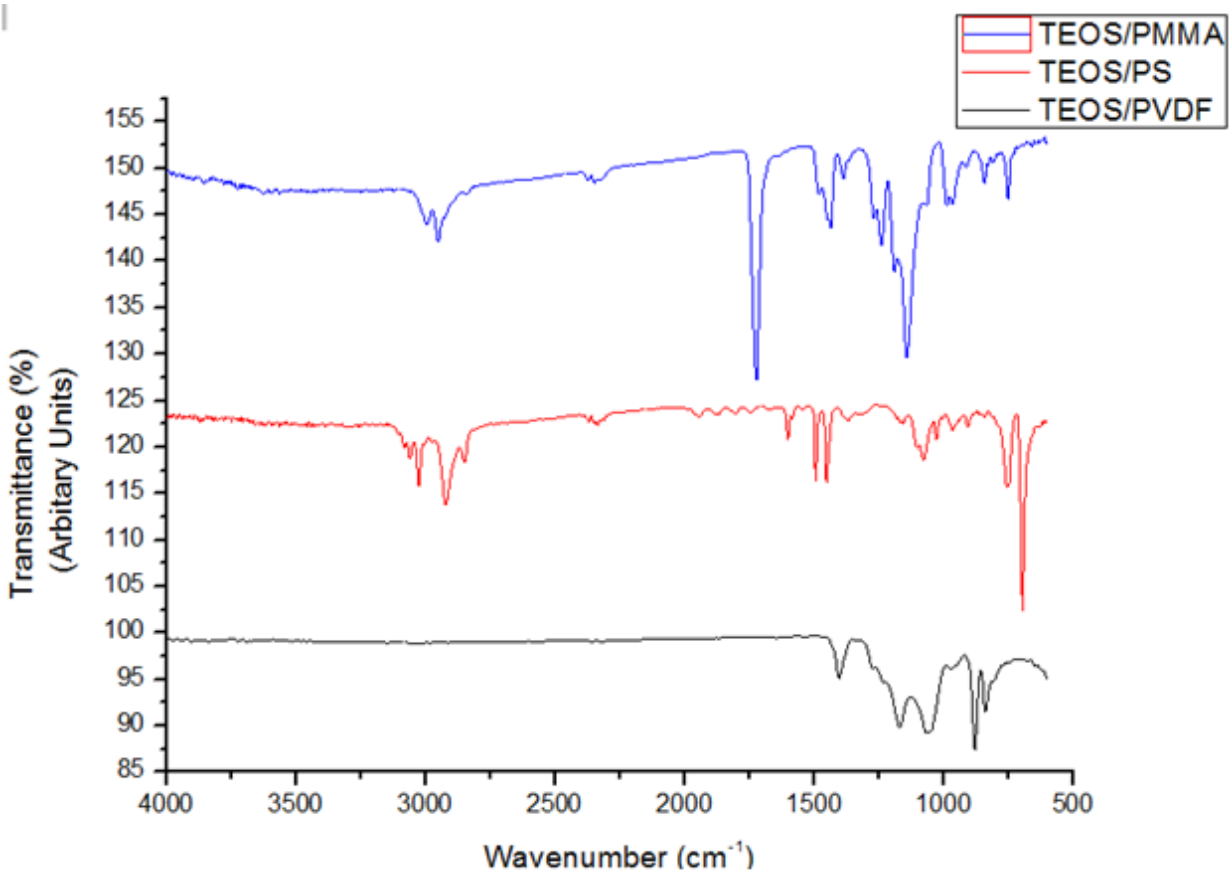

Fig.4.7 FTIR Spectra of TEOS/PVDF, TEOS/PMMA and TEOS/PS composite films

The functional groups were determined by FTIR spectra. The FTIR spectra of TEOS/PVDF, TEOS/PMMA and TEOS/PS is shown in the **Fig. 4.7**. The absorption peaks at 3439cm^{-1}, 1645cm^{-1} and 1087cm^{-1} represents –OH stretching,Si-H_2O bending vibration and Si-O-Si bond stretching respectively for pristine Tetraethoxysilane (TEOS) **[Hui Tian et al., 2009 and Violeta Purcar et al., 2013]**, whereas for pristine Polyvinylidene fluoride(PVDF) ,C-F stretching

vibration is seen at 1400cm^{-1} and 1175cm^{-1} **[F. Hamelmann et al., 2005]**.The band at 840cm^{-1} represents both β and ϒ phase, whereas the band at 796 cm^{-1} represents the α-phase **[Gaurav Mago et al., 2008]**.

In the FTIR spectra of TEOS/PVDF composite, there is a shift in the phase of PVDF. The band at 796cm^{-1} represents the α-phase of PVDF in pristine PVDF spectra, which showed a shift in the phase on adding TEOS **[Bashir Ahmed et al., 2013]**. The α-phase of PVDF at 796 cm^{-1} has been shifted to the β-phase of PVDF at 837 cm^{-1}.The absorption peak at 878 cm^{-1} represents C-C-C asymmetrical stretching vibration **[Haolong Bai et al., 2012]**.

Mixing PVDF with TEOS involves Hydrolysis and Polycondensation. For pristine TEOS, the band at 934cm^{-1} indicates the Si-OH stretching but for TEOS/PVDF composite, Si-OH bond has been formed at 970 cm^{-1} and this ensures hydrolysis. Simultaneously, the peak at 1087cm^{-1} represents Si-O-Si stretching in the cyclic structure, which has been deformed to the linear structure at 1066cm^{-1} in TEOS/PVDF composite. The band at 1168cm^{-1} has been noted as C-H rocking (CH_3) which decreases with the reaction time due to hydrolysis of TEOS.

In case of TEOS/PMMA, the absorption peaks at 1483 cm^{-1} and 1145 cm^{-1} represents deformation of CH_3 group whereas the peak at 905cm^{-1} notes the rocking mode **[Mas Rosemal et al., 2010].** As reported by Seenaa Ibrahem et al, the band at (1076-443) cm^{-1} assigns to the asymmetric stretching vibrations of Si-O-Si. The band between 990-650 cm^{-1} correspond to CH_3 symmetric bending **[Seenaa Ibrahem et al., 2014].** In FTIR spectrum, the band at 1723 cm^{-1}

denotes C-O whereas the peaks at 1434cm^{-1} and 1387 cm^{-1} represents deformation vibration of C-H bond (Hydrophobic group) in CH_2 and CH_3 **[Ying Ma et al., 2007 and Sandra Raquel Kunst et al., 2013].** By Silylation process, the Si-OR group undergoes hydrolysis and condensation. The peak present above 3200 cm^{-1},corresponds to Si-OH hydrophilic groups due to hydrolysis. Here, due to condensation two peaks were obtained at 2949 cm^{-1} and 2992 cm^{-1} which tends to C-H symmetric and asymmetric stretching and this confirms the hydrophobic group **[Marielen Longhi et al., 2015].**

The absorption peak at 3024 cm^{-1} in FTIR spectrum of TEOS/PS composite. The absorption peaks at represents aromatic C-H stretching vibration. C-H deformation vibration is seen at 694 cm^{-1}. The intense peak at 1600 cm^{-1}, 1491 cm^{-1}, 1451cm^{-1} has been obtained due to aromatic C-H bond stretching vibration **[Xin Fan et al., 2012].** The absorbance peak at 905 cm^{-1} indicates the amorphous phase **[Hew-Der Wu et al., 2001]**. The band at 1076 cm^{-1} represents asymmetric stretching vibrations of Si-O-Si **[R. K. Satvekar et al., 2012].**

4.3.1.2 Contact Angle

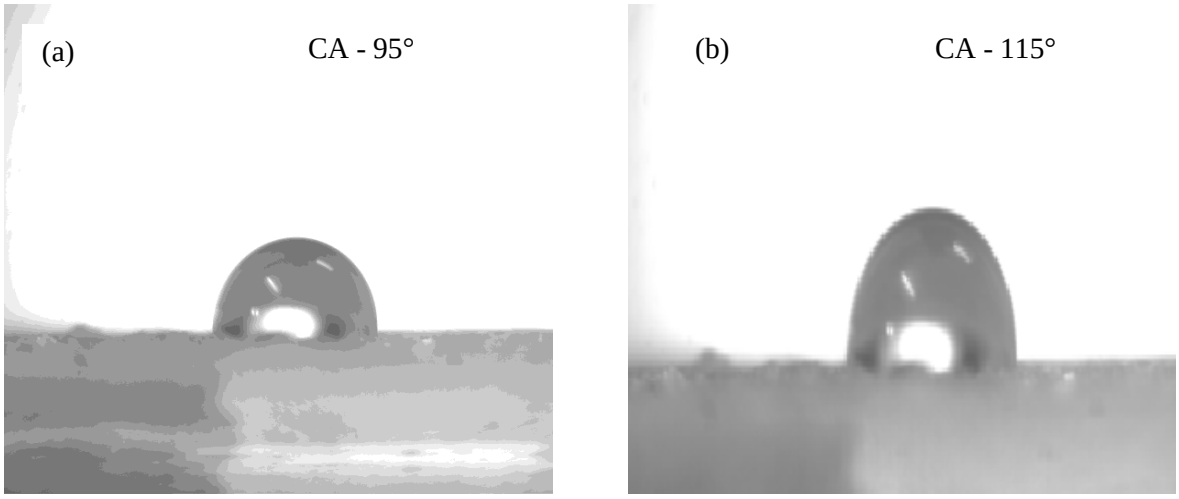

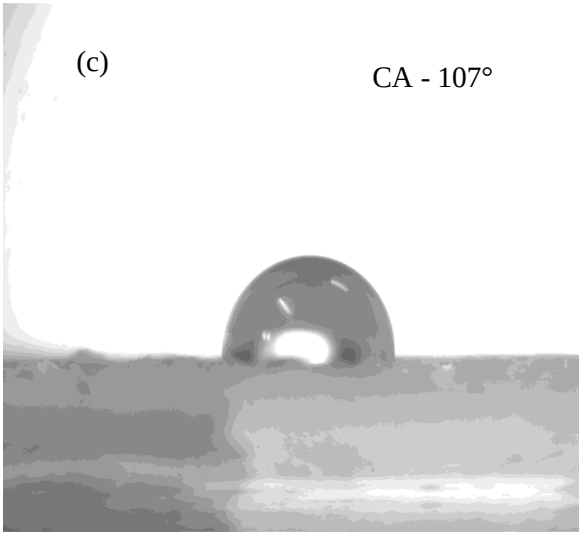

Fig.4.8 Contact angle of (a)TEOS/PVDF, (b) TEOS/PMMA, and (c)TEOS/PS

The contact angle of PVDF is 54° whereas, for TEOS/PVDF composite film shown in **Fig.4.8 (a)**, the contact angle is observed to be 92° and the film thickness also increased from 4.4μm to 5.4μm **[Xin Huang et al., 2015]**. The hydrophobic surface behaviour is also reported by other researchers Veronika V Dick et al and Jian-Hua Li et al., **[Veronika V.Dick et al., 2014] & [Jian- Hua Li et al., 2013].** In case of TEOS/PMMA and TEOS/PS composite, the contact angle is 115° and 107° respectively, **(Fig. 4.8 (b & c))** with the film thickness 11.25μm and 13.2μm thickness. On addition of TEOS, there is a change in the surface static angle. Adhesion is less for the blend of TEOS/PVDF, TEOS/PMMA, TEOS/PS and high for pristine PVDF **[A.Ananth et al., 2012] & [Shanhu Liu et al., 2015]**.As the adhesion decreases, the surface energy also increases and this results in hydrophobic surface, which is true with the composite films of PVDF, PMMA and PS.

4.3.1.3 Surface Roughness and Surface Energy

One of the primitive properties to enhance the non-wettablity of any solid surface is surface roughness and energy. The surface roughness and energy of TEOS/ PVDF, TEOS/PMMA and TEOS/PS is shown in the **Fig. 4.9, 4.10 and 4.11**. In general, wettable surfaces have less roughness and high energy whereas non-wettable surfaces have high roughness and less energy, even in micro or nano level. **Table.4.1** shows the surface roughness and energy for the Polymer-TEOS composite films. Surface energy has been computed with Hamaker's constant. Of all the three films, PMMA/TEOS was found to have higher surface roughness of 40.62 µm and less surface energy of 20.14 Jm^{-1} . The histogram for TEOS/PVDF, TEOS/PMMA and TEOS/PS have been shown in **Fig. 4.12 (a,b and c).** This implements the particle size and is found to be in the range of 150nm and 450nm with the z-steps between 700µm to 1200µm.

Table 4.1 - Calculated values of Surface energy of silane blended Polymers

Sample	Hamaker Constant ,A_n (J x 10^{-21})	Surface Roughness , Ra (µm)	Surface energy, ϒ (Jm^{-1})	Contact Angle, CA (°)	Thickness (µm)
TEOS/PMMA	1.87	40.62	20.14	115°	11.25
TEOS/PS	1.4	34.17	29.8	107°	9.32
TEOS/PVDF	1.12	29.13	49.9	92°	8.96

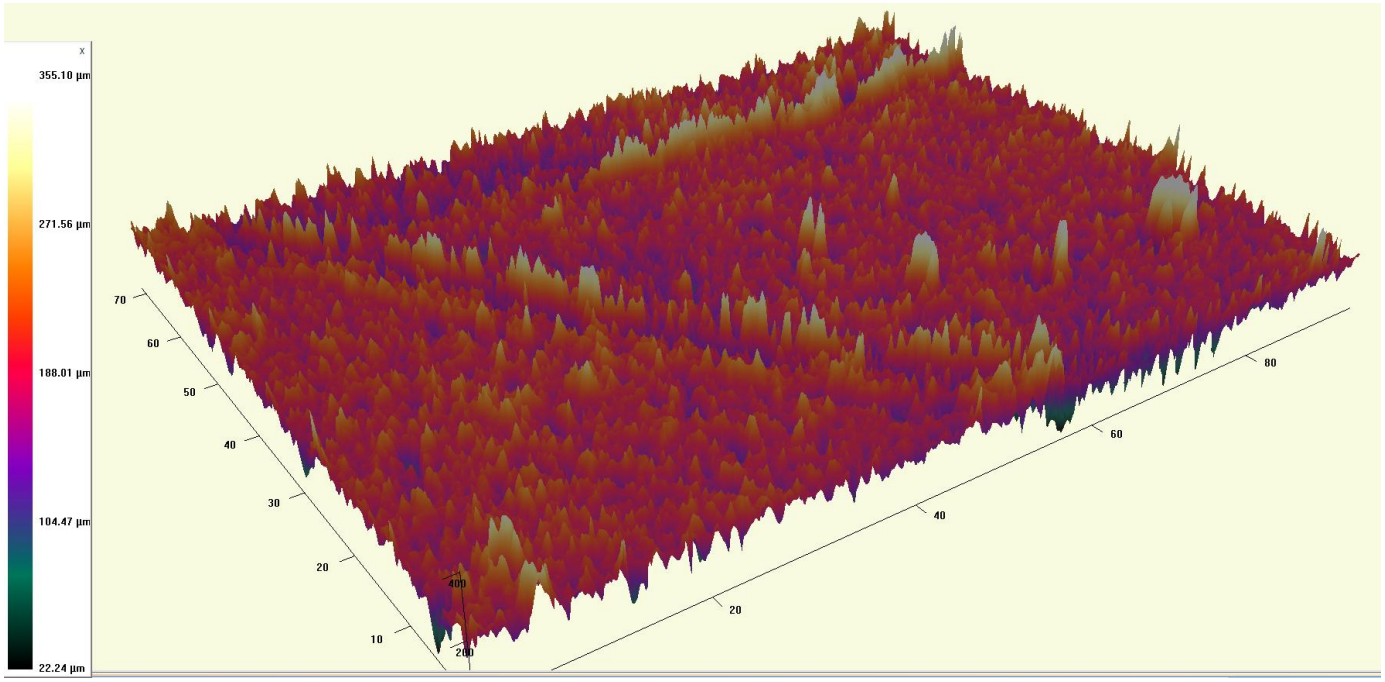

Fig.4.9 Surface Roughness of TEOS/PVDF film

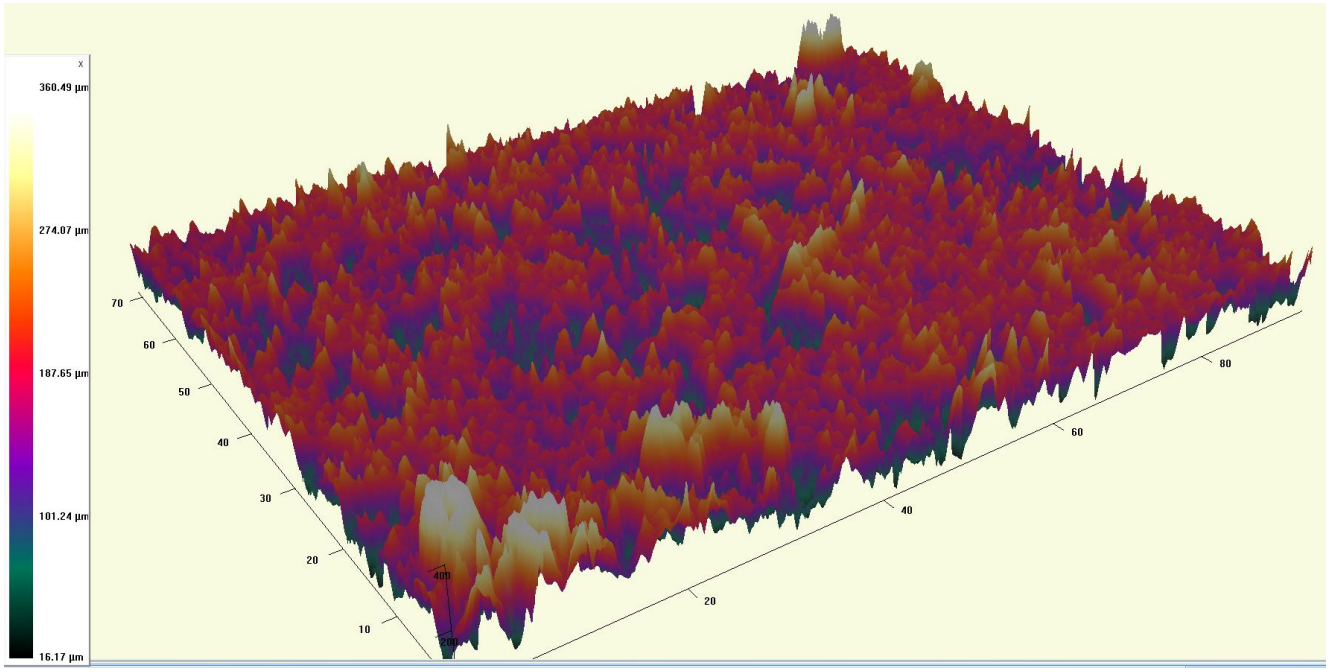

Fig.4.10 Surface Roughness of TEOS/PMMA film

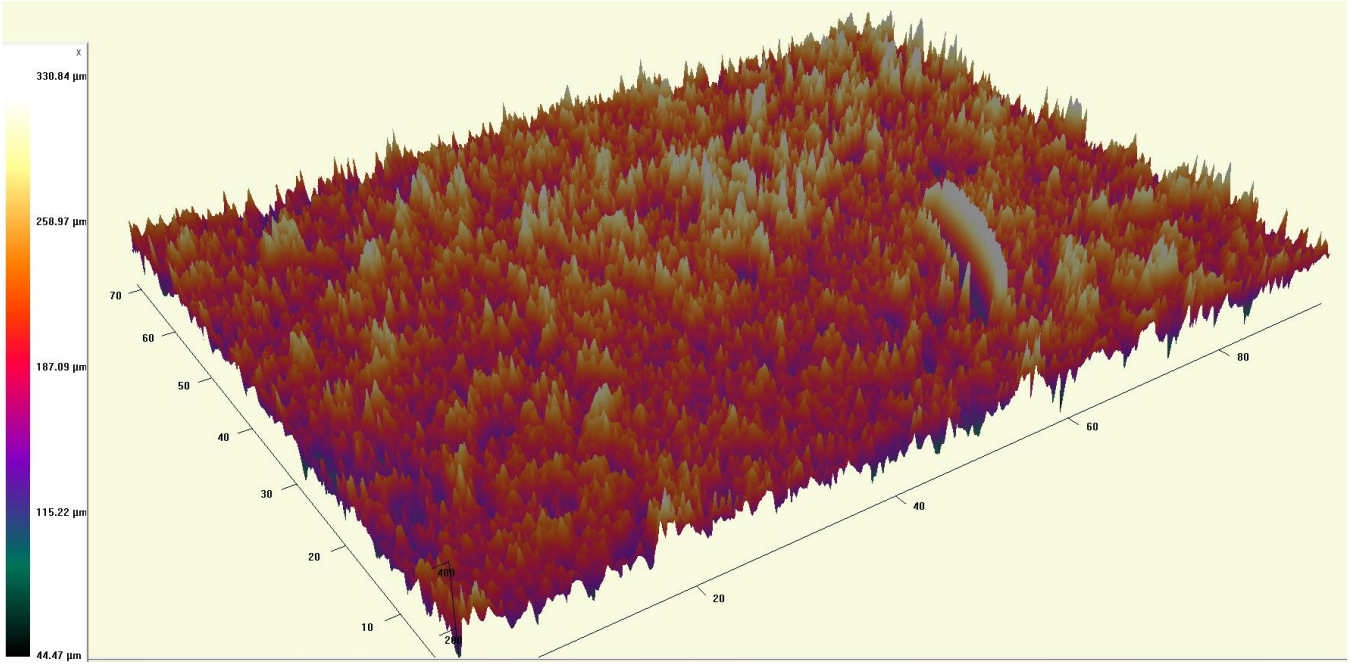

Fig.4.11 Surface Roughness of TEOS/PS film

Histogram for TEOS/PVDF, TEOS/PMMA and TEOS/PS were shown in the **Fig. 4.12 (a,b and c)** using 3D Zeta profilometer between the z-steps of 700µm to 1250µm and the average particle size for TEOS/PVDF, TEOS/PMMA and TEOS/PS is 307nm, 300nm and 262nm.

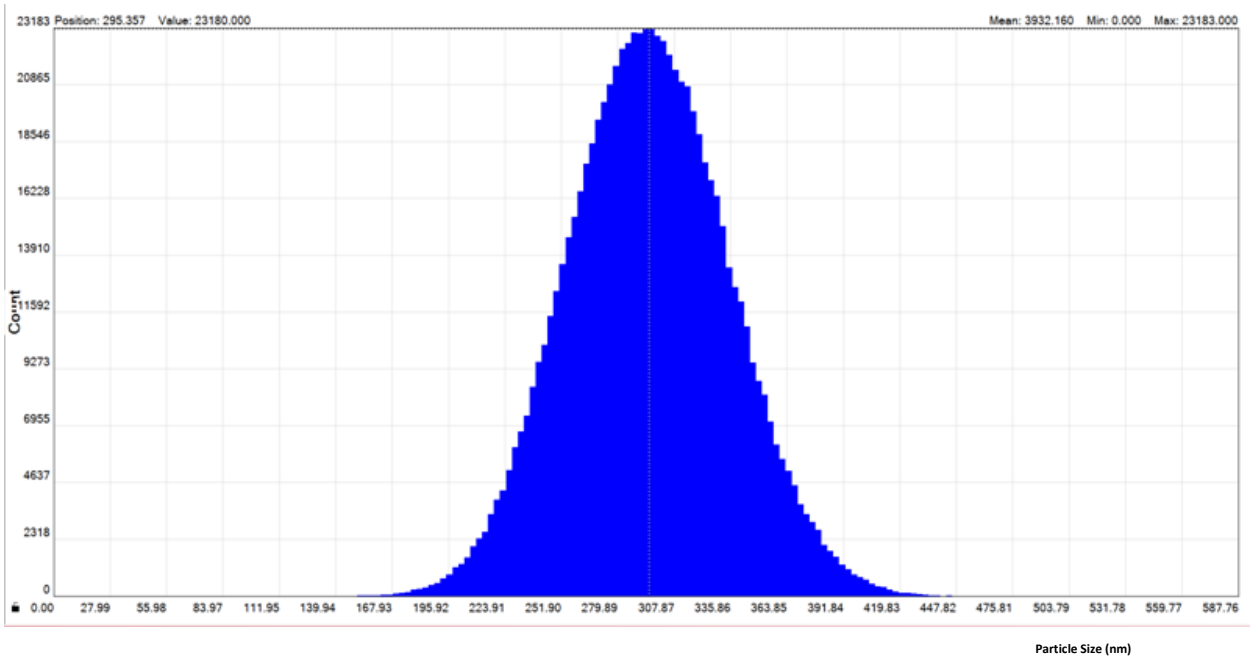

Fig. 4.12 (a) Histogram of TEOS/PVDF

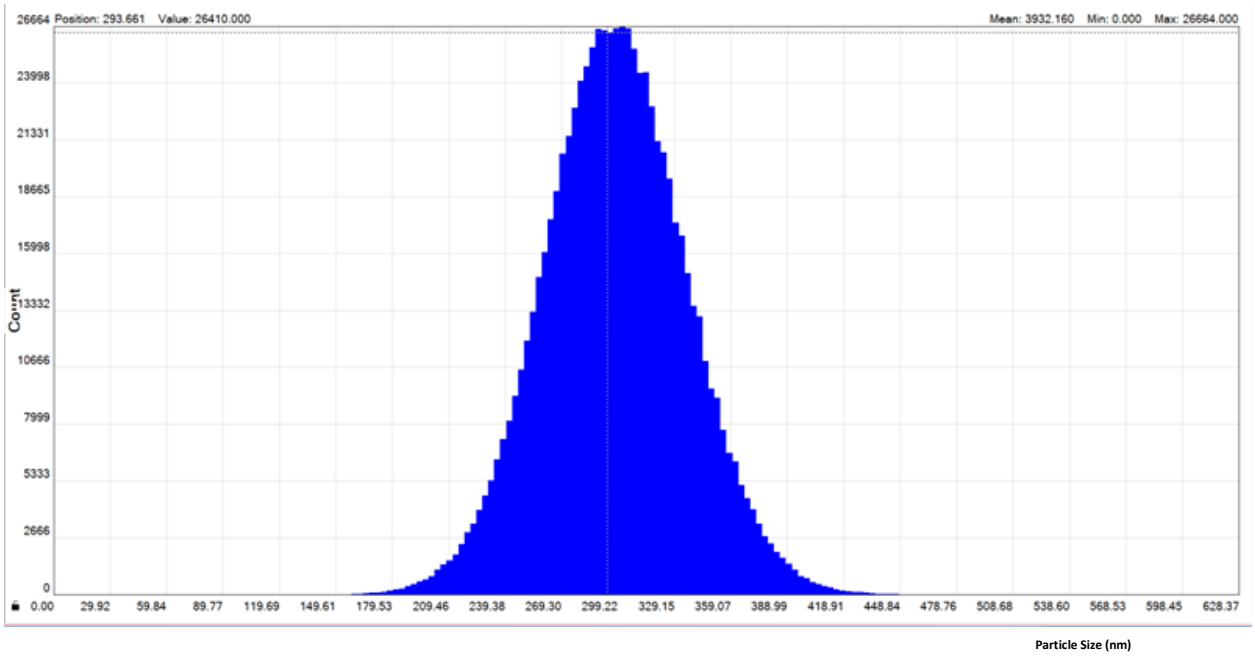

Fig. 4.12 (b) Histogram of TEOS/PMMA

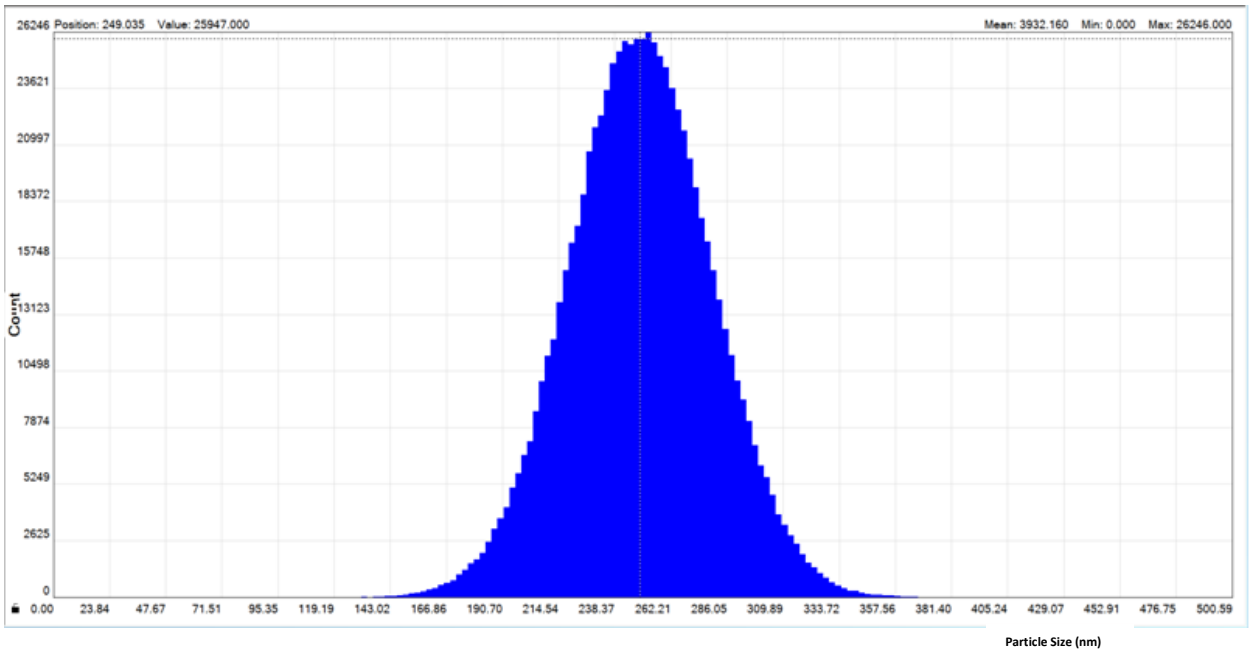

Fig. 4.12 (c) Histogram of TEOS/PS

4.3.1.4 UV-Visible Spectroscopy

The optical properties of the polymer-silane composite films were studied and the plotted spectrum is shown in the **Fig.4.13**. The spectra shows that TEOS/PVDF has higher percent of transmittance (83%) whereas TEOS/PMMA has lesser transmittance (40%). In case of TEOS/PS , the percent of transmittance is about 60%. TEOS/PVDF shows hydrophobicity with less transparency, while TEOS/PMMA, transparent film exhibited high surface roughness.

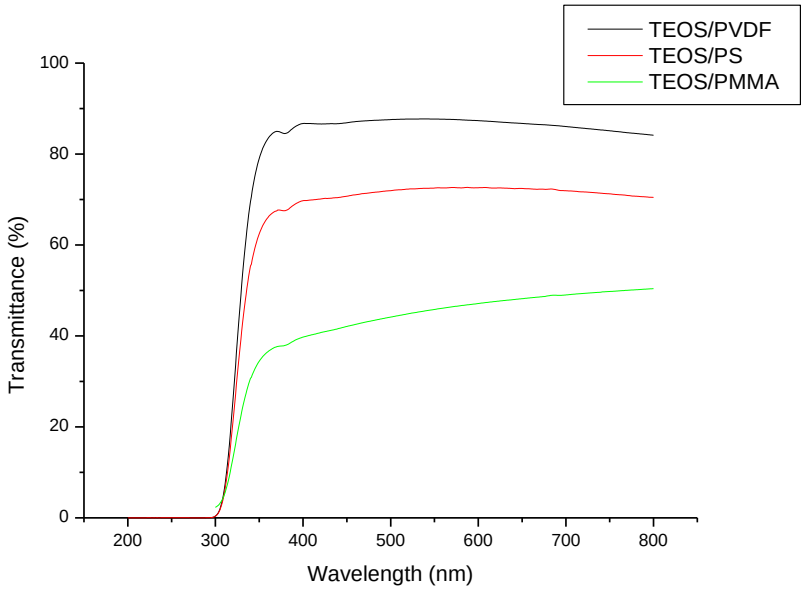

Fig.4.13 UV-Visible Spectrum of TEOS/PVDF, TEOS/PMMA and TEOS/PS

4.3.1.5 FESEM

Fig 4.14, shows the FESEM image of polymer blended TEOS. The surface morphology shows crack-free and uniform surface, which have been studied for different magnification. The particle size was observed in nanometer range (400nm). Larger the size shows winkled surface, which is due to the loss of moisture content. The Polymer blended TEOS shows a Honey-comb like structure. The smooth surfaces of TEOS have been transfigured into a non-uniform surface. The FESEM images of PVDF and TEOS blended PVDF is shown in the **fig 4.14**. On addition of TEOS to PVDF there was missile formation in its surface morphology.

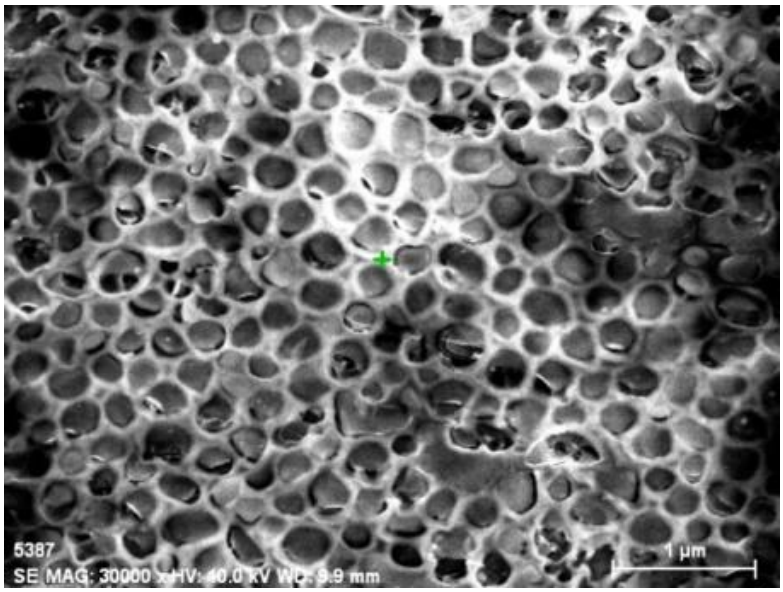

Fig.4.14 FE-SEM of PVDF/TEOS

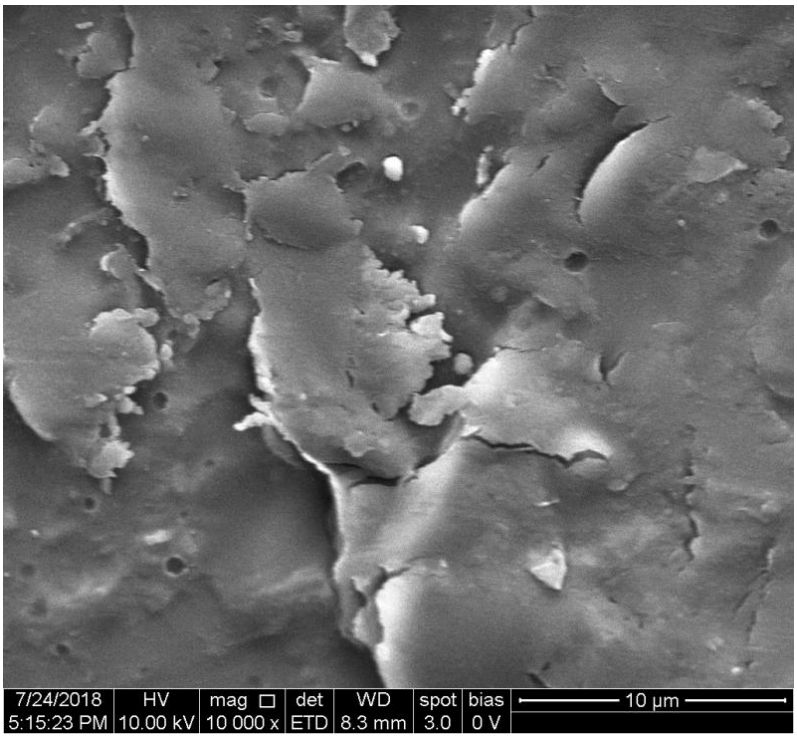

Fig.4.15 FE-SEM of PMMA/TEOS

The FESEM image of TEOS/PMMA and TEOS/PS is shown in the **Figs.4.15 and 4.16**. TEOS/PMMA surface has uneven morphology, and maybe attributed

to higher value of Ra. The TEOS/PS surface shows a lamellae morphology, which may be due to the macromolecules packed rigidly and hence can cause the increase in surface roughness. The obtained lamellae structure indicates consistency of the molecules with size varying from 407 nm to 750 nm **[Javid Rzayev., 2009]** .

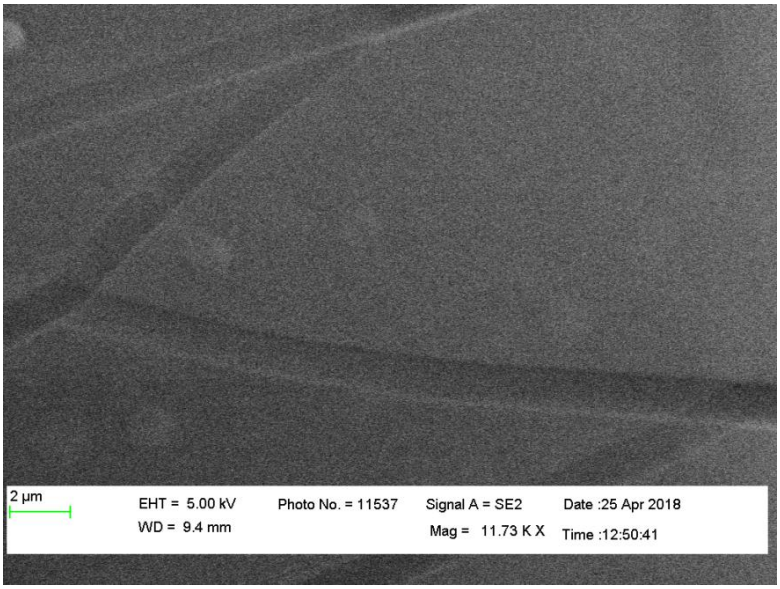

Fig.4.16 FE-SEM of PS/TEOS

With EDX, **(Fig.4.17 to 4.19)** the surface chemical analyzes was carried out and observed the following elements carbon (C), Oxygen(O), and Fluorine(F) peaks for pristine PVDF and Carbon (C), Oxygen (O), and Silica (Si) peaks for TEOS . TEOS/PVDF,TEOS/PMMA and TEOS/PS surface exhibits Carbon (C), Oxygen (O), and Silica (Si) peaks,and Fluorine (F) in addition to TEOS/PVDF surface as PVDF has fluorine as shown in **table 4.2.** This proves the deposition of dirt and impurities-free films by Sol-gel and spin-coating technique.

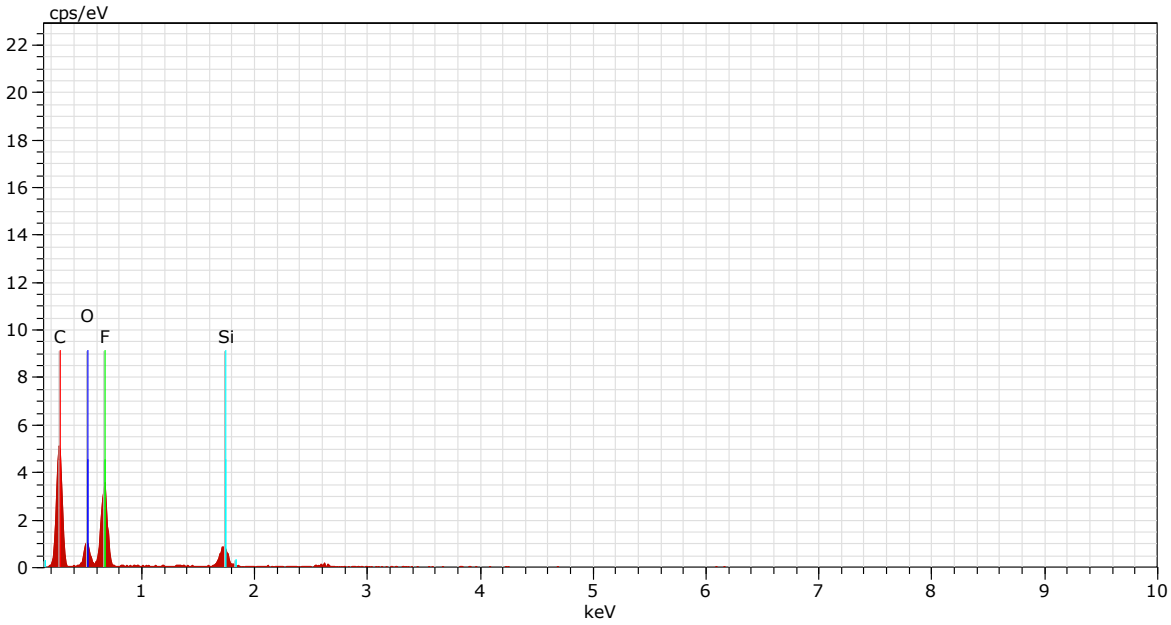

Fig.4.17 EDX of TEOS/PVDF

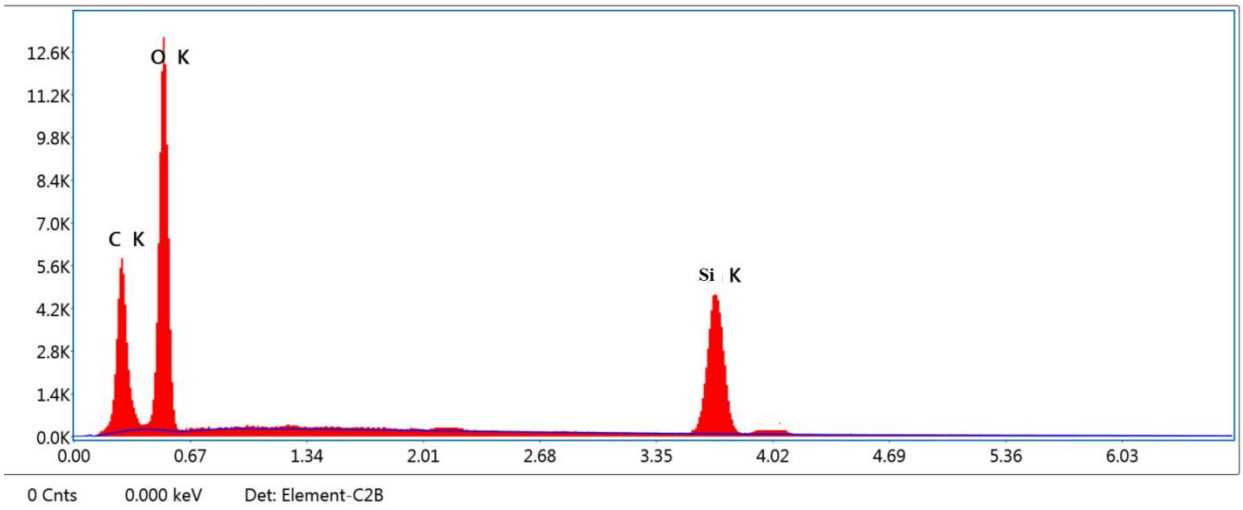

Fig.4.18 EDX of TEOS/PMMA

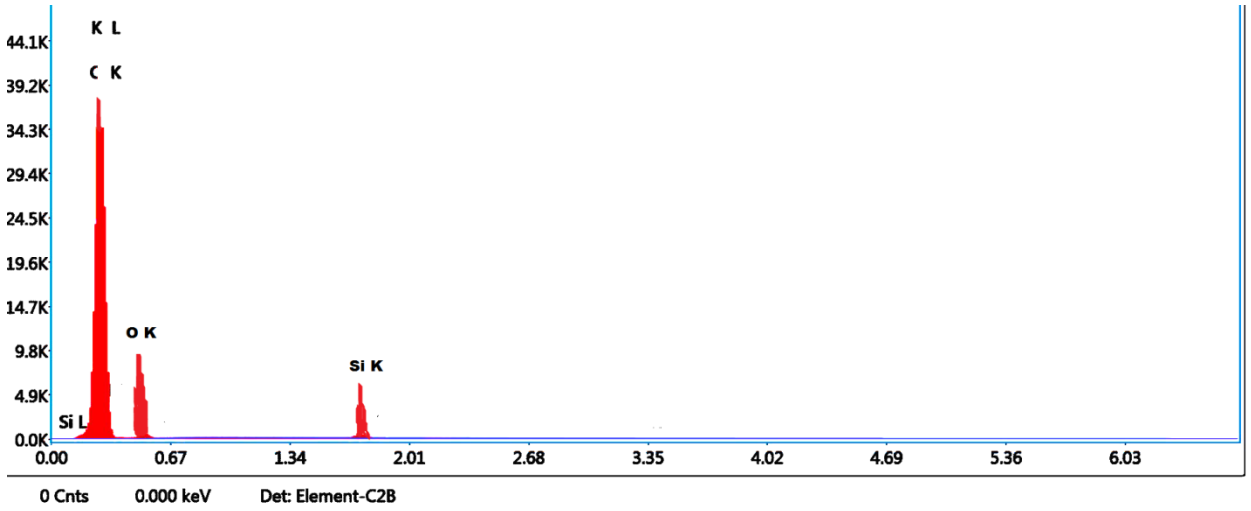

Fig.4.19 EDX of TEOS/PS

Table 4.2. Elemental composition obtained from EDX

Substrate (Glass)	Atomic Weight (%)			
	C	O	F	Si
TEOS/PVDF	59.38	11.25	26.35	3.02
TEOS/PMMA	28.12	67.26	-	4.62
TEOS/PS	92.68	6.22	-	1.1

4.3.1.6 TG-DTA

TG-DTA for TEOS/PVDF, TEOS/PMMA and TEOS/PS was plotted in the **figure 4.20,4.21 and 4.22**, treated thermally at 500°C with the heating rate of 10°C/min. In TEOS/PVDF film, the initial weight loss was of 10.24% occured at 160°C. The bump at 150°C represents the glass transition temperature. An

exothermic peak was seen at 420°C, and the corresponding weight loss resulted due to the combustion of silane material.

In case of TEOS/PMMA, weight loss takes place at 320°C, the second stage of decomposition with the corresponding exothermic peak at 300°C. Further, the two exothermic peak at 390°C and 450°C was seen in the DTA curve which may be due to the degradation of the polymeric material (PMMA) showing a chain scission of methyl methacrylate. As PMMA does not possess any α-H atoms depolymerization occurs. With TEOS/PS, single stage decomposition is seen. The volatile impurities had sharp degradation at 400°C in DTA curve and weight loss of 90.63% is seen beyond 450°C.

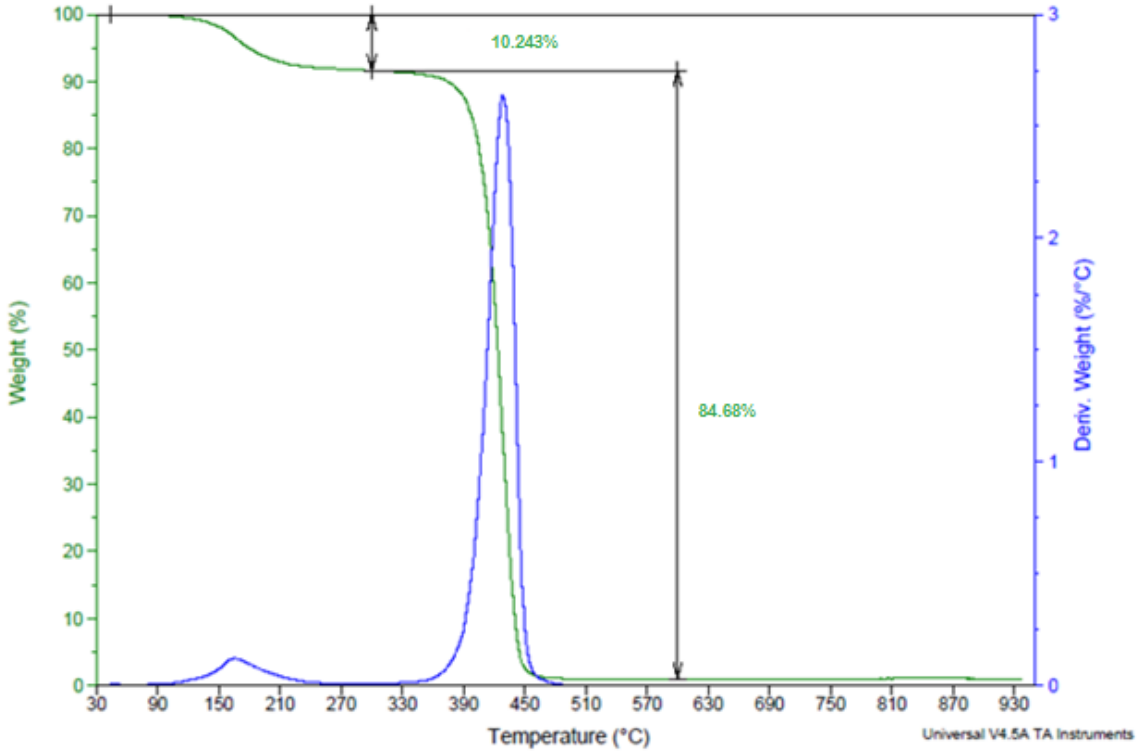

Fig. 4.20 TG-DTA for TEOS/PVDF

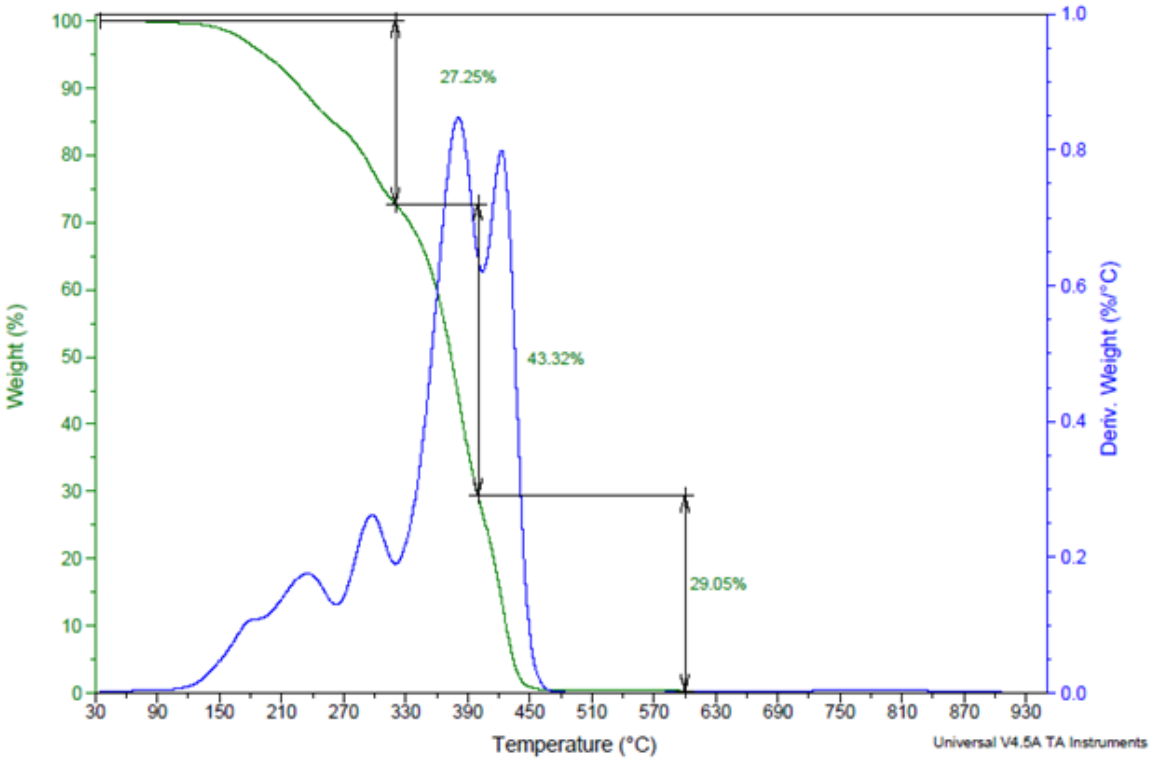

Fig. 4.21 TG-DTA for TEOS/PMMA

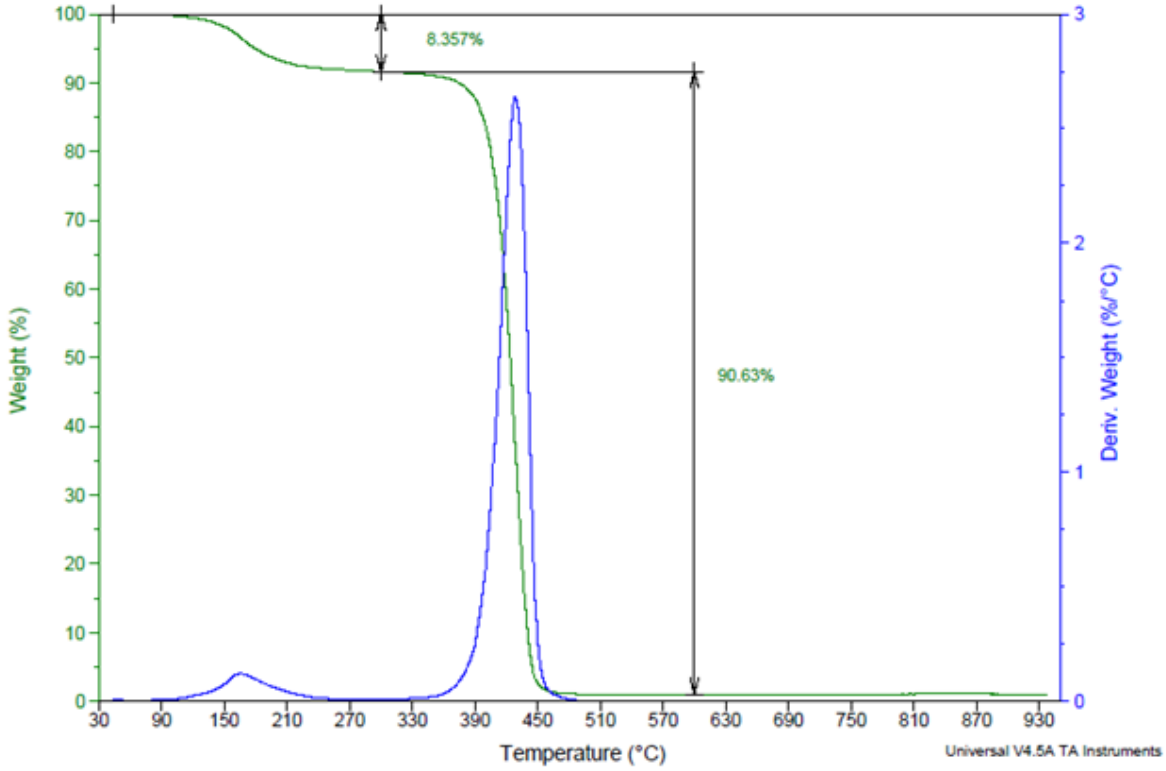

Fig. 4.22 TG-DTA for TEOS/PS

4.3.1.7 Application

Polymer-TEOS coated substrates and uncoated substrates were tested for self cleaning application. Dust particles were placed on the substrates and water droplets were allowed on it. Water spreaded out in uncoated substrates as shown in the **Fig. 4.23 (a)**. Whereas, water droplets bulked up along with the dust particles in coated substrates. Each coated substrate with the buckling of water is shown separately **(Fig.4.23 b,c,d).** 1.5 gram of dust particles were kept on coated and uncoated slides. 2 µl of water was allowed on all the coated and uncoated slides. Water spreaded along with the dust particles in uncoated substrate whereas, in the coated substrates the water gets clinged along with the dust particles making the surface clean from dust.

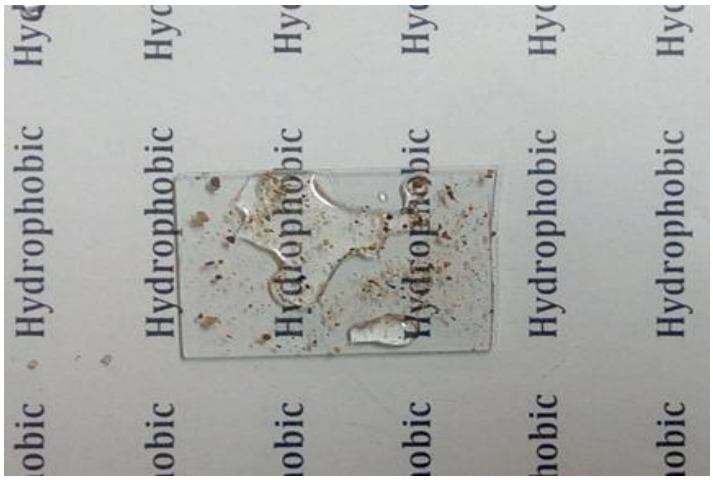

Fig. 4.23 (a) Uncoated substrate

Fig. 4.23 (b) TEOS/PVDF coated substrate

Fig. 4.23 (c) TEOS/PMMA coated substrate

Fig. 4.23 (d) TEOS/PS coated substrate

4.3.2 SET – II [MTMS + Polymer]

4.3.2.1 FTIR

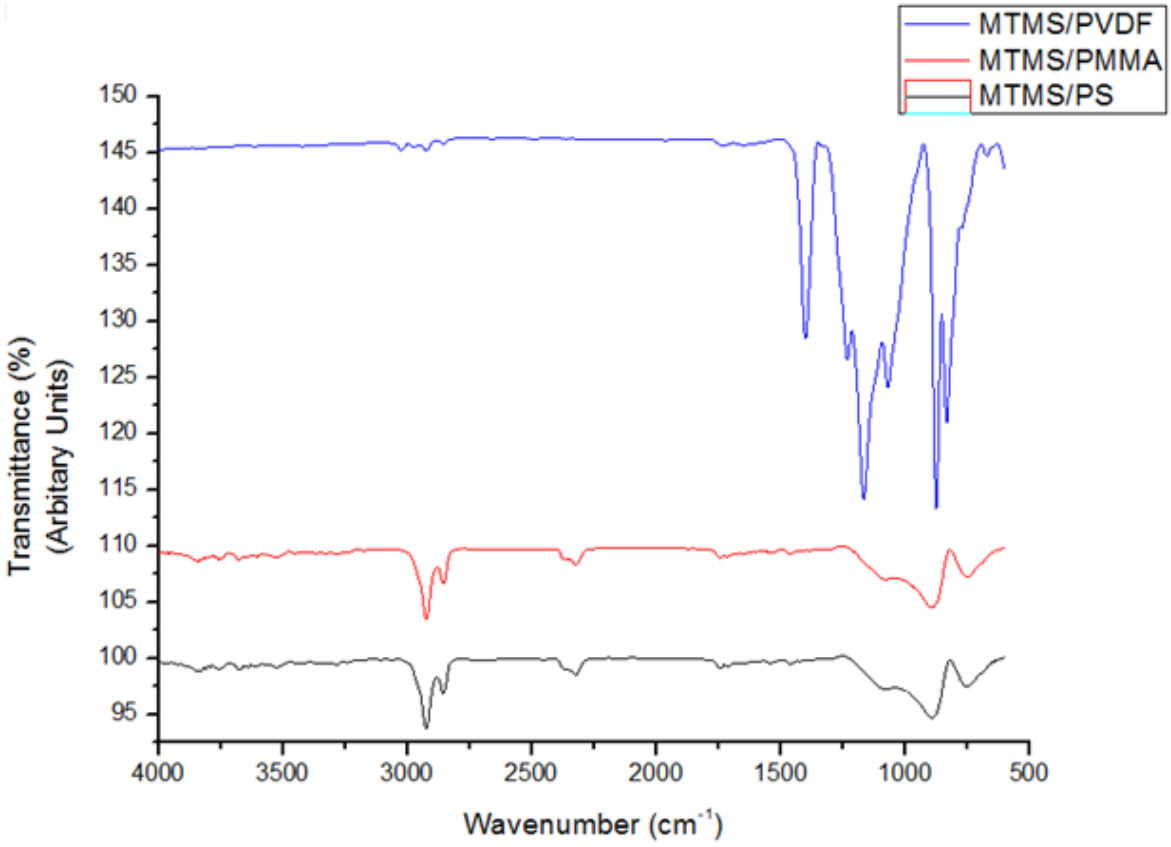

Fig.4.24 FTIR spectrum of MTMS/PVDF,MTMS/PMMA and MTMS/PS

Pristine PVDF exhibited conventional FTIR absorption peaks at 610, 759,796 and 970cm^{-1} which are characteristic of nonpolar α-phase. While the appearance of FTIR absorption peak at 835 cm^{-1} indicates the γ-phase **[Vimal K. Tiwari, et al.,2018]**. The two characteristic peaks of PVDF at 1400 and 1175cm^{-1} represents the CH_2 and CF_2 stretching vibration respectively **[Hossein Mahdavi et al., 2017]**

The characteristic bands appeared at 835, 871, 1062 cm^{-1} of pristine PVDF changes into 831, 874, 1068 $cm^{-1}$for blend, and confirms the presence of MTMS. The peak appeared at 1400 cm^{-1} of pristine PVDF is also present in the blend hence the presence of PVDF. The peaks at 3022, 3611 cm^{-1} indicates the absence of water molecule.

The functional groups of the composite films MTMS/PMMA and MTMS/PS was identified by FTIR spectra **(Fig.4.24)**.The peaks at 1029 cm^{-1} and 1103 cm^{-1} are assigned to the stretching mode of Si-O-Si. The condensation of the hydrolyzed MTMS and the presence of methyl group were indicated with C-H stretching and bending vibration modes of $Si-CH_3$ at 2970 cm^{-1}, 1408 cm^{-1} and 1269 cm^{-1}. At 763 cm^{-1}, Si-C bond is observed. **[Bi Xu et al., 2014 and D.B.Mahadik et al., 2016]**.

The absorption peaks at 727cm^{-1} and 1456cm^{-1} represents Si-C bond and bending modes of C-H bonds. The symmetric and asymmetric modes of C-H bond is seen at 2923 cm^{-1} . In this scenario, peak obtained at 3533 cm^{-1} , represents the absence of polar bond, which validates the hydrophobicity of the film **[Mahendra S.Kavale et al., 2011 and Satish A.Mahadik et al., 2013]**. The intense sharp peak at 1742 cm^{-1} denotes C=O group**.**

For Pristine Polystyrene, the peak at 2921.61 cm^{-1} represents the C-H stretching vibration mode, whereas this peak has been shifted to 2854 cm^{-1} in MTMS composited Polystyrene representing the inclusion of methenyl group. The band at 1141cm^{-1} represents the O-Si-O bond. The peak at 3520.42 cm^{-1} represents

the absence of polar bond. This ensures hydrophobicity of films **[Xin Fan et al., 2012].**

4.3.2.2 Contact Angle

The contact angle for the composite films MTMS/PVDF, MTMS/PMMA and MTMS/PS was observed as 132°, 112° and 119° and are shown in the **Figs.4.25 (a) , (b) and (c).** The hydrophobic surface behavior is also reported by other researchers Popat G. Pawar et al and Shanhu Liu et al., **[Popat G. Pawar et al., 2017 and Shanhu Liu et al., 2015].** The adhesion property is less for the composite films upon adding silane to the polymer. As the adhesion decreases, the surface energy increases and this results in hydrophobic nature, for all the three composite films of PVDF, PMMA and PS with MTMS.

(a) CA - 132°

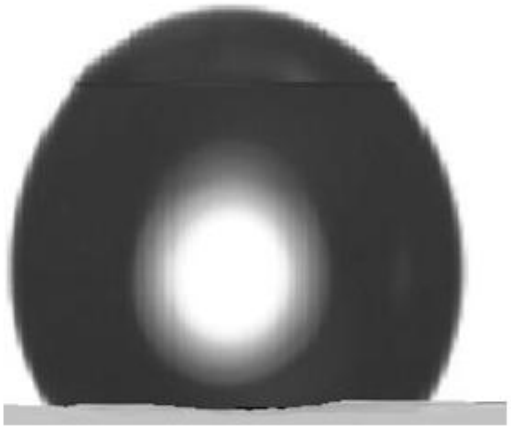

(b) CA - 112°

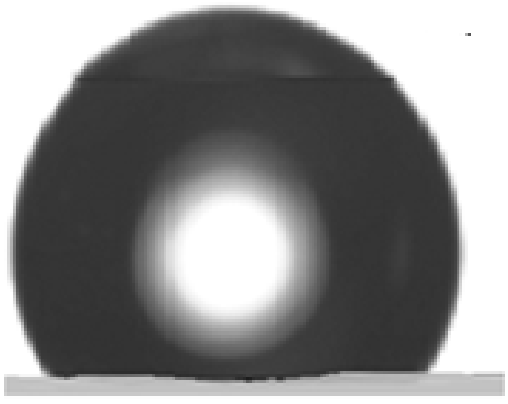

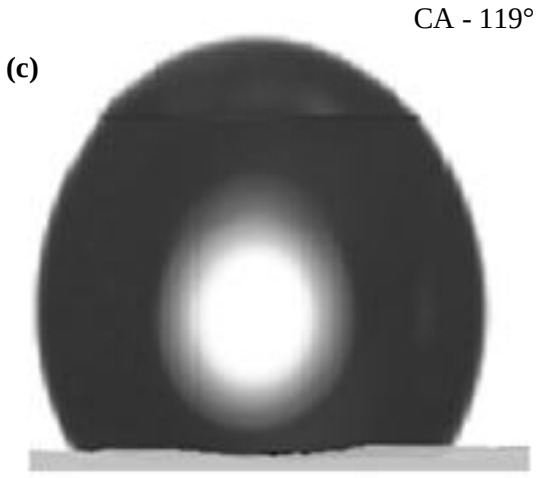

Fig.4.25 Contact Angle for (a) MTMS/PVDF, (b) MTMS/PMMA and (c) MTMS/PS

4.3.2.3 Surface Roughness and Surface Energy

The thickness and surface roughness of the films were measured using Zeta Profilometry **(Figs.4.26,4.27,4.28).** It is quantified by the deviations of the normal vector. If these deviations are large, the surface is rough and for small deviations, the surface is smooth. It was found that MTMS/PVDF has higher surface roughness (R_a) compared to MTMS/PMMA and MTMS/PS with higher peak height, Rp ranging between 250µm to 500µm.

Table. 4.3 - Surface Roughness and Thickness Measurement of spin-coated films

Sample	Hamaker Constant A_n (J x 10^{-21})	Surface Roughness , Ra (µm)	Surface energy, Ɣ (Jm^{-1})	Contact Angle, CA (°)	Thickness (µm)
MTMS/PVDF	1.12	60.76	18.26	132°	15.2
MTMS/PS	1.4	55.85	22.5	119°	12.4
MTMS/PMMA	1.87	52.55	32.5	112°	14.6

The intermolecular interactions at an interface, can be dispersive force, energetically homogeneous or heterogeneous interactions and bonding states the surface energy **[Soo-Jin Park et al., 2011]**. In case of polymers, such surface energy can be measured by indirect methods based on wettability. The Lifshitz theory of Van der Waals interaction can be used to explain the attraction between two uncharged macroscopic surfaces across air or water **[Calcum J.Durmmond et al., 1997]**. As noted by J.Vial et al., **[J.Vial et al., 1991]** the surface energy can be calculated once the Hamaker constant (A_H) / (A_n) is known.

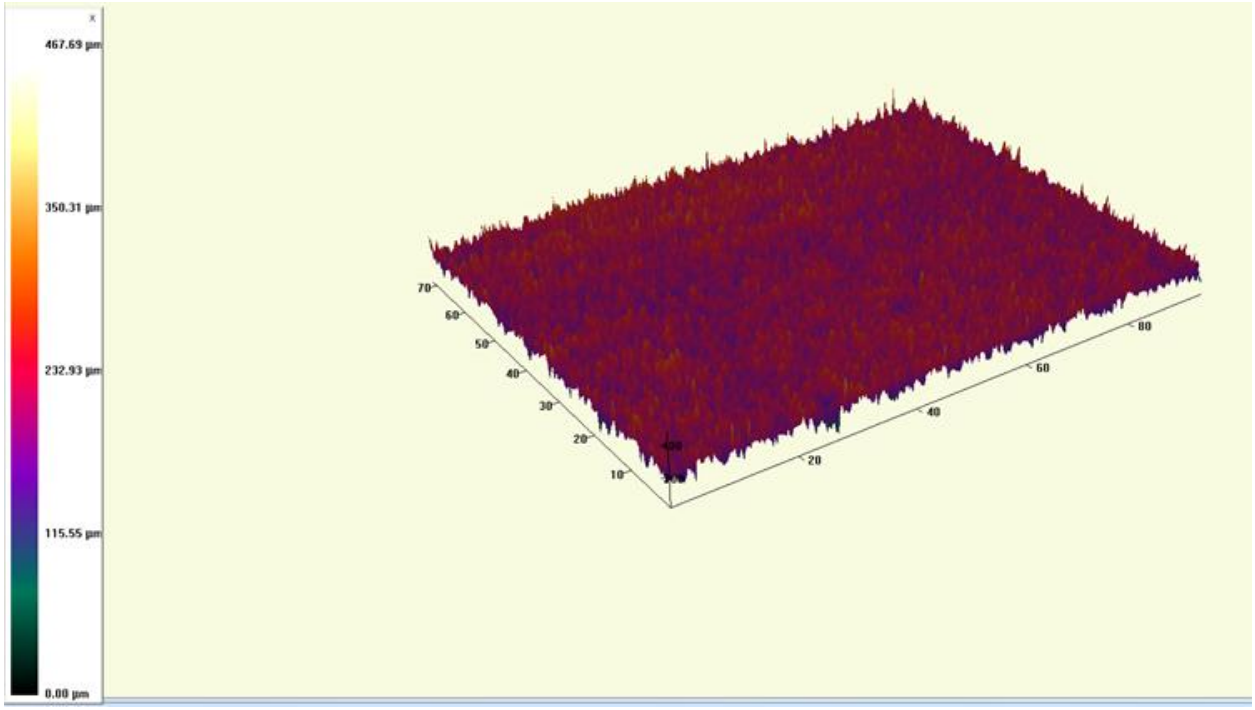

Fig. 4.26 Surface Roughness of MTMS/PVDF

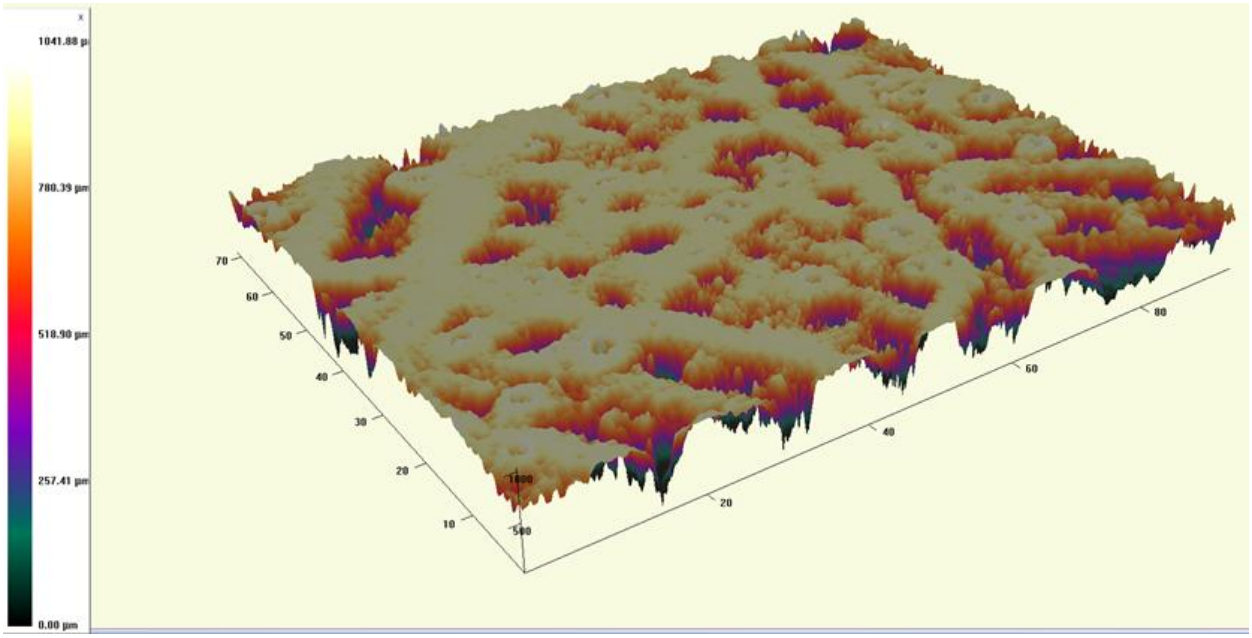

Fig. 4.27 Surface Roughness of MTMS/PMMA

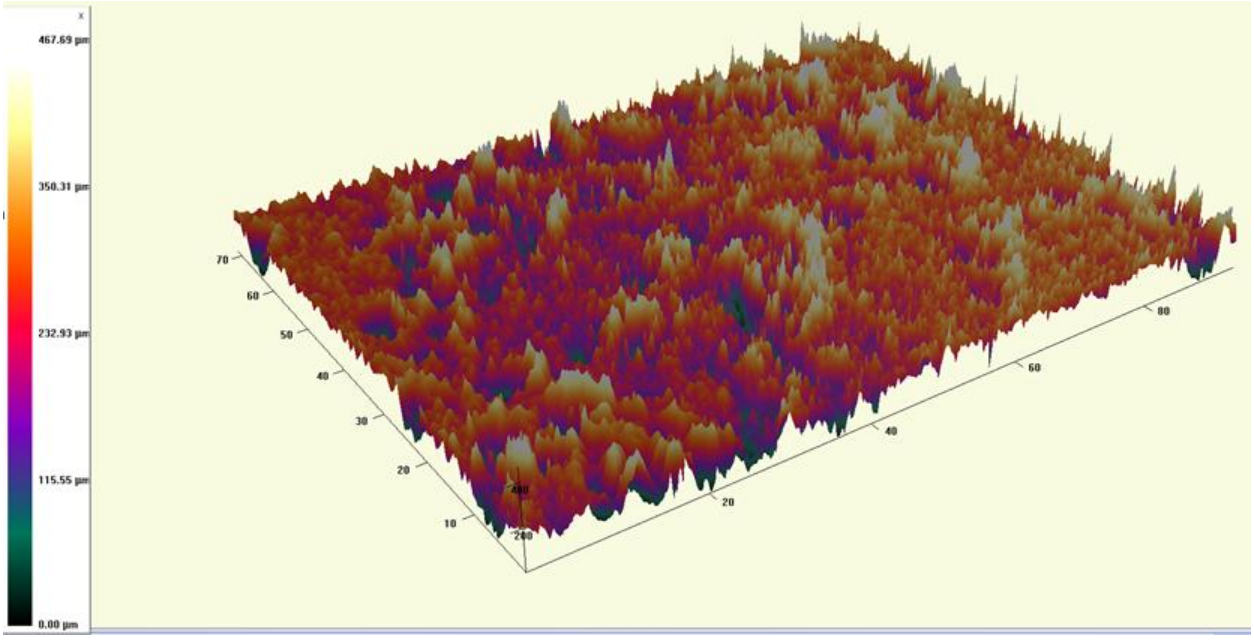

Fig. 4.28 Surface Roughness of MTMS/PS

4.3.2.4 UV-Visible Spectroscopy

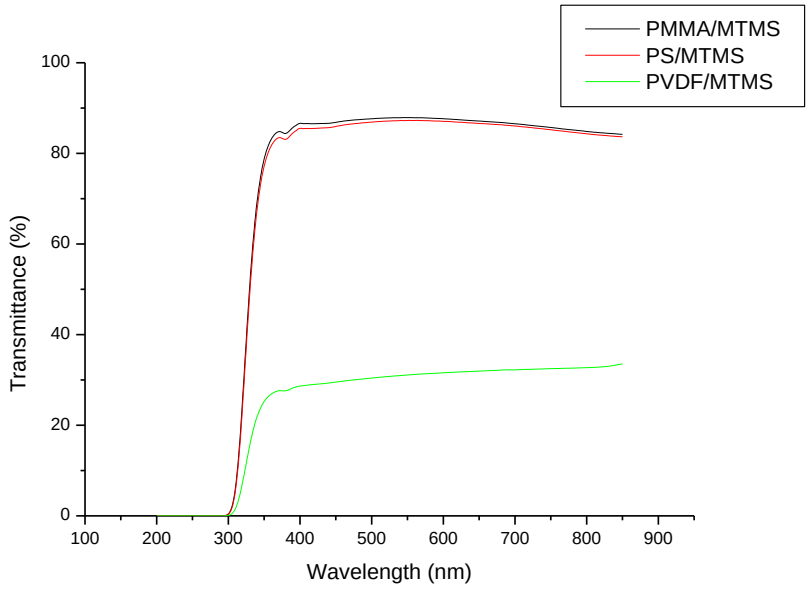

Fig. 4.29 UV-Visible Spectrum for MTMS/PVDF, MTMS/PMMA and MTMS/PS

The UV-Visible spectrum for MTMS/PVDF, MTMS/PMMA and MTMS/PS has been plotted as shown in **Fig.4.29**.MTMS/PVDF has less percentage of transmittance (22%), with higher surface roughness and contact angle. As roughness increases the absorption of the film increases thereby decreasing the transmittance of the film. MTMS/PMMA film has cutoff wavelength at 390 nm and 89% transmittance. MTMS/PS exhibited the cutoff wavelength at 385 nm, and transmittance of 85 %. In both the composite films, the optical clarity was good, as the transmittance is higher, which enables the use in applications like Coatings on spectacle lenses, CD cases, cosmetic containers and many household appliances.

4.3.2.5 FESEM

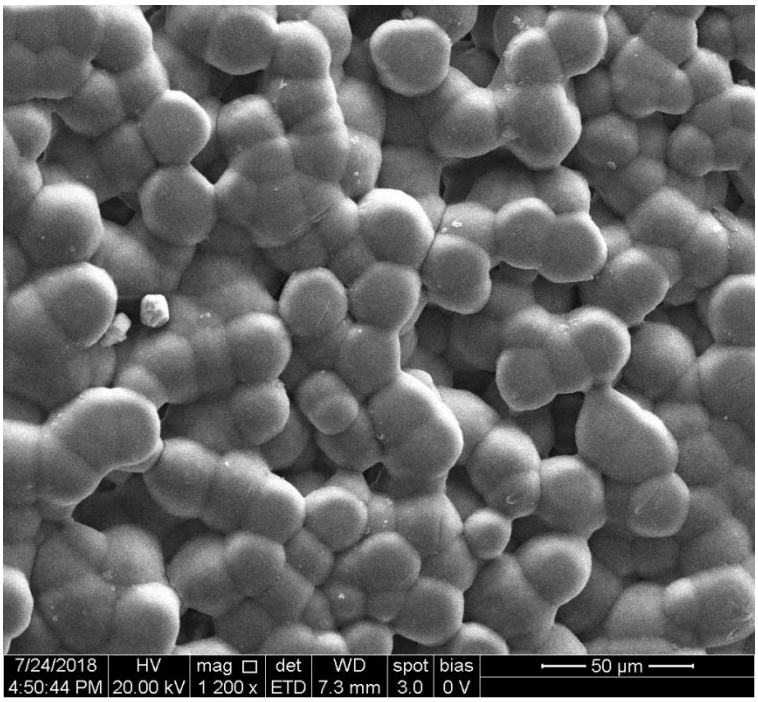

Fig.4.30 FE-SEM of MTMS/PVDF

Microstructure images of the membrane surfaces were obtained using a scanning electron microscope. **Fig.4.30** shows the FE-SEM picture of the MTMS/PVDF film formed from the composite particles. It reveals that the films are composed of microsized particles, and these microsized particles provides an appropriate surface roughness for the treated substrates. With the addition of MTMS more and more nanospheres were observed on the membrane surface, which gradually construct hierarchical structures that are crucial for super-nonwettability. The enhanced surface roughness can effectively guarantee the water trapping ability and reinforce the oil-repellency of the membranes **[Zhenxing Wang et al., 2018]**

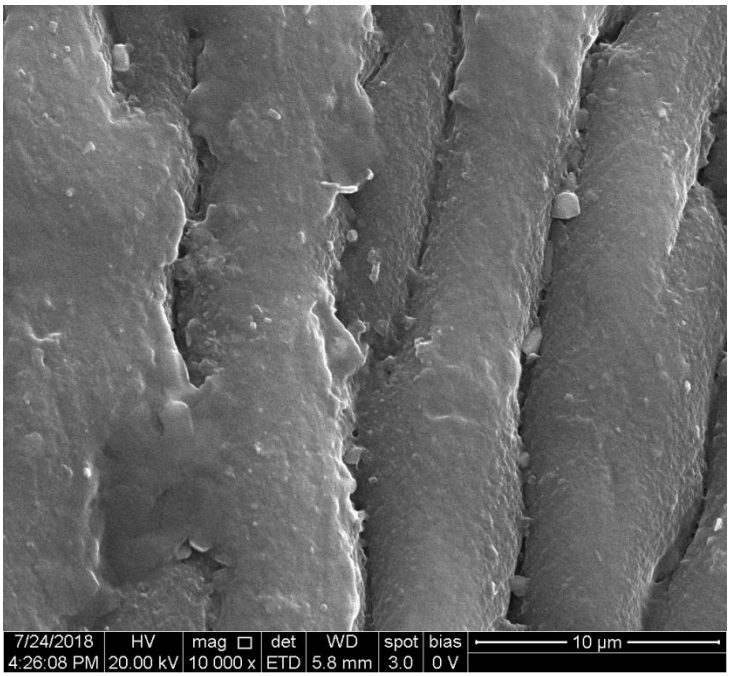

Fig. 4.31 FE-SEM of MTMS/PMMA

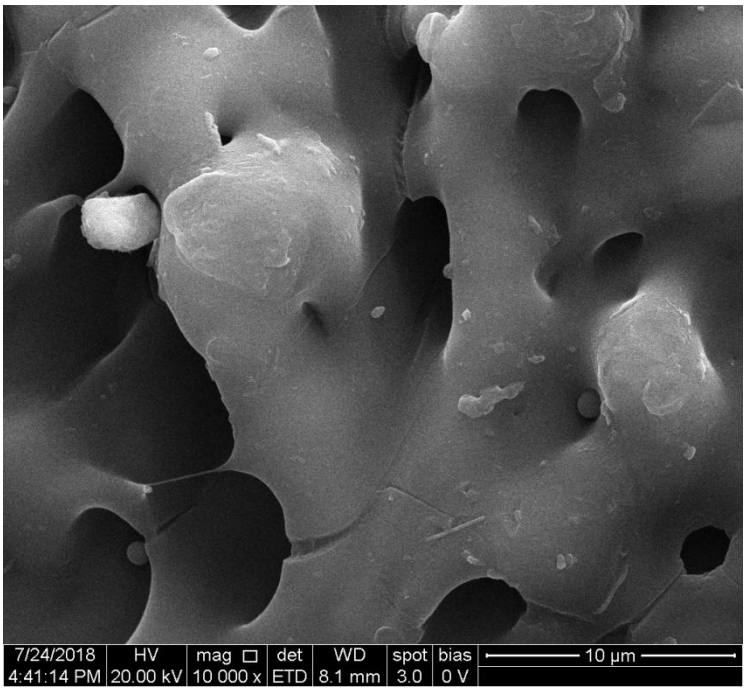

Fig.4.32 FE-SEM of MTMS/PS

From the **Fig.4.31**, the FESEM images of MTMS/PMMA was shown. The surface morphology of Spin-coated processed silica composited acrylic polymer

(PMMA), a flap-repeated pattern surface with average particle size of 282nm was observed. With Fig.4.32, MTMS/PS surface morphology was shown. Unoccupied voids were formed, due to the loss of moisture content and the average particle size of 324nm was obtained. **Fig. 4.33 (a), (b) and (c)** represents the histogram for PVDF/MTMS, PMMA/MTMS & PS/MTMS obtained from 3D Zeta profilometry between the z-steps of 600µm to 1250µm with the particle size ranging between 150nm to 460nm.

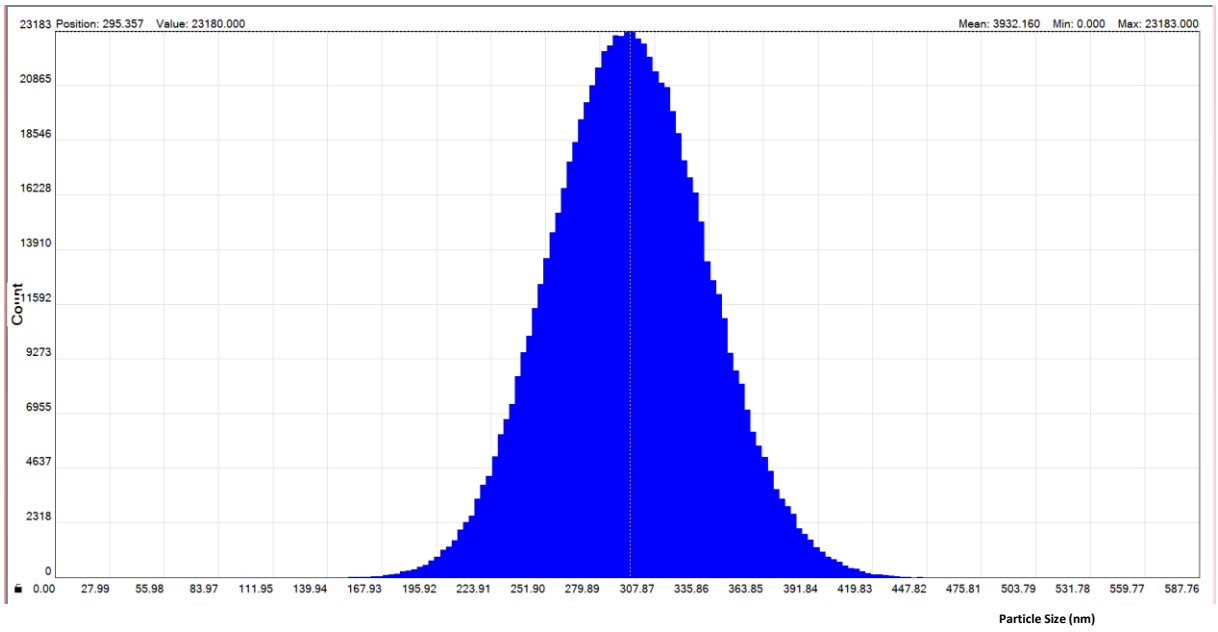

Fig.4.33 (a) Histogram for PVDF/MTMS

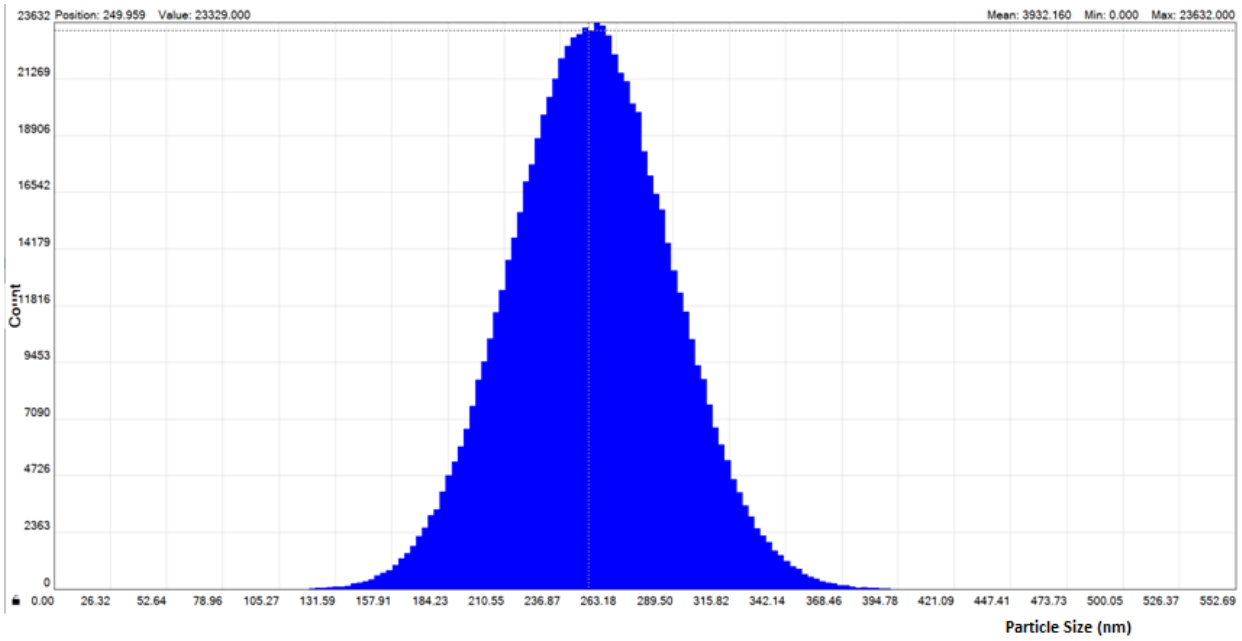

Fig.4.33 (b) Histogram for PMMA/MTMS

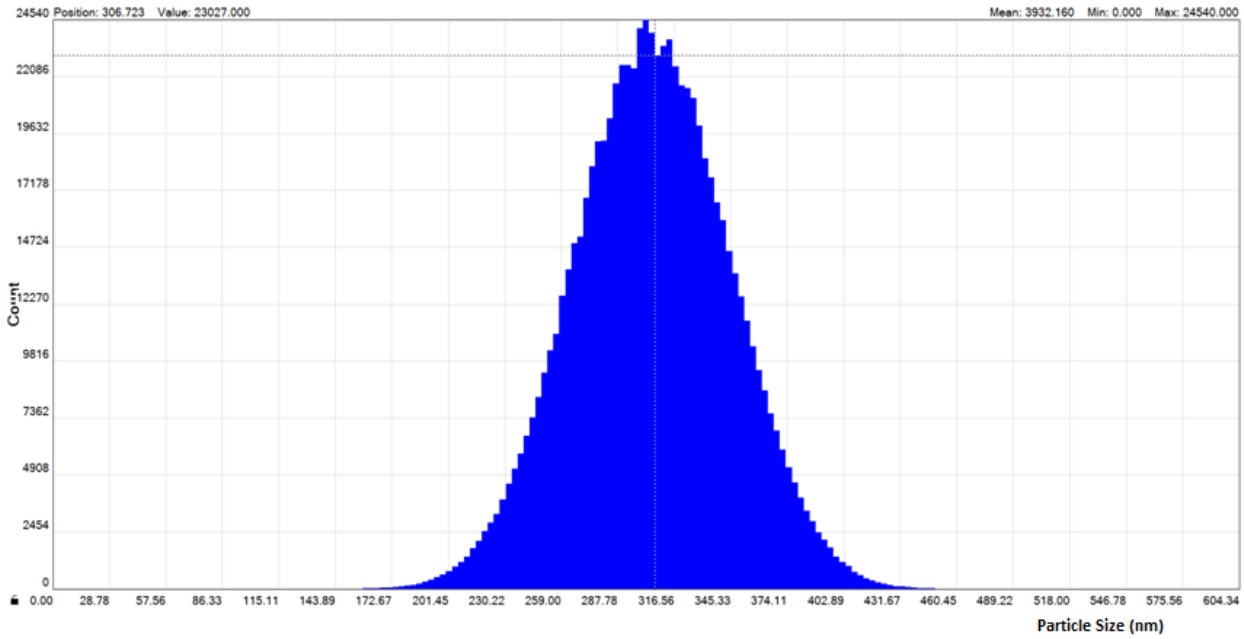

Fig.4.33 (c) Histogram for PS/MTMS

With EDX, the surface chemical analyzes was carried out and observed the following elements carbon (C), Oxygen(O), and Silica (Si) peaks for MTMS/PVDF, MTMS/PMMA as well as for MTMS/PS. Fluorine (F) is also

present in MTMS/PVDF film. The atomic weight percentage for the composite films are tabulated in **table 4.4**. This confirms that the films are impurity-free and has the appropriate elemental composition.

Table 4.4. Elemental composition obtained from EDX

Sample	Atomic Weight (%)			
	C	O	Si	F
MTMS/PVDF	57.45	11.52	3.87	27.16
MTMS/PMMA	95.56	2.39	2.05	-
MTMS/PS	96.43	2.25	1.32	-

4.3.2.6 TG-DTA

Initial weight loss for MTMS/PVDF film was at about 65ºC was mainly due to solvent evaporation. Major weight loss was observed in the range 400-500ºC for the prepared sample. This could be corresponds to structural decomposition of the polymer blend and their complexes. The sample is stable upto 520ºC as shown in **Fig.4.34**. A sharp and large exothermic peak appeared at 490 ºC concurrent with an appreciable weight loss of about 74.73% and this indicate the complex decomposition of the film, which is in agreement with the TG curve. From the above discussion, it is concluded that the thermal stability limit of the blend is 460º C**. [K Naveen Kumar et al., 2012].**

TG-DTA for MTMS/PMMA and MTMS/PS was plotted in the **Figs.4.35 and 4.36**, treated thermally at 500°C with the heating rate of 10°C/min. It was found that upto 150°C , there is no weight loss, and beyond 200°C ,there is a

decrease in weight of the material with a weight loss of 2.811%. Moreover, the composite PMMA/MTMS sample displayed no residual material formation at temperatures of up to 350°C. This behaviour also indicates the random chain scission process of PMMA polymer that occurs during degradation. Beyond 380°C, there is a drastic weight loss **[Nidal Wanis Elshereksi et al., 2014 and Piotr Galka et al., 2014]**. From the DTA curve, sharp exothermic peak was observed at 420°C representing the combustion of the silane .

The TGA curve of MTMS/PS represents that there is no weight loss upto 150°C. Weight loss of 19.70% occured between 300°C and 330°C due to the adsorbed water with a exothermic peak at 300°C and beyond 450°C there is a drastic loss of 65.96 % due to depolymerization. An exothermic peak centered at 392°C was observed in DTA curve, attributed to the decomposition and combustion of the silane. **[Silvano Rodrigo Valandro et al., 2014 and Qingshan Lu et al., 2010].**

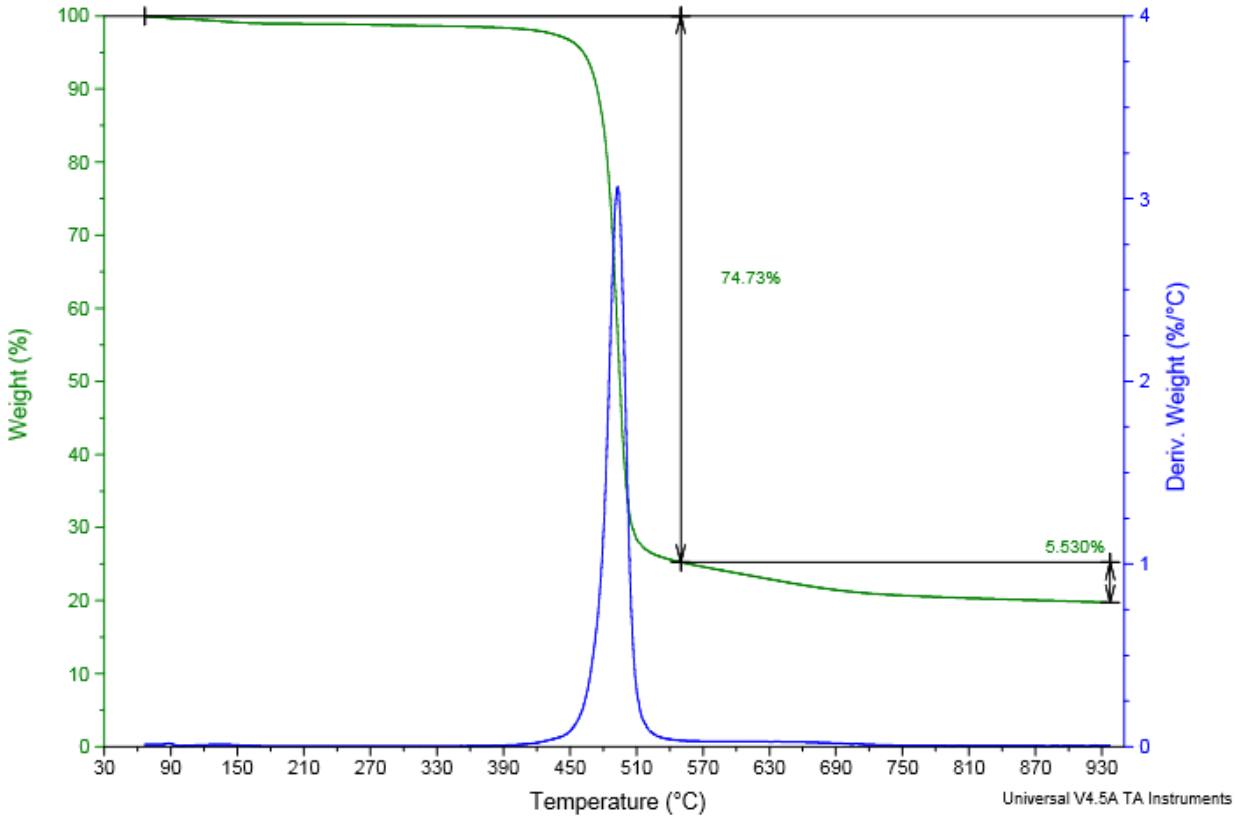

Fig. 4.34 TG-DTA of MTMS/PVDF

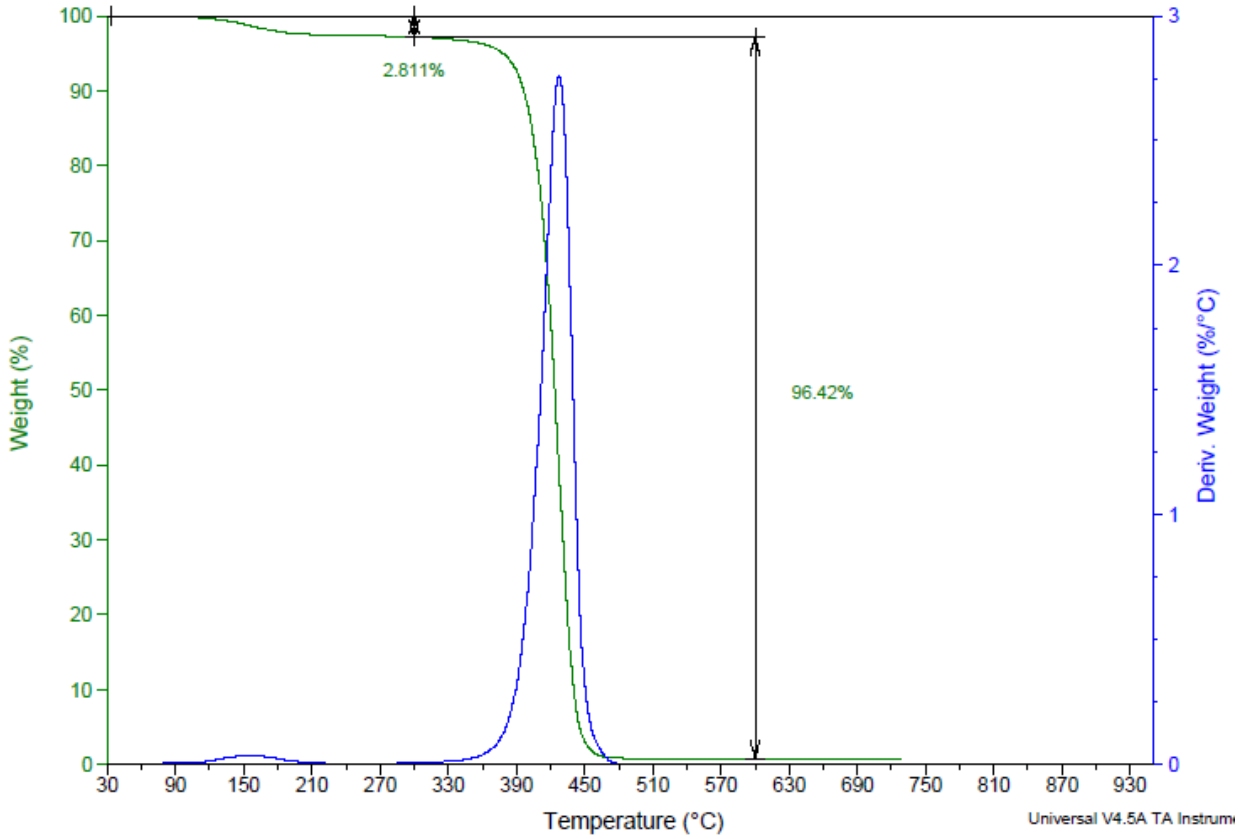

Fig. 4.35 TG-DTA for MTMS/PMMA

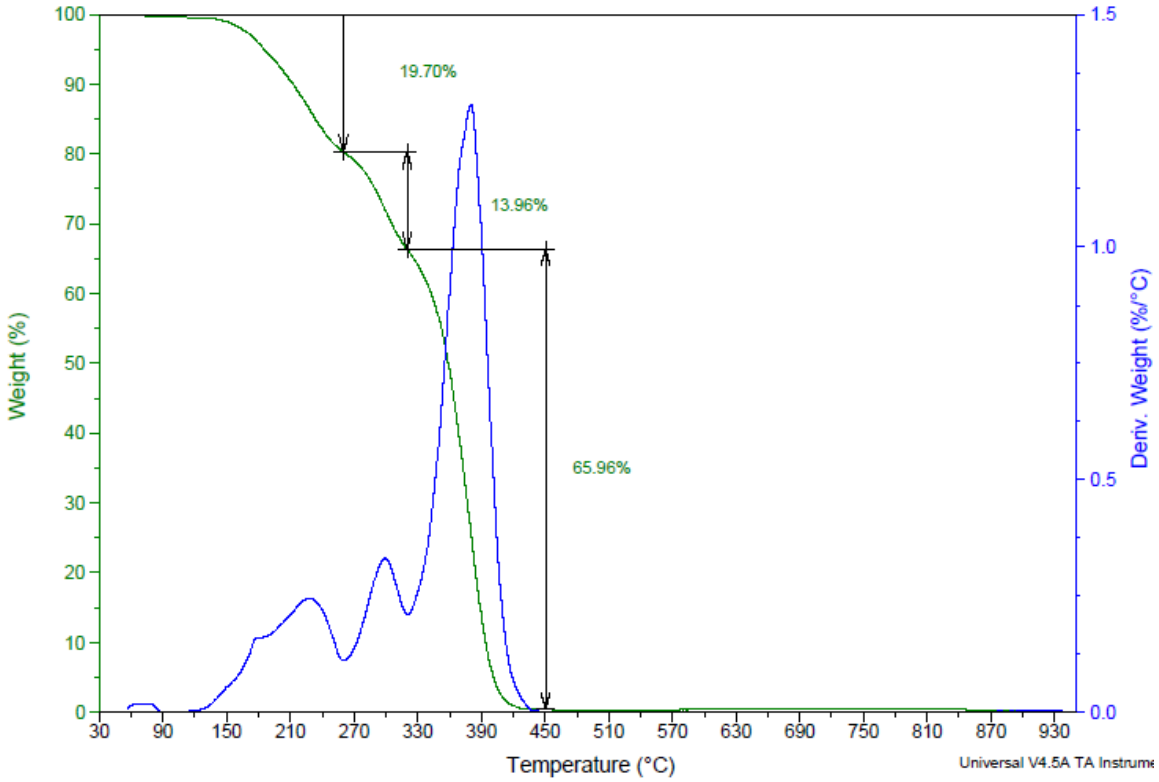

Fig.4.36 TG-DTA for MTMS/PS

4.3.2.7 Application

Polymer- MTMS coated glass substrates were tested for self-cleaning. 2 gram of dust particles were kept on the coated glass substrates. 2µl of water was allowed on the substrate, made the slides dirt-free as the water droplet got clinged to the surface along with the dust particles shown in **Fig. 4.37 (a), (b) and (c).**

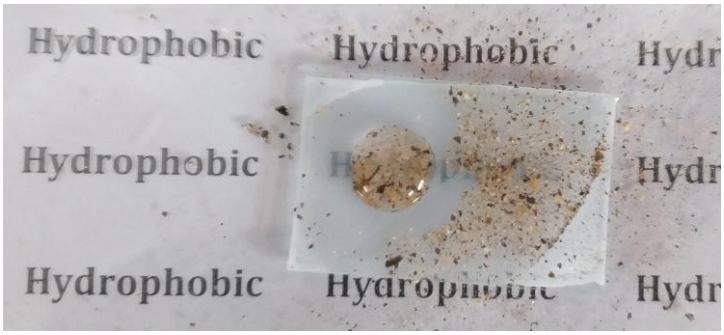

Fig. 4.37 (a) PVDF/MTMS coated substrate

Fig. 4.37 (b) PMMA/MTMS coated substrate

Fig. 4.37 (c) PS/MTMS coated substrate

4.3.3 SET – III [PDMS + Polymer]

4.3.3.1 FTIR

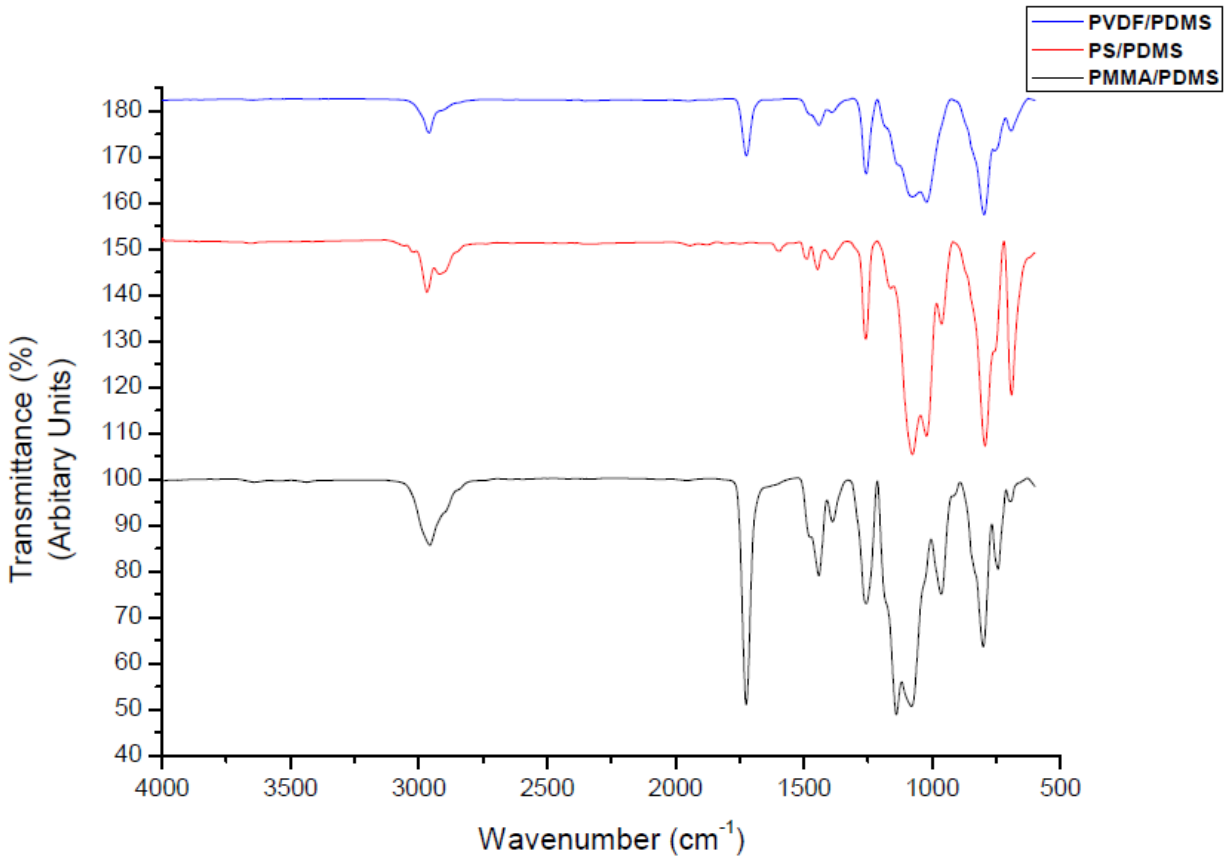

Fig. 4.38 FTIR Spectrum of PDMS/PVDF, PDMS/PMMA and PDMS/PS

The functional groups of the composite films PDMS/PVDF, PDMS/PMMA and PDMS/PS elucidated by FTIR spectra are shown in the **Fig.4.38**. The peak at 797 cm^{-1} is due to the vibration of PVDF crystalline phase **[Zhao-Tong Qu et al., 2018]**. 1022 cm^{-1} assigned to the stretching mode of Si-O-Si vibration. The peaks at 1257 cm^{-1} and 1441 cm^{-1} denotes symmetrical and asymmetrical deformation of CH_3 bonds in Si-CH_3 groups **[A Groza et al., 2015]**.

The peak at 1724 cm^{-1} corresponds to C=O stretching vibration of acrylate **[Paula Ferreira et al., 2013 and Hualin Chen et al., 2009]**. The band at

1139 cm^{-1} attributes to the vibration of C-O-C group. The bands at 1443 cm^{-1} and 749 cm^{-1} were seen due to the vibrations ofs α- methylene group **[S Sathya et al., 2016]** whereas the peak at 1253 cm^{-1} shows the deformation of CH_3 in PDMS **[A Groza et al., 2015]**.

The peak at 690 cm^{-1} corresponds to the aromatic CH deformation vibration of PS. The sharp peaks at 795 cm^{-1} and 1258 cm^{-1} represents Si-CH_3 bond. Si-O-Si stretching vibration is seen at 1021 cm^{-1} . The peak at 2962 cm^{-1} attributes to the presence of methylene group of PDMS **[Helyati Abu Hassan Shaari et al., 2018 and Mesut Akgun et al., 2005]**. When all the three polymers are mixed with PDMS, hydrophobicity is achieved (i.e) there is absence of polar bond in all the three composite films.

4.3.3.2 Contact Angle

The contact angle for the composite films PDMS/PVDF,PDMS/PMMA and PDMS/PS is 148°, 153° and 135° and are shown in the **Figs.4.39 (a), (b) and (c).** The adhesive force defines the strength of interaction between a droplet and the solid surface, it is measured at the instance when a water droplet separates from the surface, the adhesive force observed to vary with the distance that the droplet/substrate travels [**Xia Zhang et al., 2017**]. The adhesion property is less for the composite films upon adding silane to the polymer. In all the three composite films, the adhesion decreases, the surface energy increases, resulting in super hydrophobicity.

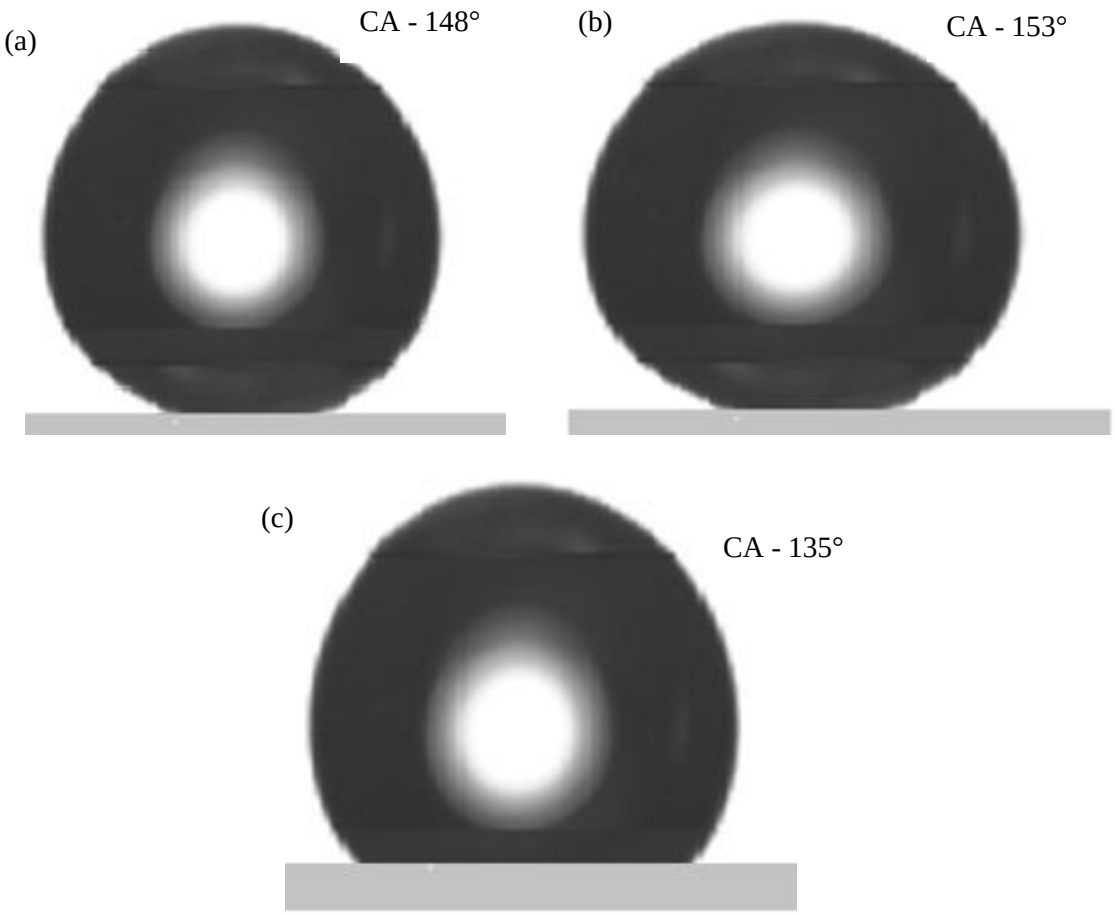

Fig.4.39 Contact angle for (a)PDMS/PVDF, (b)PDMS/PMMA,and (c) PDMS/PS

4.3.3.3 Surface Roughness and Surface Energy

Surface roughness is an important criteria, to be noted to develop hydrophobic surfaces. Using Zeta Profilometry, the thickness and surface roughness of the films, were measured **(Figs.4.40,4.41 and 4.42)**. Roughness plays an important role in determining how real object will interact with its environment and promote adhesion. Surface roughness is expected to increase the interaction of solid- fluid interface and decrease the slippage [**S C Yang., 2006**]. The surface roughness (R_a) of PDMS/PMMA was found to be higher than that of PDMS/PVDF and PDMS/PS. The peak depth (Rp) ranges between 333.71µm to 589.96 µm. **Table**

4.5 shows the measured values of surface roughness and thickness of the composite films. Superhydrophobic nature was observed for all the films upon mixing rubbery like PDMS due to the presence of strong methoxy group.

Table. 4.5 - Values of Surface Roughness and Thickness

Sample	Hamaker Constant A_n (J x 10^{-21})	Surface Roughness, Ra (µm)	Surface energy, Ɣ (Jm^{-1})	Contact Angle, CA (°)	Thickness (µm)
PDMS/PMMA	5.186	69.43	11.05	153°	18.1
PDMS/PVDF	3.405	67.81	15.18	148°	15.3
PDMS/PS	7.85	55.85	19.25	135°	13.2

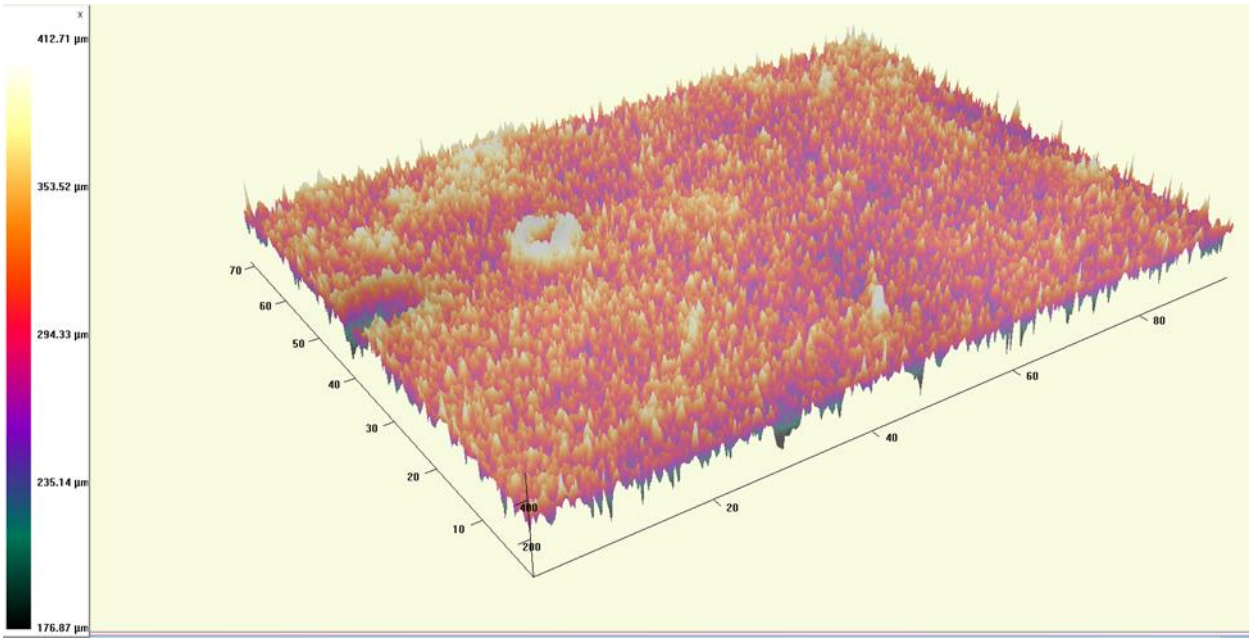

Fig. 4.40 Surface Roughness of PDMS/PVDF

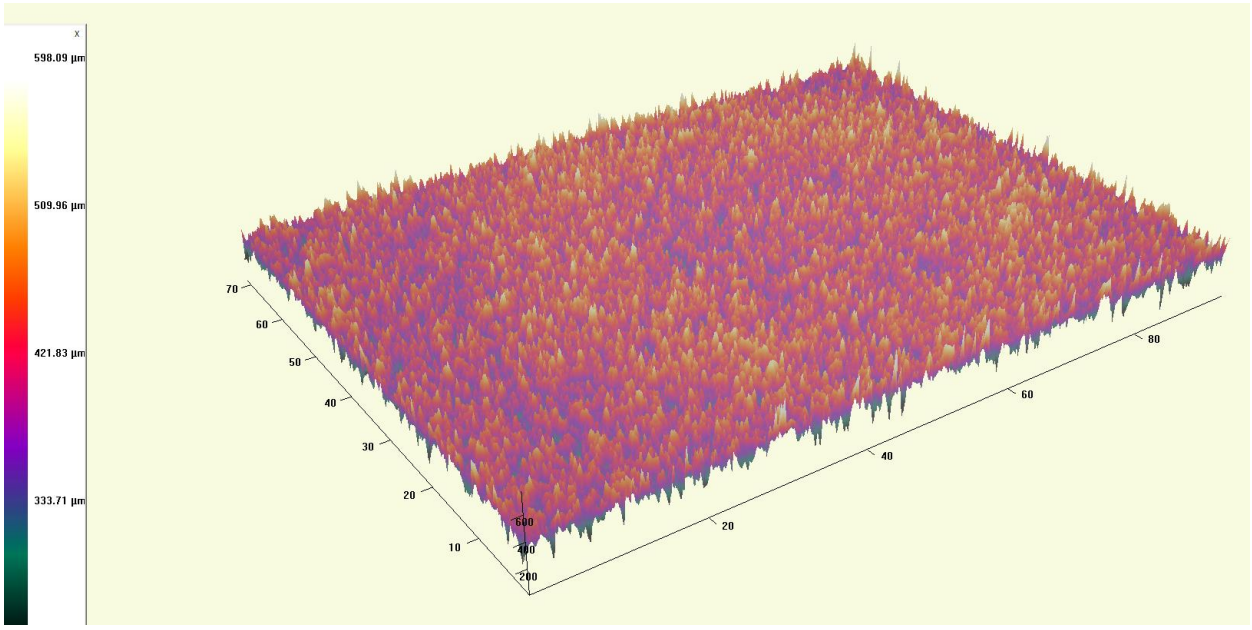

Fig. 4.41 Surface Roughness of PDMS/PMMA

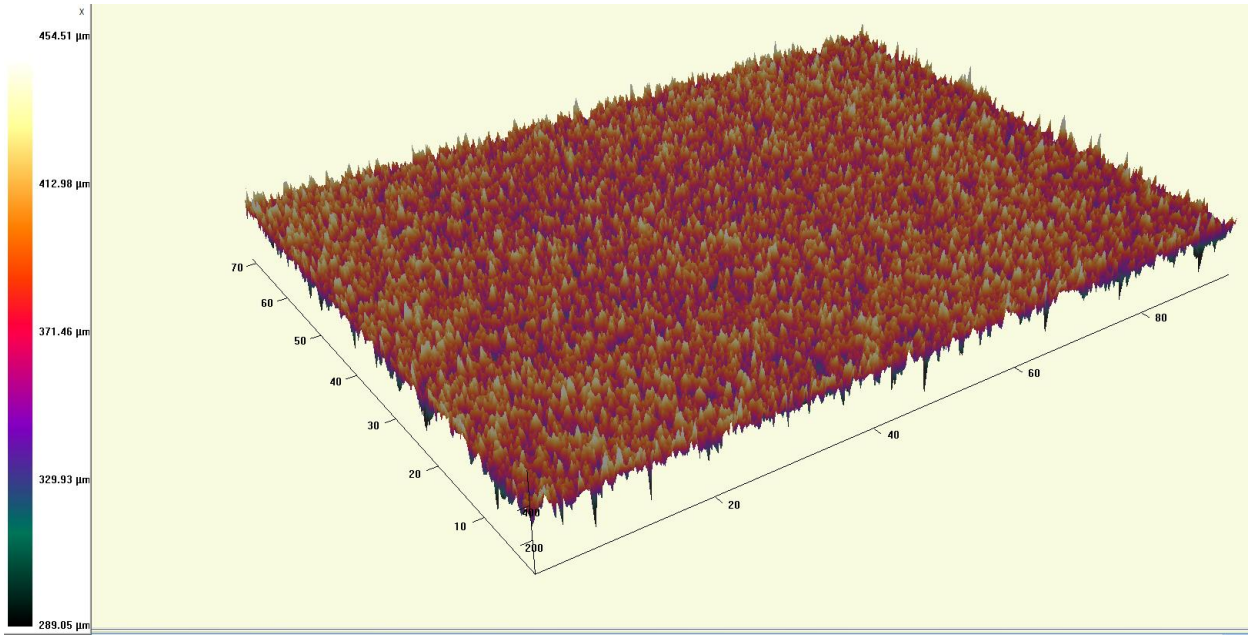

Fig. 4.42 Surface Roughness of PDMS/PS

4.3.3.4 UV-Visible Spectroscopy

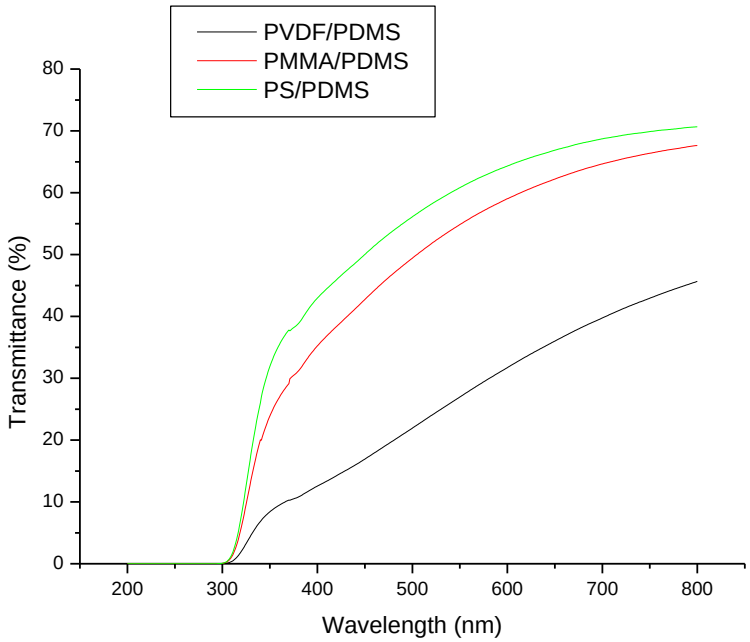

Fig. 4.43 UV-Visible spectrum of PDMS/PVDF, PDMS/PMMA and PDMS/PS

The UV-Visible spectrum for PDMS/PVDF, PDMS/PMMA and PDMS/PS has been plotted in **Fig.4.43**. The reduction in % of transmittance and increase in CA with high thickness was observed. This maybe due to the rougher surface morphological structure, which acted as light scattering centres, and hence results in reduced transparency **[Hui Liu et al.,2017]**. PVDF/PDMS composite has the lowest transparency percentage with higher contact angle. The transmittance values of PDMS/PMMA and PDMS/PS lies in the range between 30% to 70% whereas in the case of PDMS/PVDF, transmittance percentage drops below 40%.

4.3.3.5 FESEM

The surface morphology of the prepared composite films is shown in the **Figs.4.44, 4.45 and 4.46.** PDMS/PVDF SEM image shown in **Fig.4.44** has sphere formation with the average particle size of 804 nm. PDMS/PMMA **(Fig.4.45)** shows more rougher surface than PDMS/PS which exhibited average particle size of 745nm and this may be attributed to higher contact angle of 153° for PMMA/PDMS. In all the three composite films, the crystallite/sphere formation is due to the presence of PDMS. **Figs.4.47 (a), (b) and (c)** represents the histogram for PVDF/PDMS, PMMA/PDMS & PS/PDMS obtained from 3D Zeta profilometry between the z-steps of 700µm to 1300µm. The average particle size lies between 150nm to 580nm.

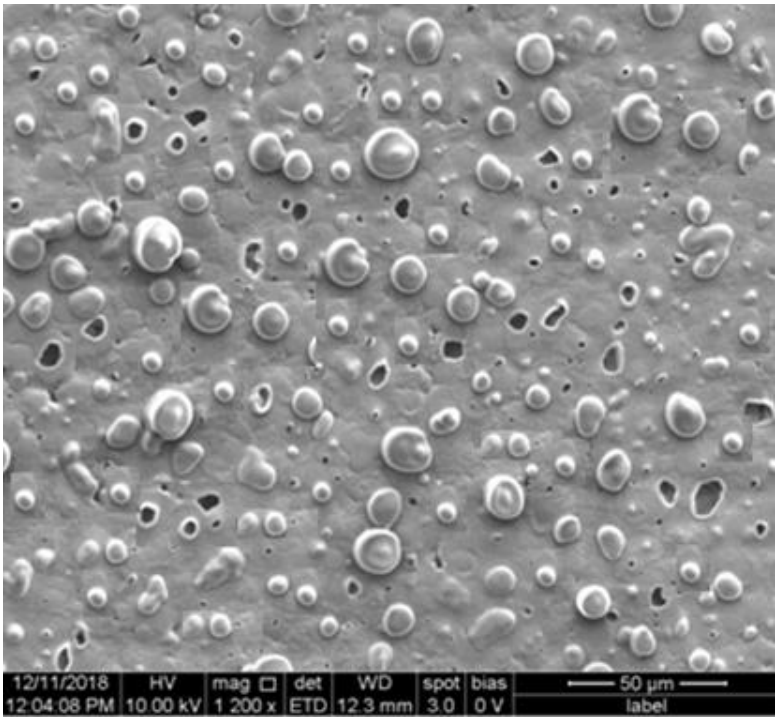

Fig. 4.44 FE-SEM OF PDMS/PVDF

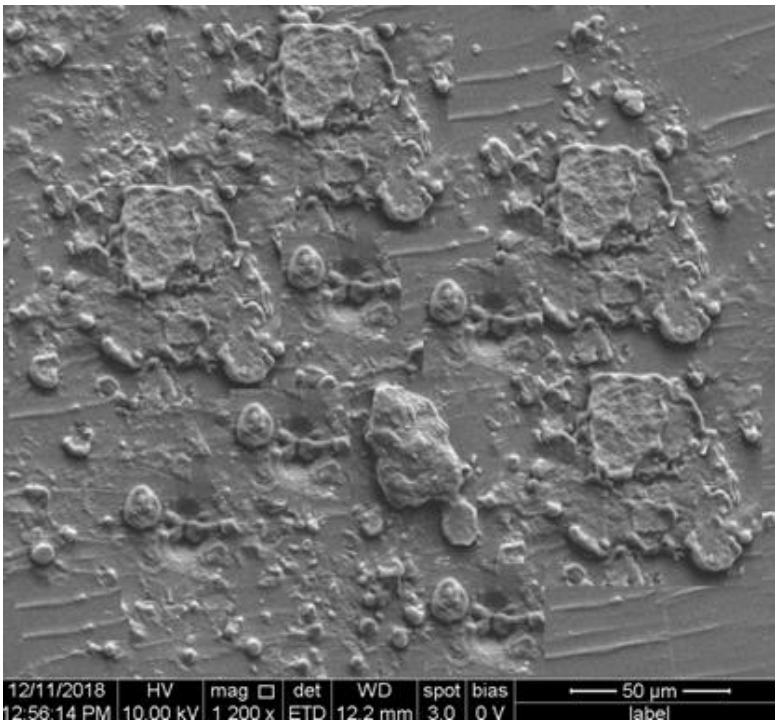

Fig. 4.45 FE-SEM of PDMS/PMMA

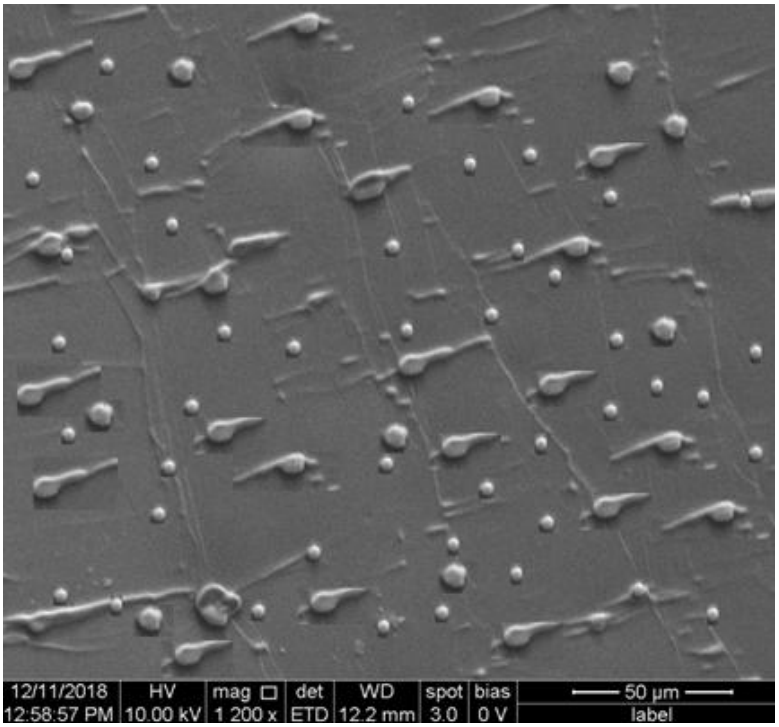

Fig. 4.46 FE-SEM of PDMS/PS

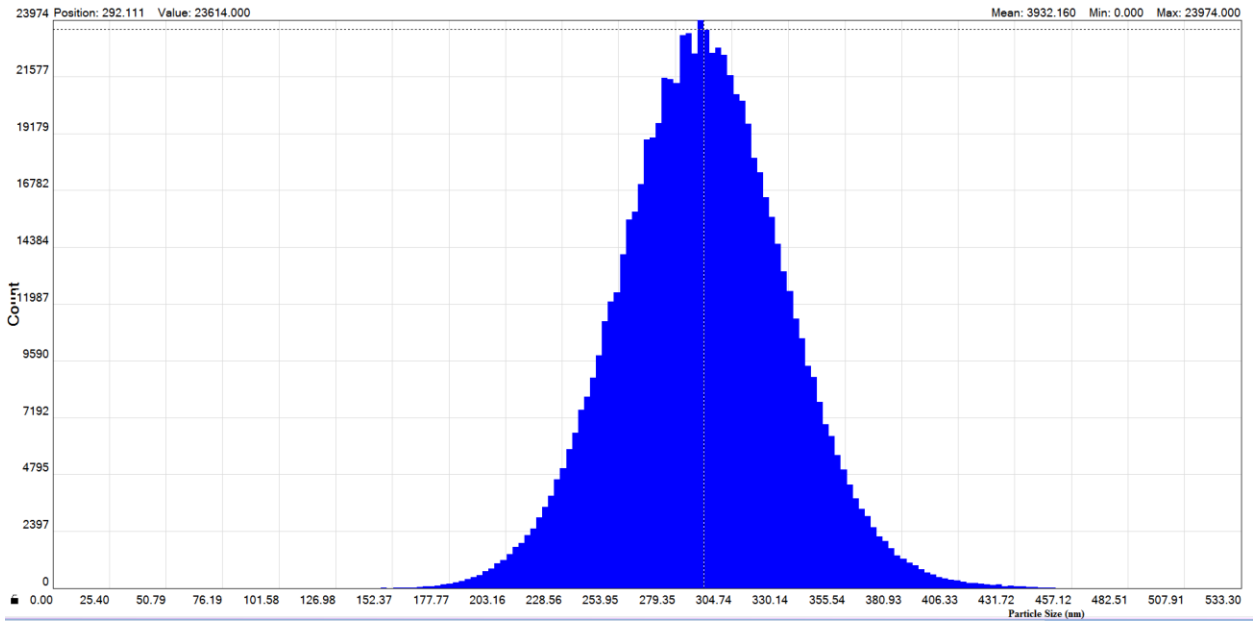

Fig. 4.47 (a) Histogram of PDMS/PVDF

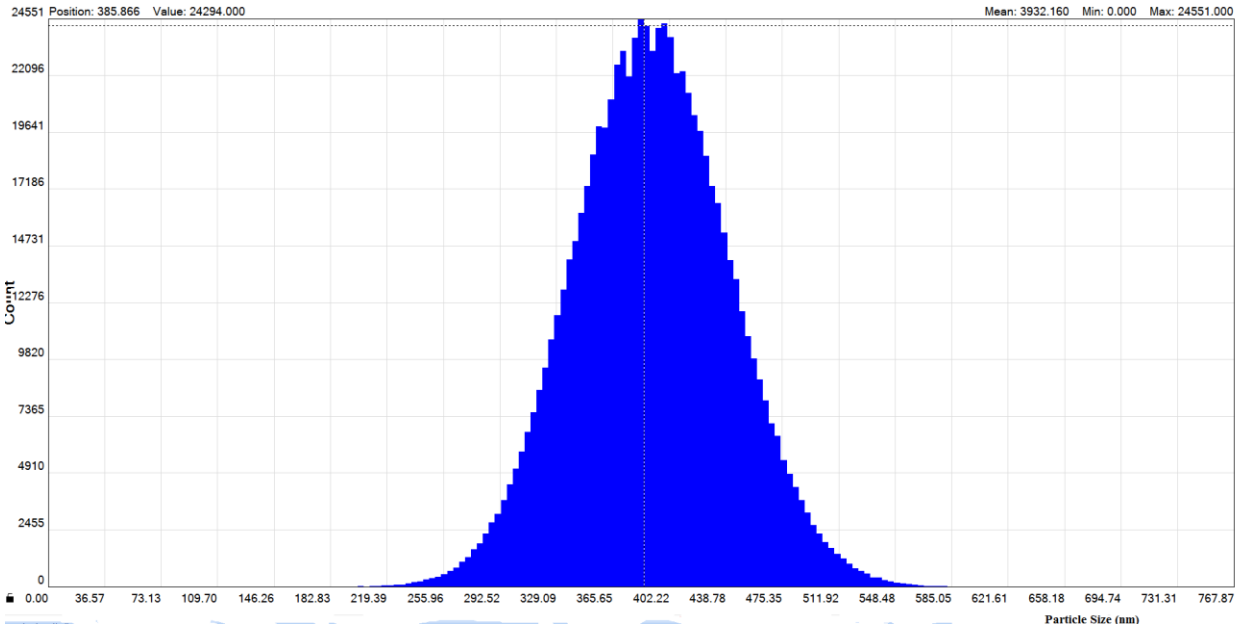

Fig. 4.47 (b) Histogram of PDMS/PMMA

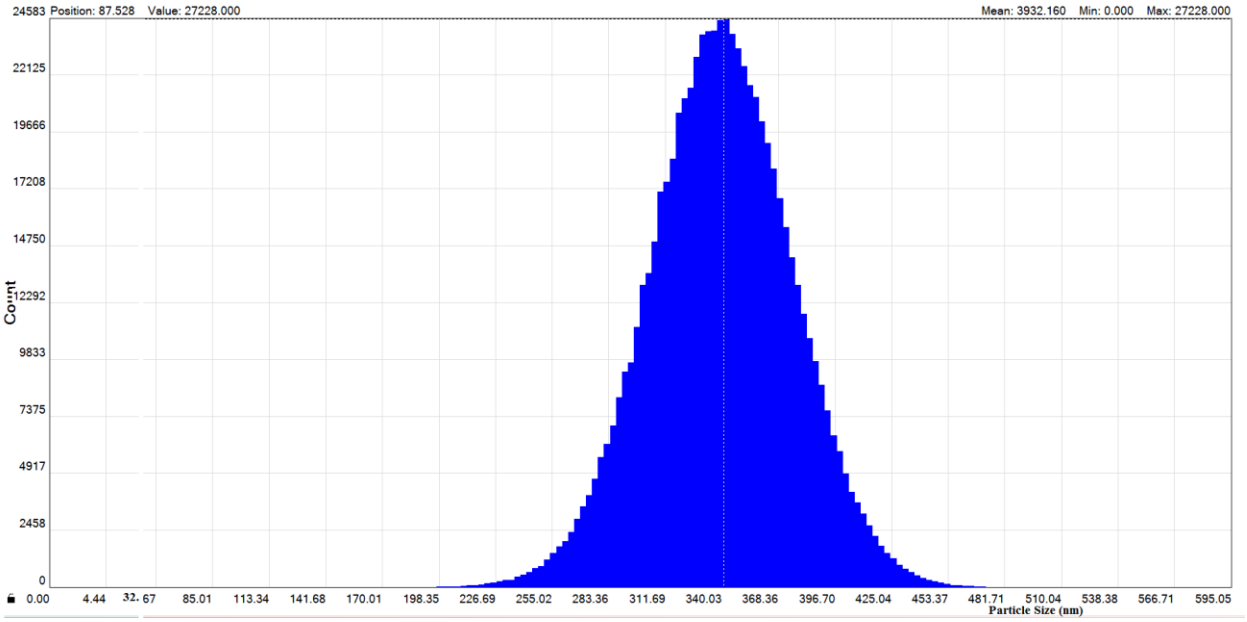

Fig. 4.47(c) Histogram of PDMS/PS

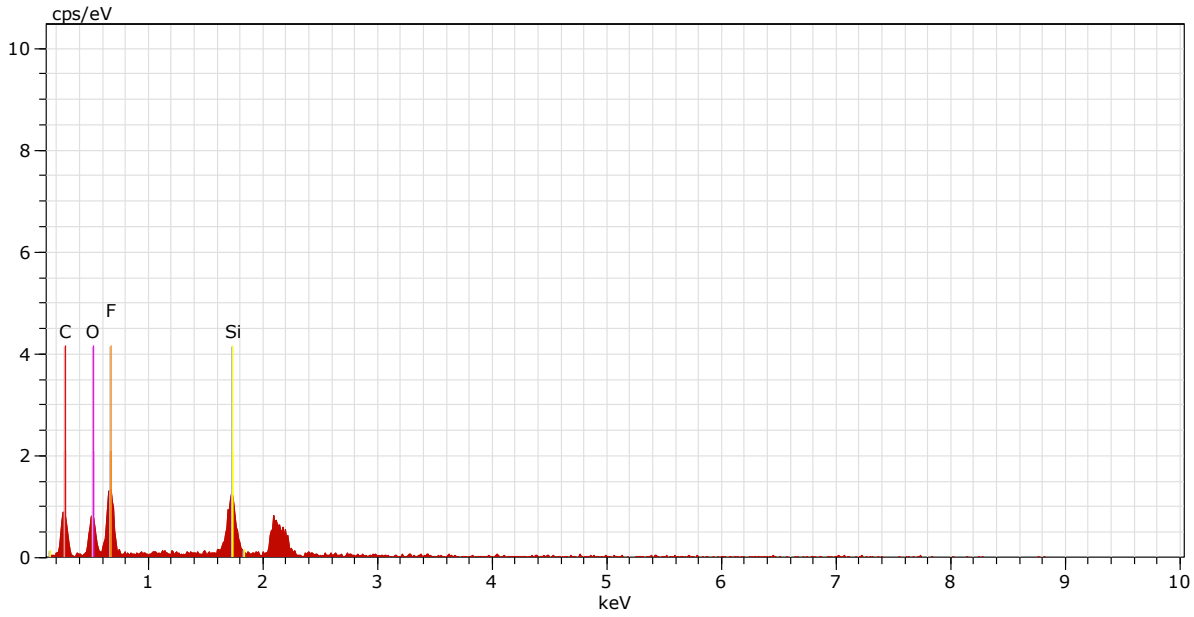

Fig. 4.48 EDX of PDMS/PVDF

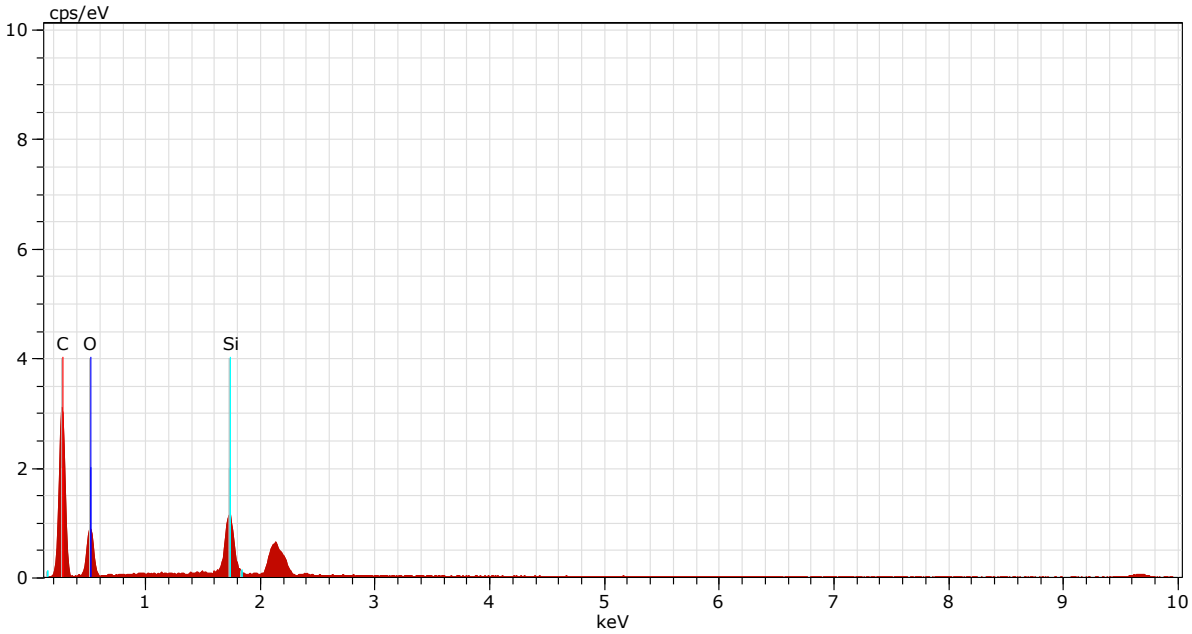

Fig.4.49 EDX of PDMS/PMMA

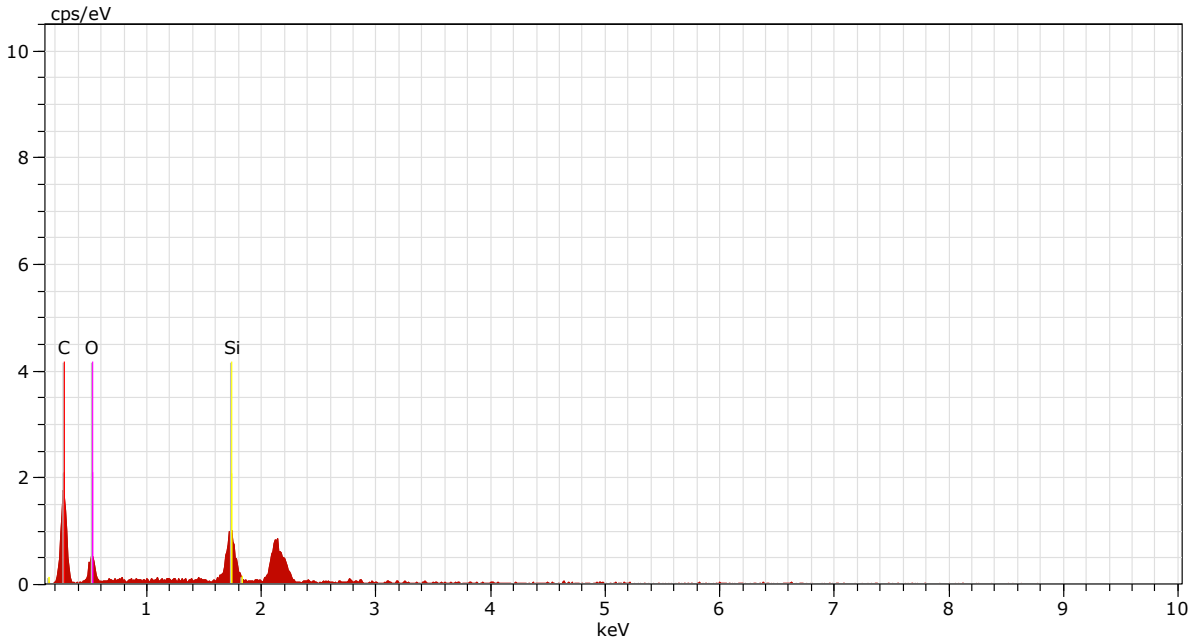

Fig. 4.50 EDX of PDMS/PS

The surface chemical analyzes was carried out with EDX and observed the following elements Carbon (C), Oxygen(O), and Silica (Si) for PDMS/PMMA as

well as for PDMS/PS and in addition Fluorine (F) of 17.5 % was obtained for PDMS/PVDF film. The atomic weight percentage for the composite films are tabulated in **table 4.6**. This proves that the composite films were dirt and impurity-free.

Table 4.6. Elemental composition obtained from EDX

Sample	Atomic Weight (%)			
	C	O	Si	F
PDMS/PVDF	43.06	19.84	10.31	26.79
PDMS/PMMA	72.76	20.86	6.38	-
PDMS/PS	72.70	18.57	8.73	-

4.3.3.6 TG-DTA

In **Fig.4.51**, thermal analysis of PDMS/PVDF was shown. Due to solvent evaporation, there is a initial weight loss at 65°C. Single stage decomposition is seen. Major weight loss was observed in the range 400-500ºC for the prepared sample which is due to the structural decomposition of the polymer and its complexes. The sample is stable upto 450ºC. A sharp and large exothermic peak was noted at 490 ºC concurrent with an appreciable weight loss of about 70.23% and this indicate the complex decomposition of the film, which is in agreement with the TG curve. **[K Naveen Kumar et al., 2012].**

TG-DTA for PDMS/PMMA and PDMS/PS was plotted in the **Figs.4.51 and 4.52**, treated thermally at 500°C with the heating rate of 10°C/min. There is no weight loss upto 160°C. Beyond 210°C, there is a weight loss of 4.127%.There is no residual material formation upto 360°C. This behaviour also

indicates the random chain scission process of that occurs during polymer degradation **[Nidal Wanis Elshereksi et al., 2014]**. From the DTA curve, a sharp exothermic peak is observed at 430°C representing the combustion of the silane. The TGA curve of PDMS/PS shows that there is no weight loss upto 140°C. 21.37% of weight loss is seen between 270°C and 330°C which is due to the adsorbed water. There is a drastic weight loss of 67.82% beyond 450°C due to the decomposition of the material. An exothermic peak centered at 390°C observed in DTA curve maybe attributed to the combustion of the silane.

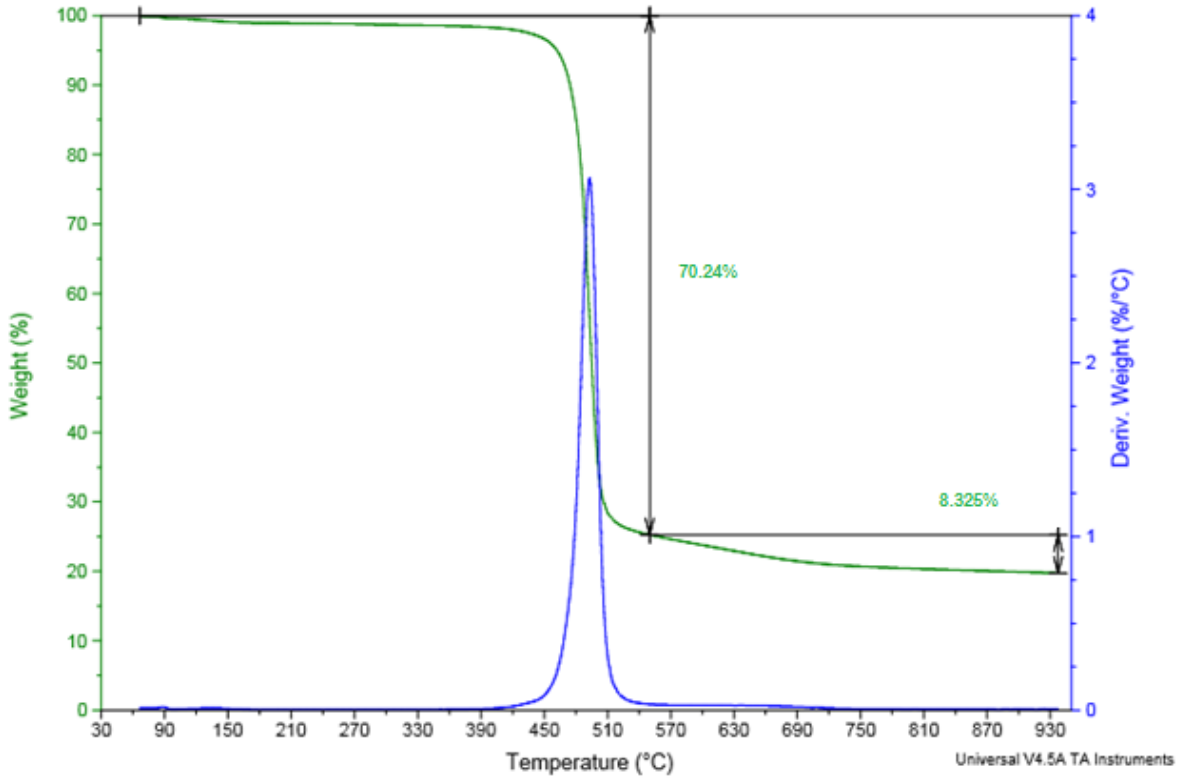

Fig.4.51 TG-DTA for PDMS/PVDF

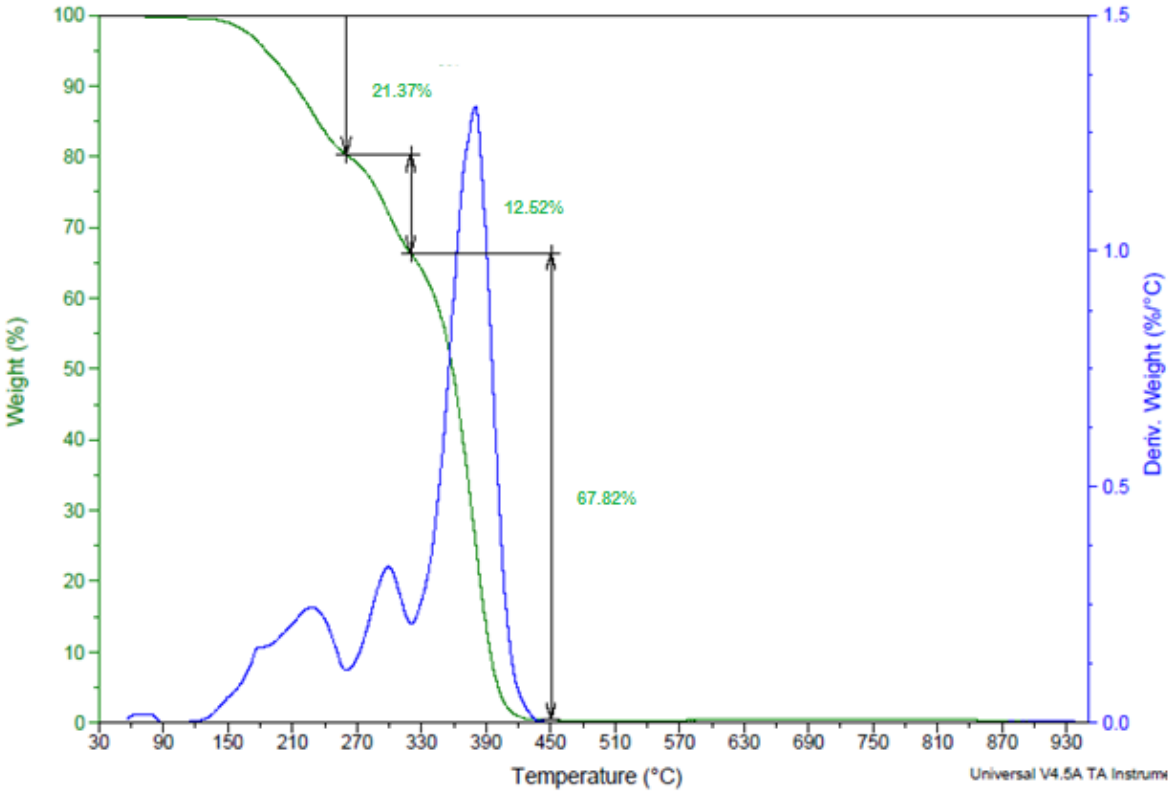

Fig.4.52 TG-DTA for PDMS/PMMA

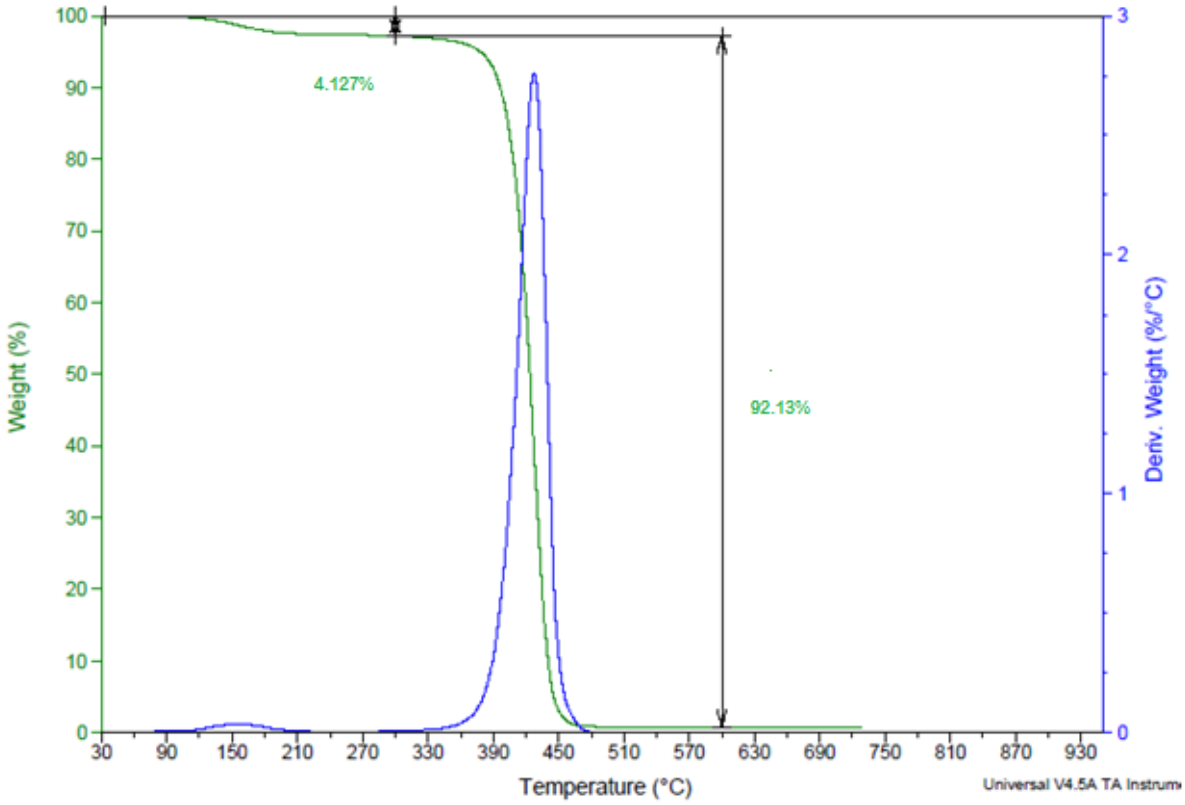

Fig.4.53 TG-DTA for PDMS/PS

4.3.3.7 Application

Polymer-PDMS coated glass substrates were shown in the **Fig.4.54 (a), (b) and (c)**. The glass substrates were coated and tested for self-cleaning. 3 gram of dust particles were kept on the coated substrate. 4µl of water made surface dirt-free. The dust particles clinged to the water droplet. The prepared solution were coated on filter paper and tested for oil-water separation. 10 ml of oil (Kerosene) and 30ml of water were mixed and allowed to filter through the coated filter paper as shown in the **Fig. 4.55**. It was found that water get separated and the oil remained back. PMMA/PDMS coated filter paper filtered about 25.5ml of water as shown in the **Fig.4.55**.

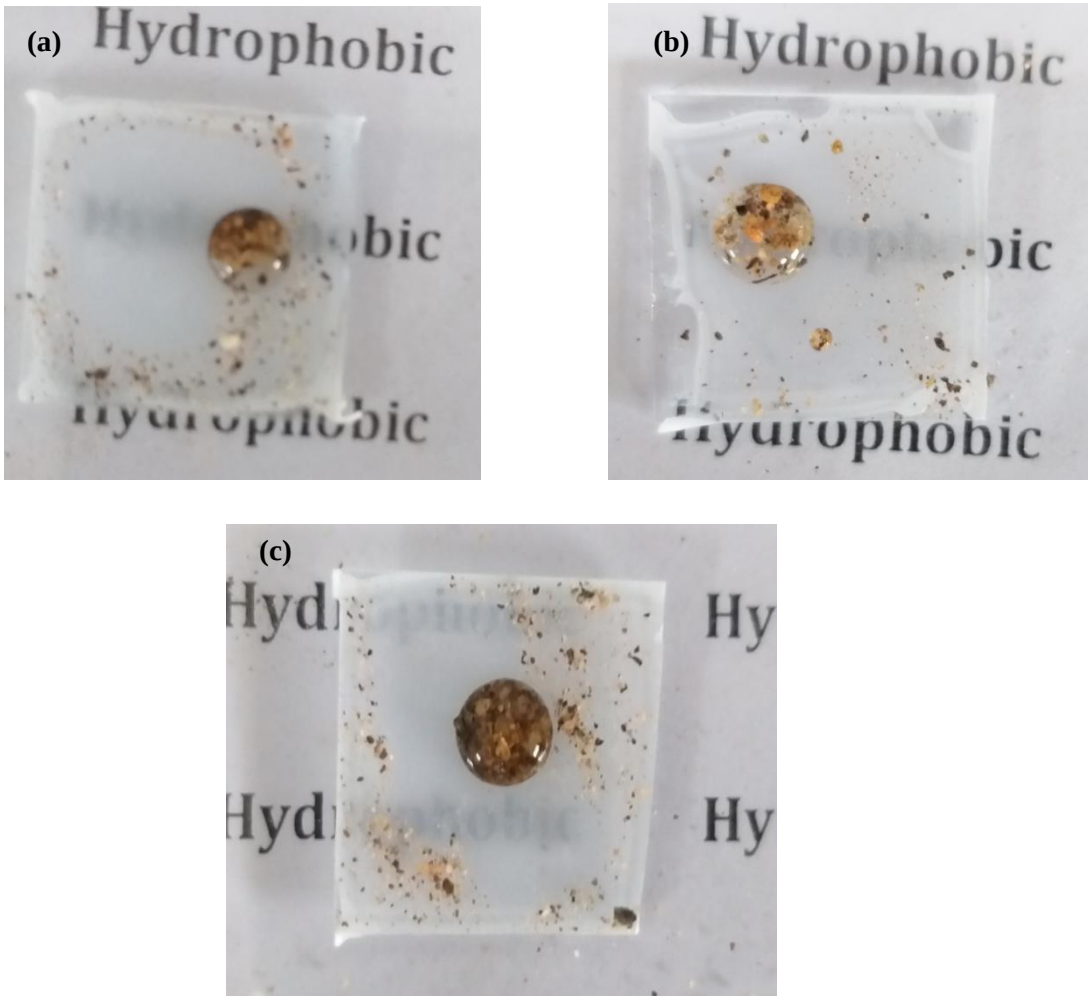

Fig. 4.54 (a) PDMS/PVDF, (b) PDMS/PMMA and (c) PDMS/PS coated subtrates showing Self cleaning property.

Step- I

(Mixture of Kerosene oil& Water)

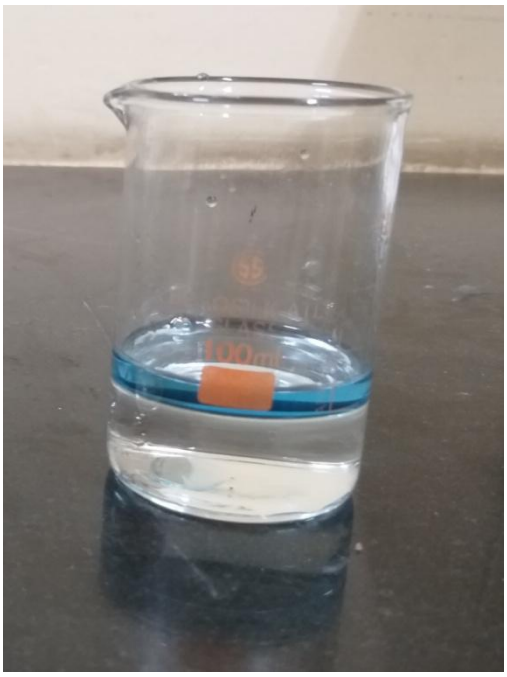

Step- II

(a) PVDF/PDMS

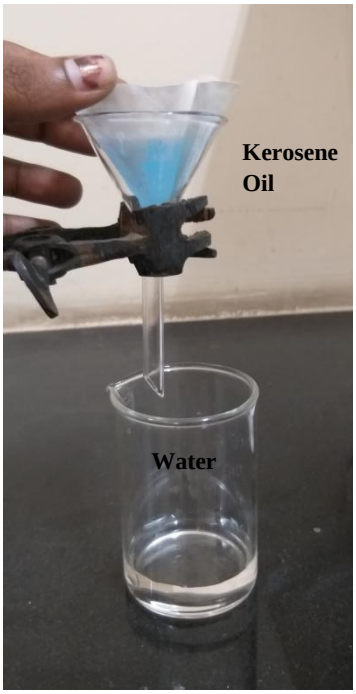

(b) PMMA/PDMS

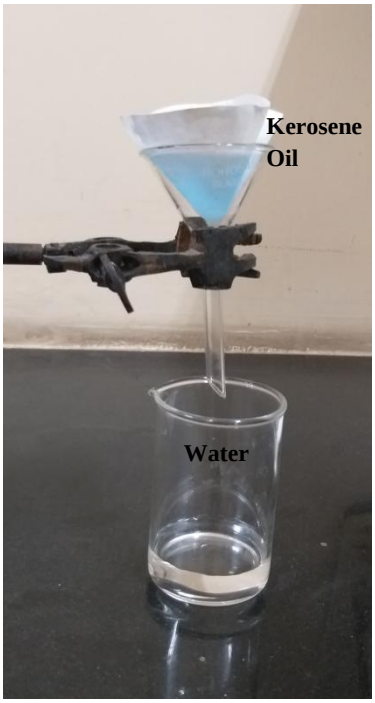

(c) PS/PDMS

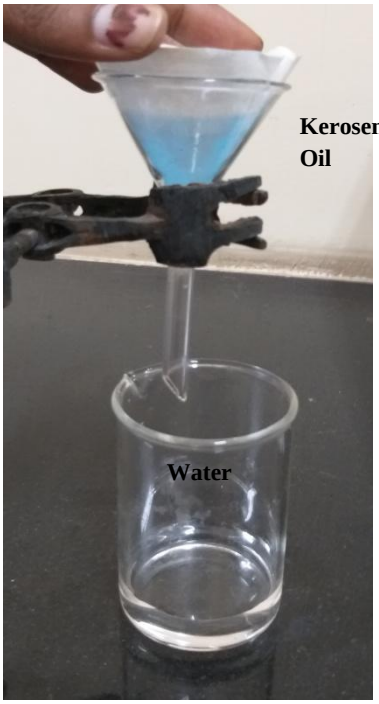

Step- III

Filtered Water

Fig. 4.55 Step I-III shows the oil-water separation

4.3.4 SET – IV [TEOS + MTMS + Polymer]

4.3.4.1 FTIR

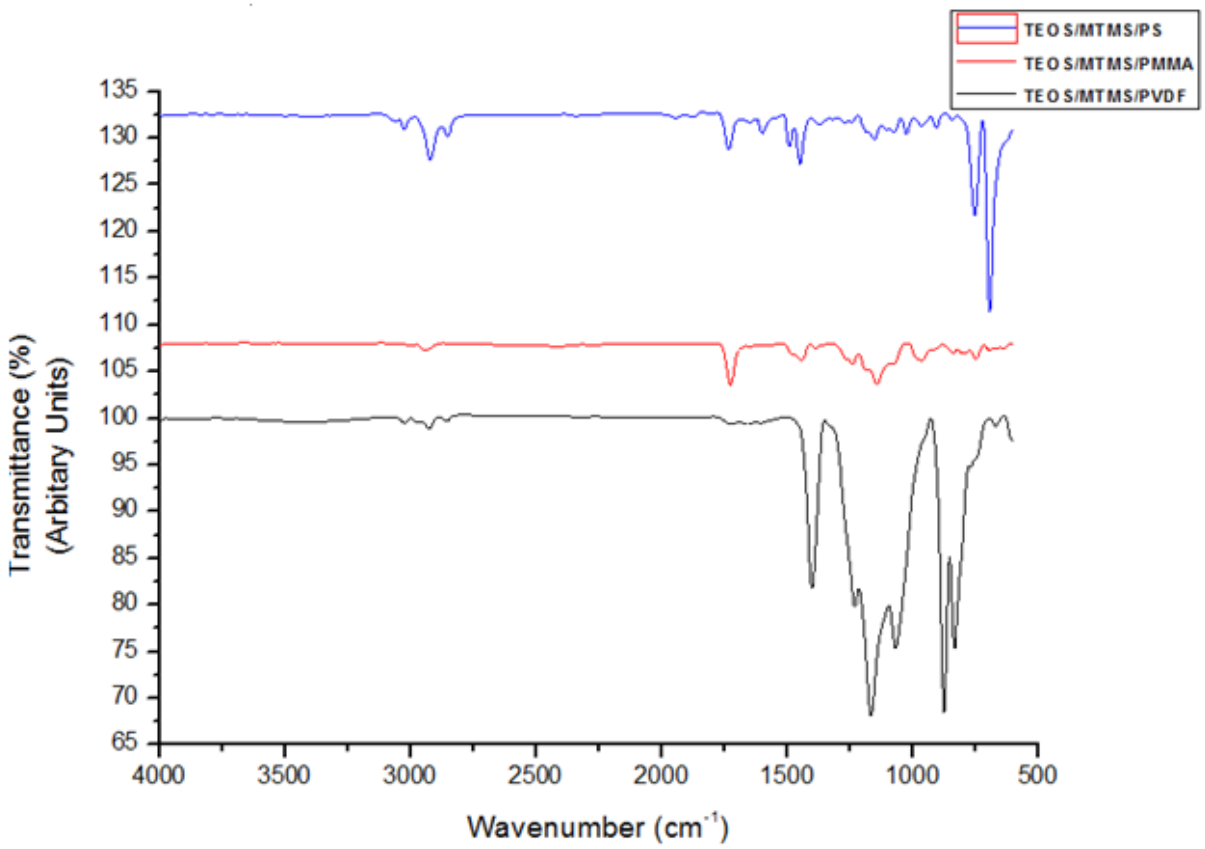

Fig.4.56 FTIR Spectrum of TEOS/MTMS/PVDF, TEOS/MTMS/PMMA and TEOS/MTMS/PS

The functional groups have been determined with FTIR spectroscopy. The spectrum of TEOS/MTMS with PVDF,PMMA and PS were shown in the **Fig.4.56**. The peak at 767 cm^{-1} and 832 cm^{-1} refers to the non-polar α-phase and ϒ-phase of PVDF seen in TEOS/MTMS/PVDF film **[Vimal K. Tiwari, et al.,2018]**. The peak at 1400 cm^{-1} and 1165 cm^{-1} shows CH_2 and CF_2 stretching vibration **[Hossein Mahdavi et al., 2017].** With the presence of silane , Si-O-Si stretching has been deformed to linear structure. Beyond, 3000 cm^{-1} , absence of polar

bond is observed. The absorption peak at 1145 cm^{-1} represents Si-O-Si group and the peak at 1386 cm^{-1} shows O-CH_3 deformation of PMMA **[Mas Rosemal et al.,2010 and Seenaa Ibrahem et al.,2014].** The peak at 1725cm^{-1} assigns to the C=O stretching bond **[Ying Ma et al., 2007 and Mas Rosemal et al., 2010].** Due to condensation two peaks were obtained at 2949 cm^{-1} and 2992 cm^{-1} which can be attributed to C-H symmetric and asymmetric stretching **[Marielen Longhi et al., 2015].** The weak absorption peaks at 1440cm^{-1} and 2947 cm^{-1} were due to the stretching and bending modes of C-H bonds **[D.B.Mahadik et al., 2016].** In this scenario, a small or negligible peak is obtained at 3433 cm^{-1} and 3735 cm^{-1} representing the absence of polar bond, which proves that the composite film is hydrophobic. **[Mahendra S.Kavale et al., 2011 and Satish A. Mahadik et al.,2013]**.

TEOS/MTMS/PS spectrum is shown in the **Fig.4.56**. The sharp peak at 692cm^{-1} represents the PS templates, and the presence of phenyl group is shown between 692cm^{-1} to 1596 cm^{-1} [**Xin Fan et al., 2012**]. The peak at 1105 cm^{-1} confirms the Si-OH group. The weak absorption peaks at 1447cm^{-1} and 2920 cm^{-1} may be due to the stretching and bending modes of C-H bonds [**Mas Rosemal et al., 2010**]. Si-O-Si stretching of the silane group is observed at 921 cm^{-1} and 1151 cm^{-1}[**Violeta Purcar et al., 2012 and Seenaa Ibraheem et al., 2014**].

4.3.4.2 Contact Angle

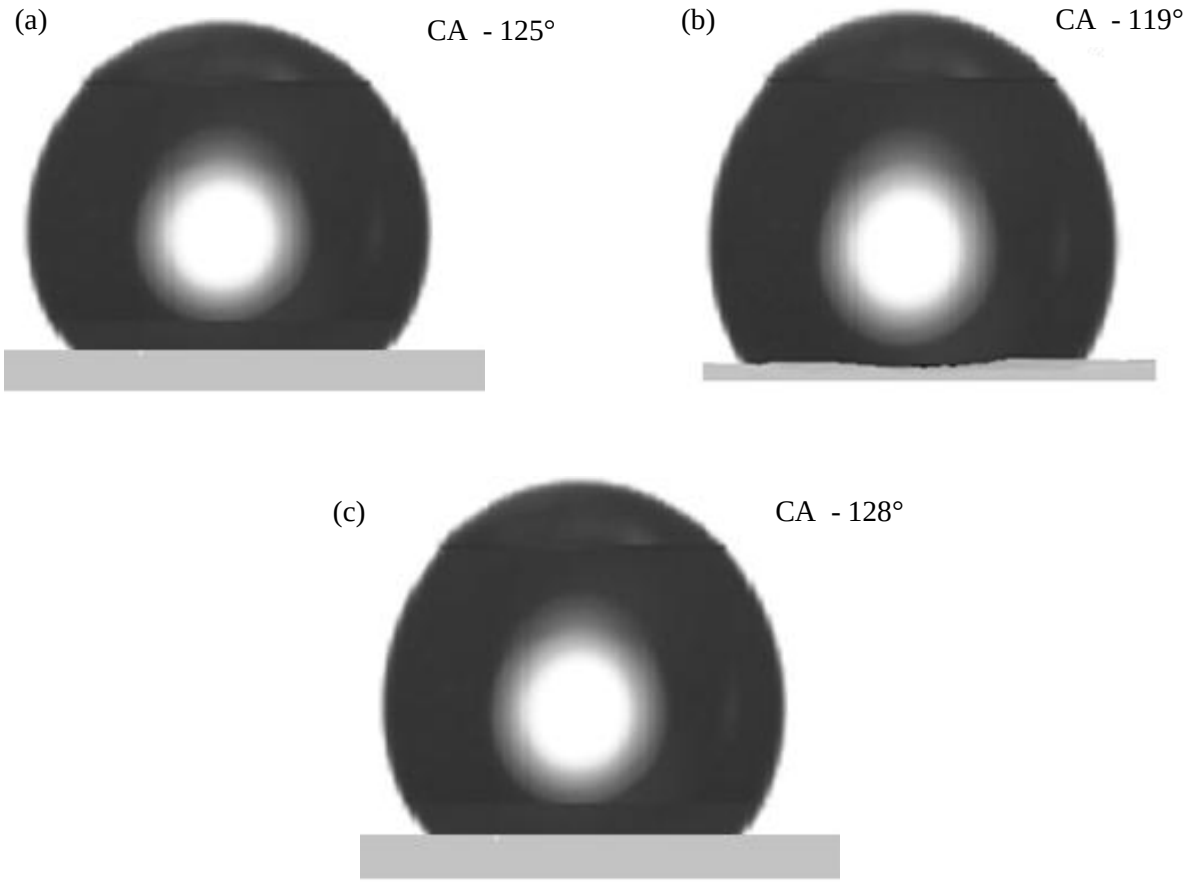

Fig. 4.57 Contact Angle of (a)TEOS/MTMS/PVDF, (b)TEOS/MTMS/PMMA and (c)TEOS/MTMS/PS

With the measured contact angle, the surface energy can be calculated as both are related to the young's equation. **Fig. 4.57 (a), (b) and (c)** shows the contact angle of TEOS/MTMS with PVDF, PMMA and PS with the CA measurement of 125°, 119° and 128°. TEOS/MTMS/PS shows higher contact angle.

4.3.4.3 Surface Roughness and Surface Energy

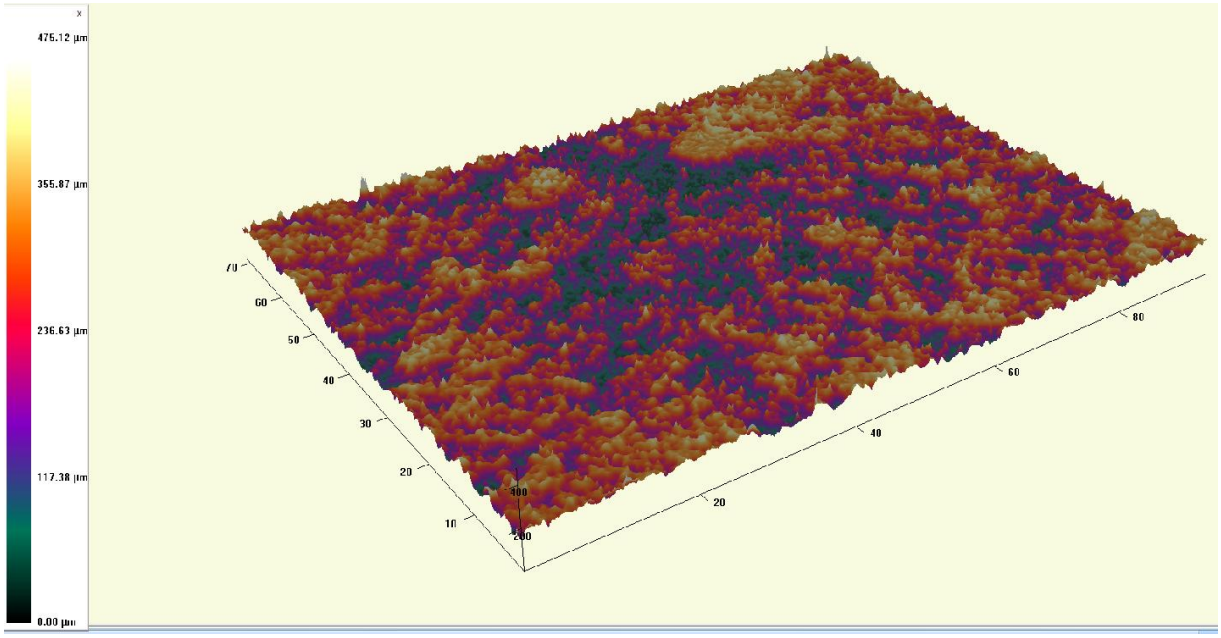

Fig. 4.58 Surface Roughness of TEOS/MTMS/PVDF

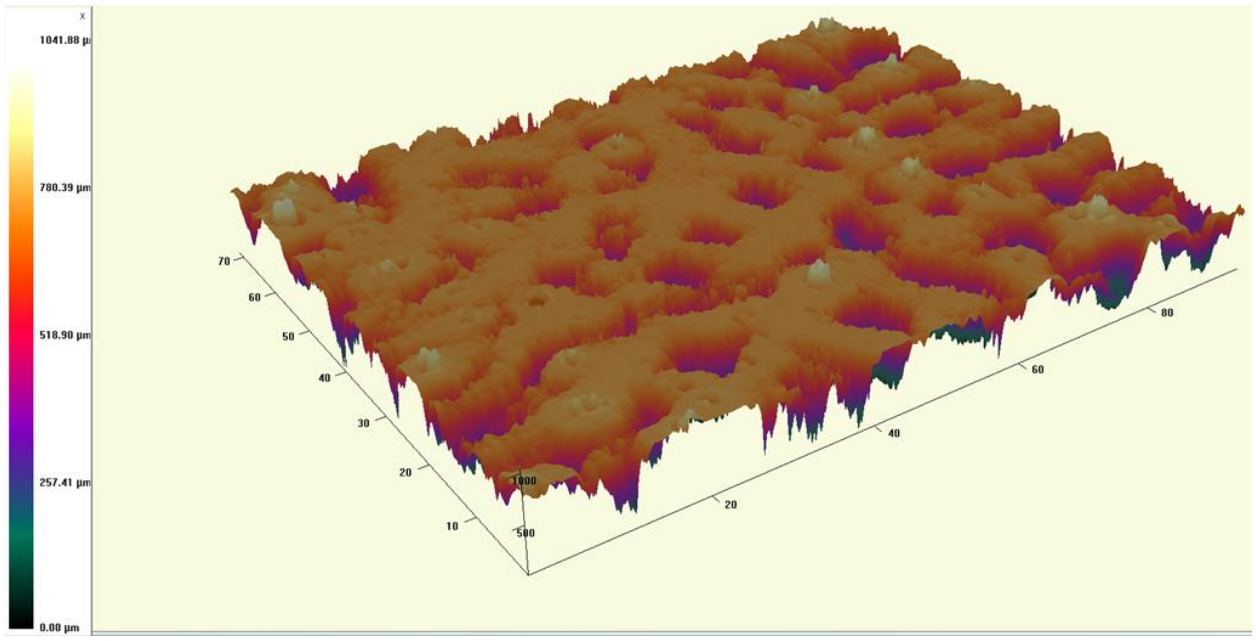

Fig.4.59 Surface Roughness of TEOS/MTMS/PMMA

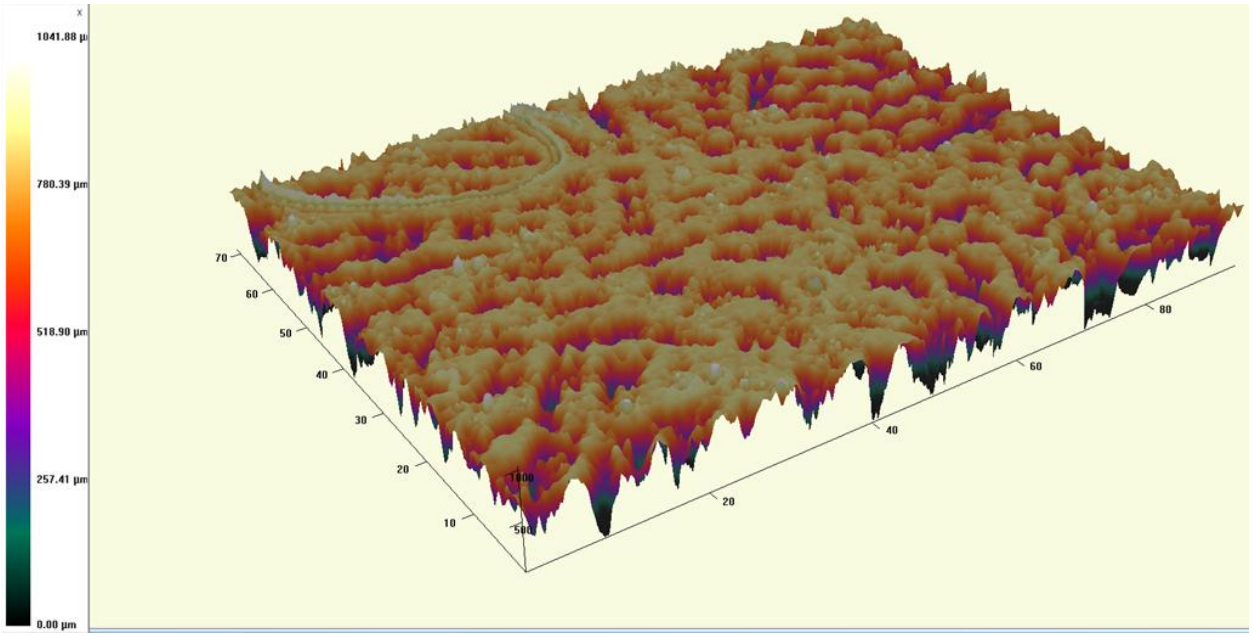

Fig. 4.60 Surface Roughness of TEOS/MTMS/PS

The Surface roughness of TEOS/MTMS/Polymer have been shown in the **Fig. 4.58,4.59 and 4.60.** TEOS/MTMS/PS has higher surface roughness with the peak height (Rp) ranging between 147.11 µm to 336.00 µm. Higher the surface roughness, higher will be the contact angle with reduction in surface energy.

The phenomenon caused by intermolecular interactions at an interface states the surface energy, which can be dispersive force, energetically homogeneous or heterogeneous interactions and bondings [**Soo-Jin Park et al., 2011**]. In case of polymers, such surface energy can be measured by indirect methods based on wettability. The attraction between two uncharged macroscopic surfaces across air or water can be explained with Lifshitz theory of Van der Waals interaction [**Calcum J. Drummond et al., 1997**]. The surface energy/surface tension can be calculated once the Hamaker constant (A_H) / (A_n) is known as discussed earlier

by [**J.Vial et al.,**]. The computed surface energy values are tabulated in **table.4.7**

Table.4.7 - Surface Roughness and Thickness Measurement of the coated films

Sample	Hamaker Constant A_n (J x 10^{-21})	Surface Roughness, Ra (μm)	Surface energy, Ɣ (Jm^{-1})	Contact Angle, CA (°)	Thickness (μm)
TEOS/MTMS/PS	1.962	59.96	18.57	128°	15.8
TEOS/MTMS/PVDF	2.086	57.64	17.49	125°	14.2
TEOS/MTMS/PMMA	1.524	44.37	21.4	119°	13.2

4.3.4.4 UV-Visible Spectroscopy

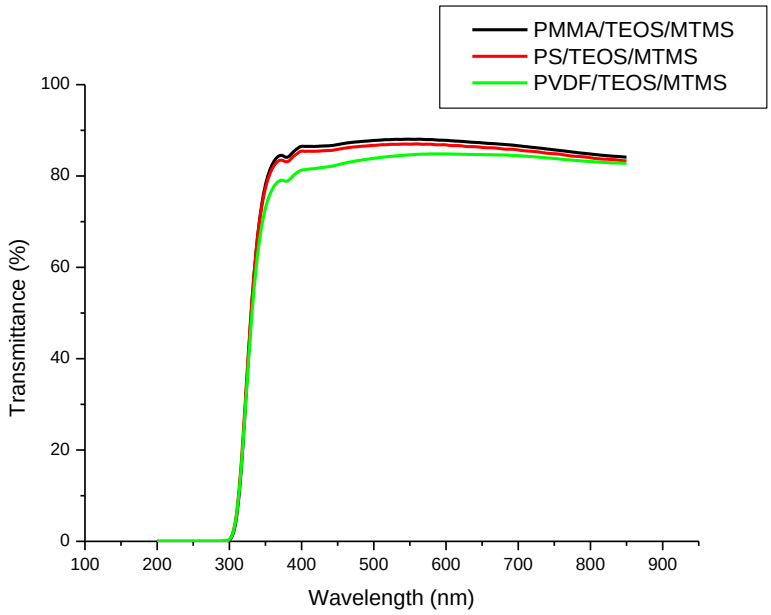

Fig. 4.61 UV-Visible Spectrum of TEOS/MTMS/PVDF, TEOS/MTMS/PMMA and TEOS/MTMS/PS

The UV-Visible spectra for TEOS/MTMS/PVDF, TEOS/MTMS/PMMA and TEOS/MTMS/PS is shown in **Fig. 4.61**. Cut-off wavelength of TEOS/MTMS/PVDF is at 381 nm, and has 80% transmittance. The cut-off wavelength for TEOS/MTMS/PMMA is 379 nm , with the transmittance of 85 % and for TEOS/MTMS/PS is 374nm and effective high transmittance of 84%. For the polymer solutions mixed with silanes (TEOS/MTMS), the transmittance percentage is higher than 80, in the entire visible-region and hence can be used in the self cleaning application for Solar panels and window screens.

4.3.4.5 FESEM

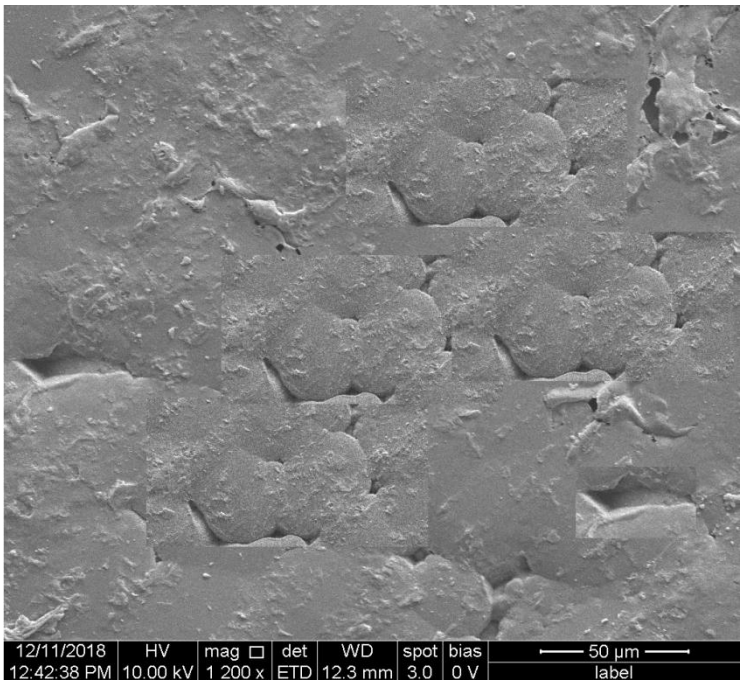

Fig. 4.62 FE-SEM of TEOS/MTMS/PVDF

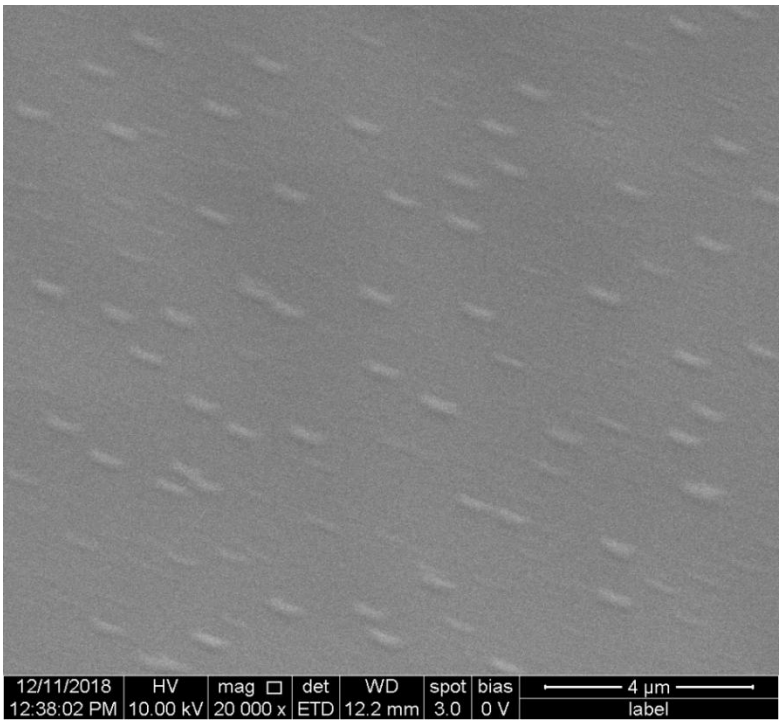

Fig. 4.63 FE-SEM of TEOS/MTMS/PMMA

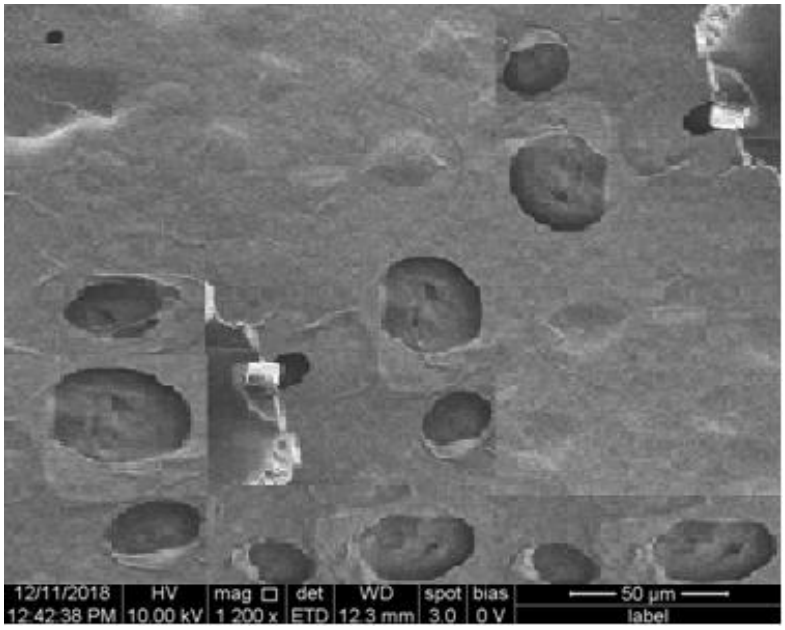

Fig.4.64 FE-SEM of TEOS/MTMS/PS

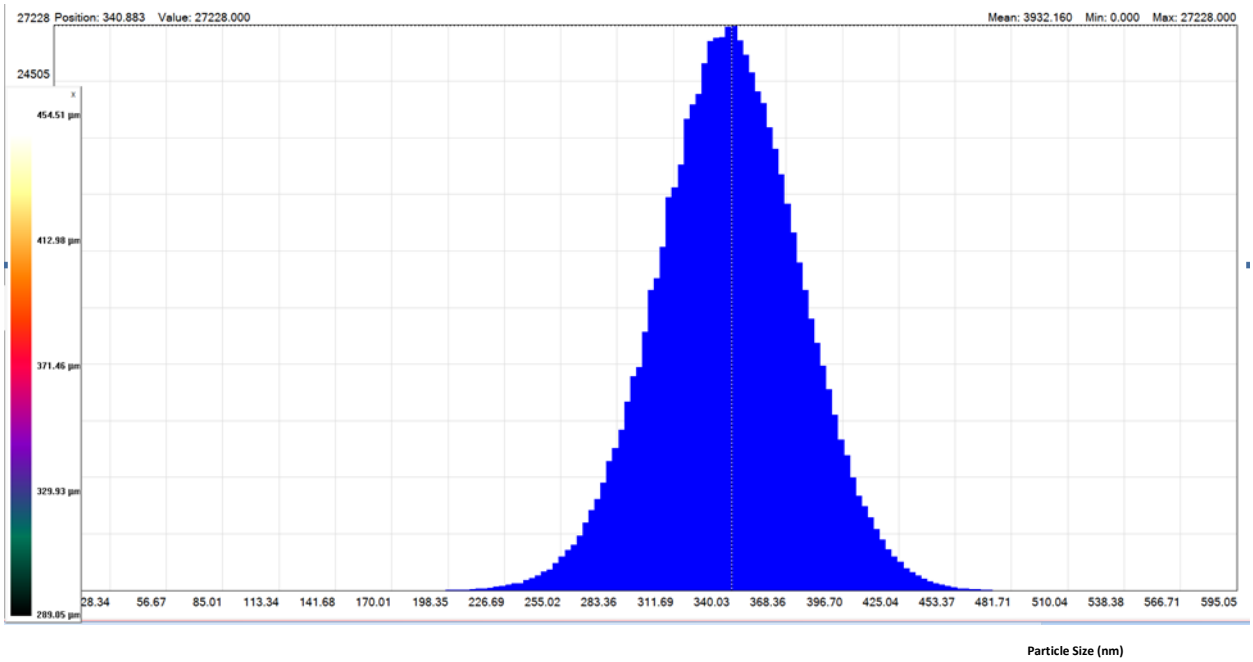

Fig. 4.65 Histogram of TEOS/MTMS/PVDF

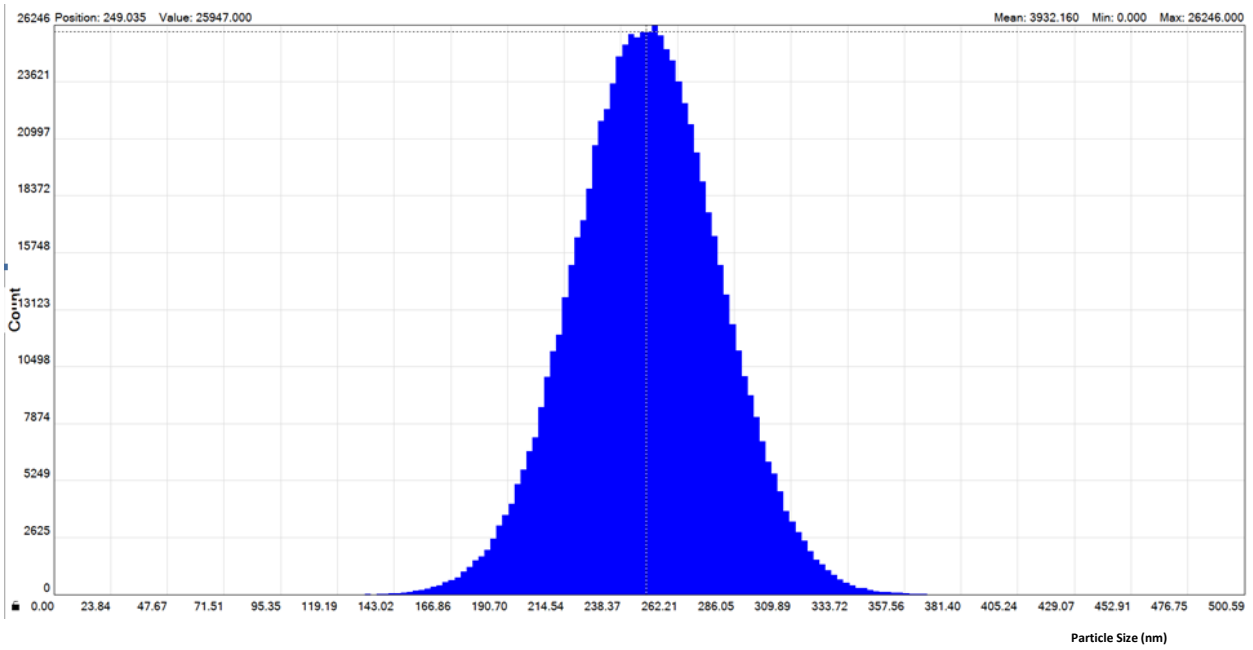

Fig.4.66 Histogram of TEOS/MTMS/PMMA

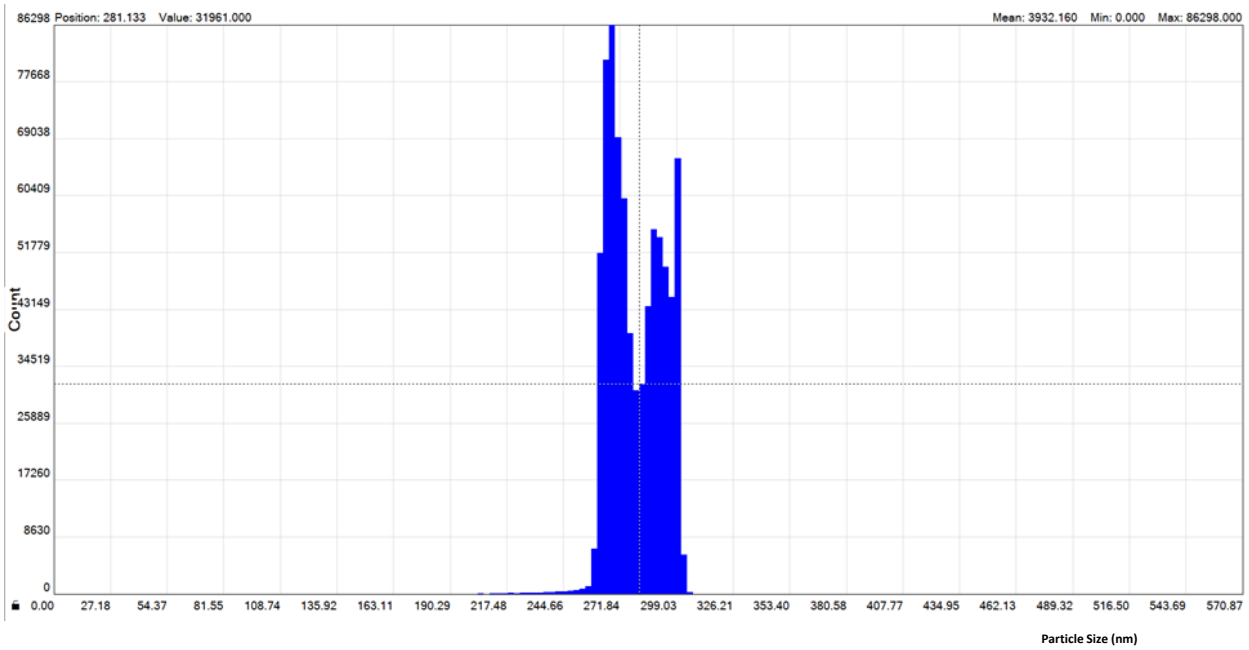

Fig.4.67 Histogram of TEOS/MTMS/PS

The morphology of the composite films were identified with FE-SEM. TEOS/MTMS/PVDF morphology is shown in the **Fig.4.62**, which implements rough surface. **Fig.4.63** represents the morphology of Silanes/PMMA. The surface is found to be smoother with spherical crystallites scattered, confirming the silanes composited with the acrylic polymer (PMMA) with the particle size of 283nm as explained by [**Chandan Kumar et al.,**]. Such surface formation hold good for hydrophobicity. The morphology of Silanes with Polystyrene film is shown in **Fig.4.64**. Unoccupied voids were formed, with noted particle size of 345nm and due to these voids, % of transmittance for PS is also closer to PMMA. Histogram of TEOS/MTMS/Polymer is shown in the **Fig.4.65, 4.66 and 4.67** between the z-steps of 800µm to 1450µm.

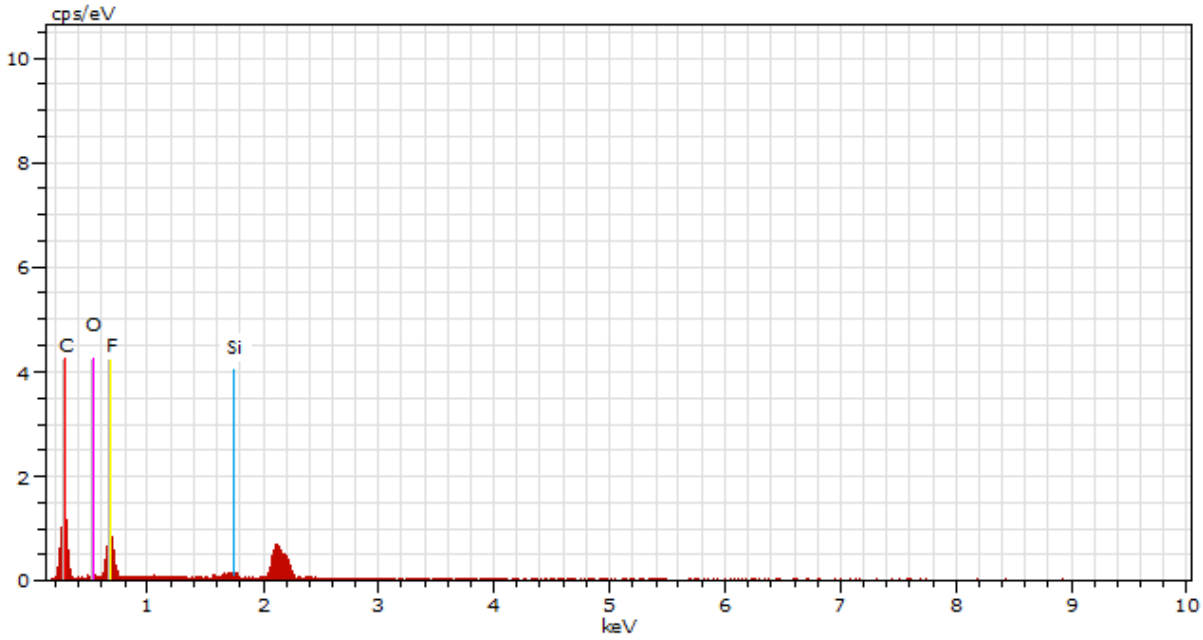

Fig. 4.68 EDX of TEOS/MTMS/PVDF

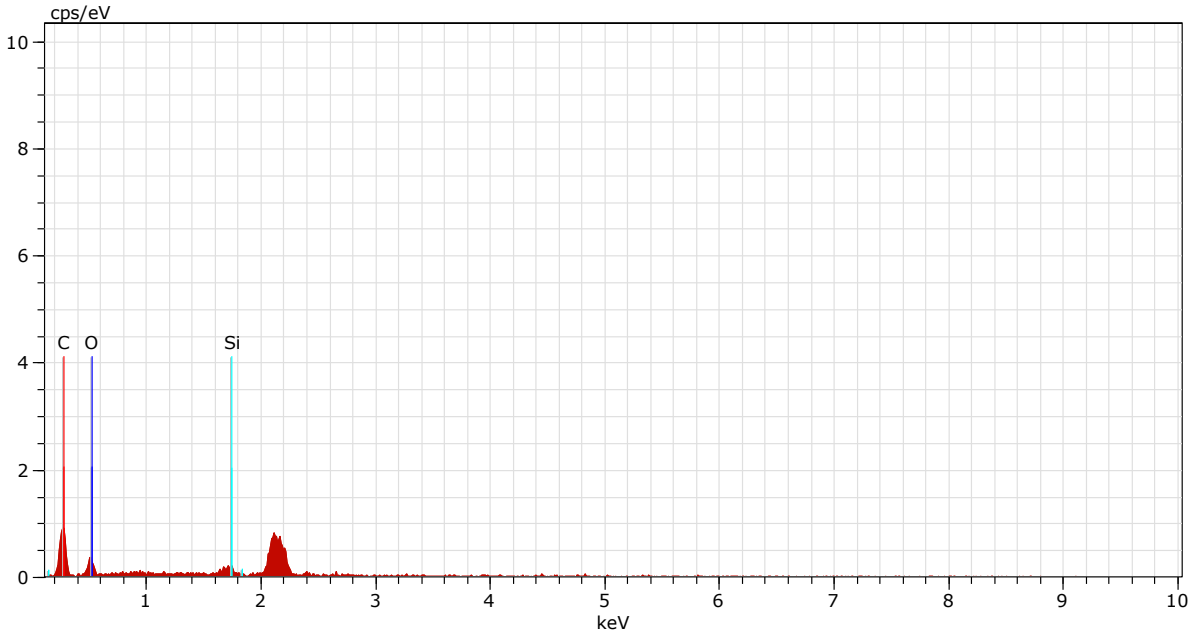

Fig. 4.69 EDX of TEOS/MTMS/PMMA

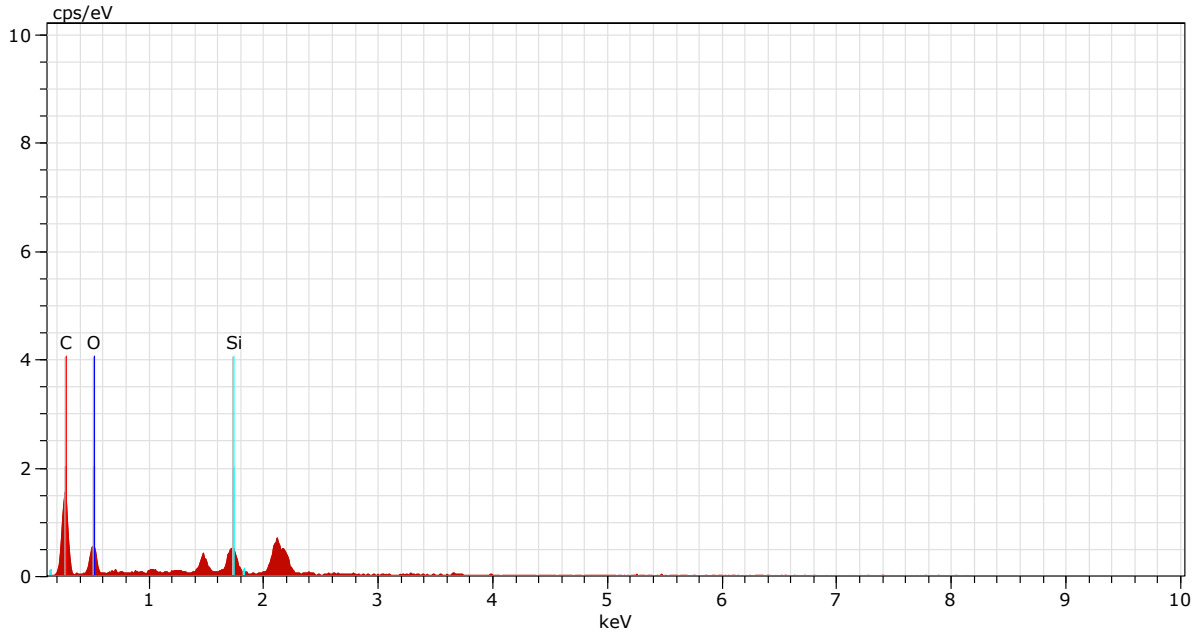

Fig. 4.70 EDX of TEOS/MTMS/PS

With EDX, **(Fig.4.68,4.69 & 4.70)** the surface chemical analyzes was carried out and observed the following elements Carbon (C), Oxygen(O), and Silica (Si) presence for TEOS/MTMS/PMMA as well as for TEOS/MTMS/PS. TEOS/MTMS/PVDF has all the above mentioned elements including Fluorine (F). The atomic weight percentage for the composite films are tabulated in **Table.4.8** .The spin-coated films were impurity-free and ensures the presence of constituent elements.

Table 4.8 Elemental composition obtained from EDX

Substrate (Glass)	**Atomic Weight (%)**			
	C	O	Si	F
TEOS/MTMS/PVDF	48.16	2.69	28.17	20.98
TEOS/MTMS/PMMA	70.18	26.91	2.91	
TEOS/MTMS/PS	69.60	24.72	5.68	

4.3.4.6 TG-DTA

TG-DTA curve for TEOS/MTMS/PVDF is shown in the **Fig.4.71**.It represents a single stage decomposition, with an exothermic peak at 480°C and the weight loss was about 76.23%, which is due to the volatile and polymeric materials. In case of TEOS/MTMS/PMMA (**Fig.4.72**), it is multi-stage decomposition due to no intermediates. Initially 16.58% of the material is decomposed at about 300°C , Single stage decomposition is seen for TEOS/MTMS/PS (**Fig.4.73**). Beyond 410°C, exothermic peak was seen due to the degradation of polymer material. The weight loss is about 91.88%.

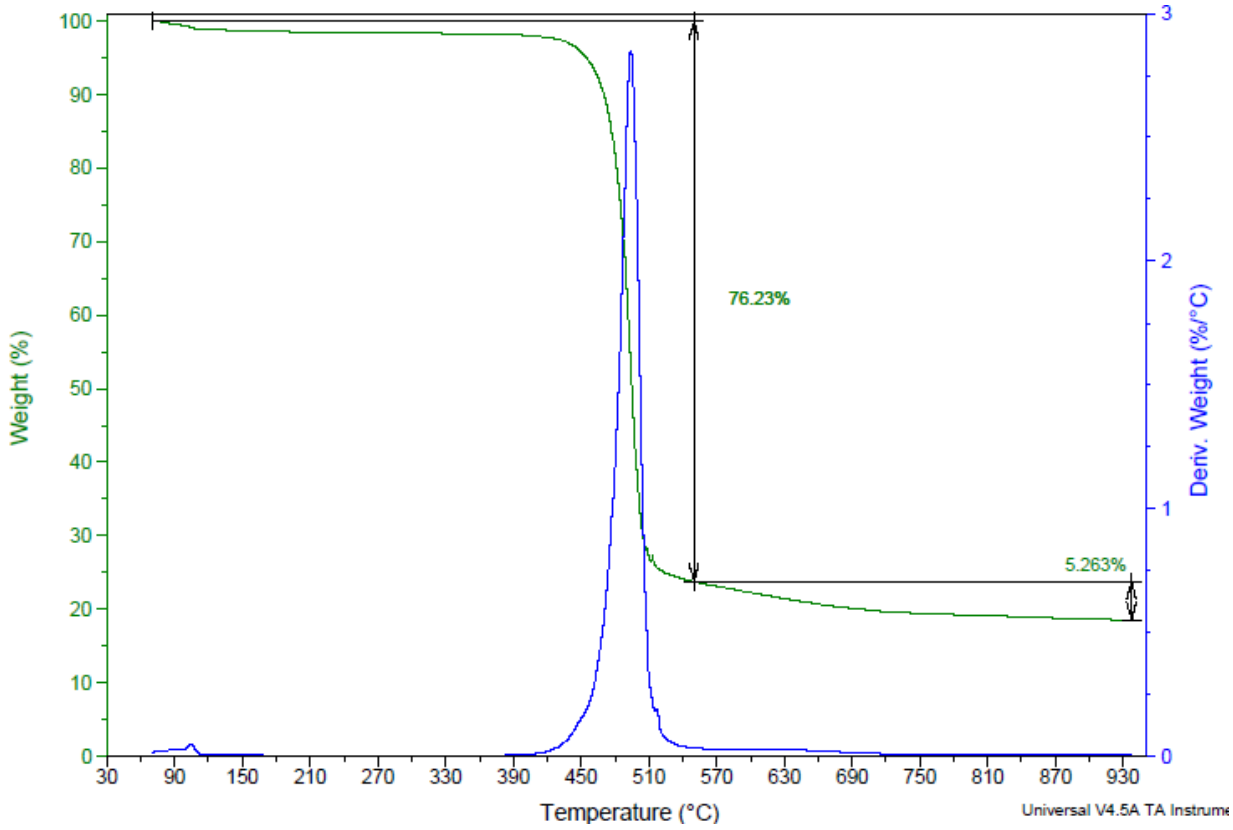

Fig. 4.71 TG-DTA for TEOS/MTMS/PVDF

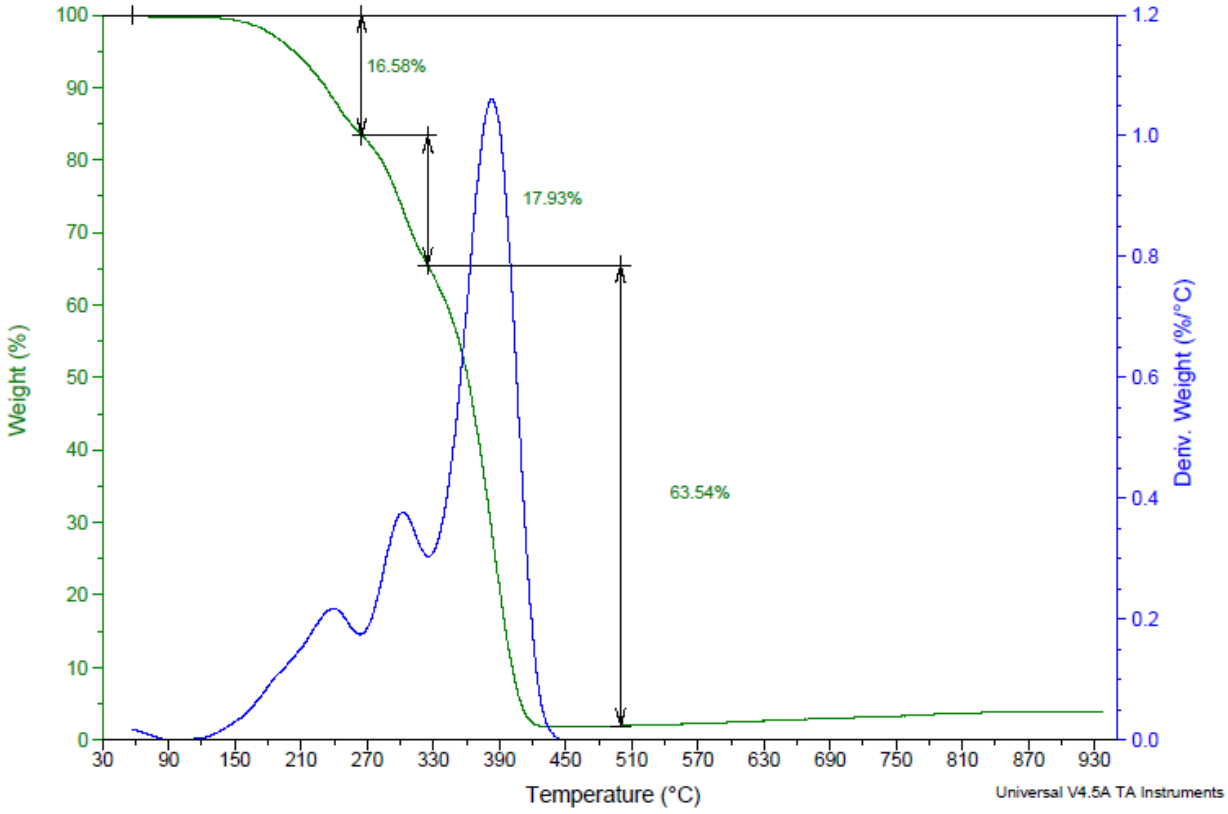

Fig. 4.72 TG-DTA for TEOS/MTMS/PMMA

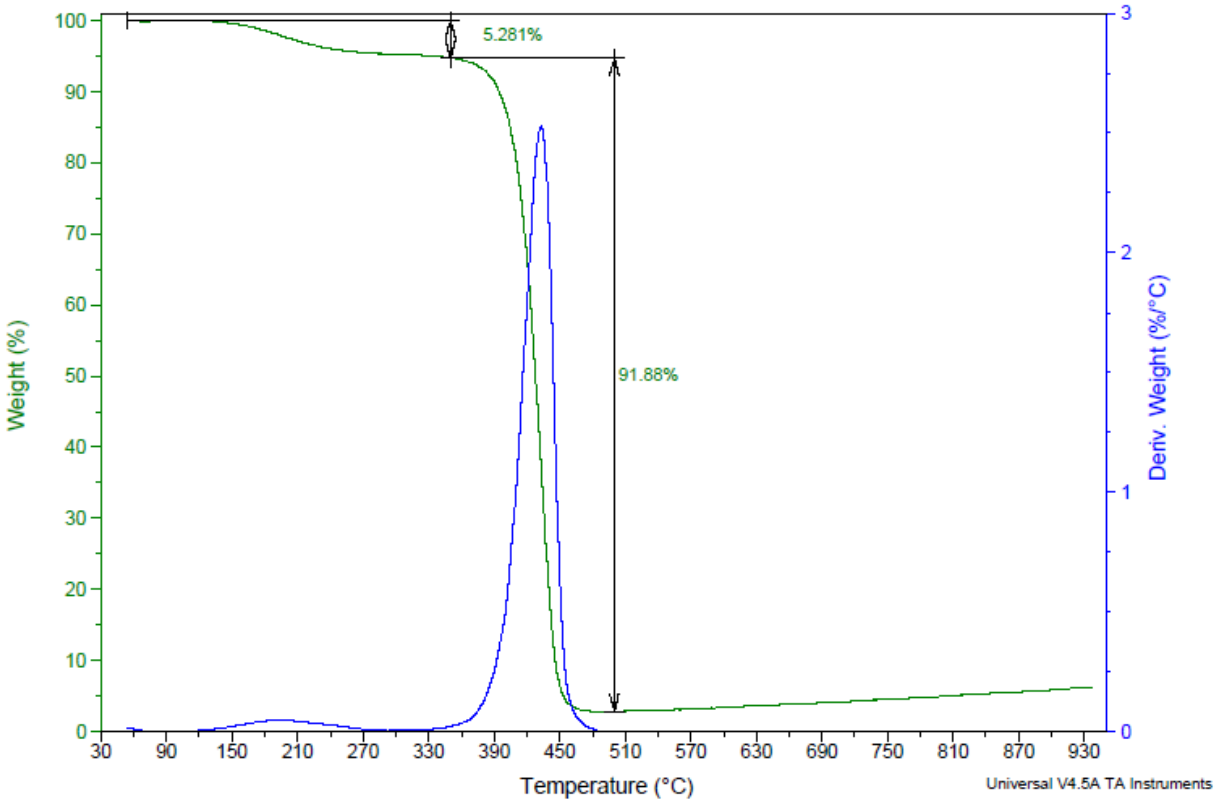

Fig.4.73 TG-DTA for TEOS/MTMS/PS

4.3.4.7 Application

The substrates were coated with TEOS/MTMS and three other polymers (PVDF, PMMA and PS. 2 grams of dust particles were kept on the coated substrates. 3µl of water is allowed on the same substrates. The coated substrates were found to behave hydrophobically as the dust particles on the substrates got clinged to the water droplet as shown in **Fig. 4.74 (a), (b) and (c).**

Fig.4.74 (a) TEOS/MTMS/PVDF coated substrate

Fig.4.74 (b) TEOS/MTMS/PMMA coated substrate

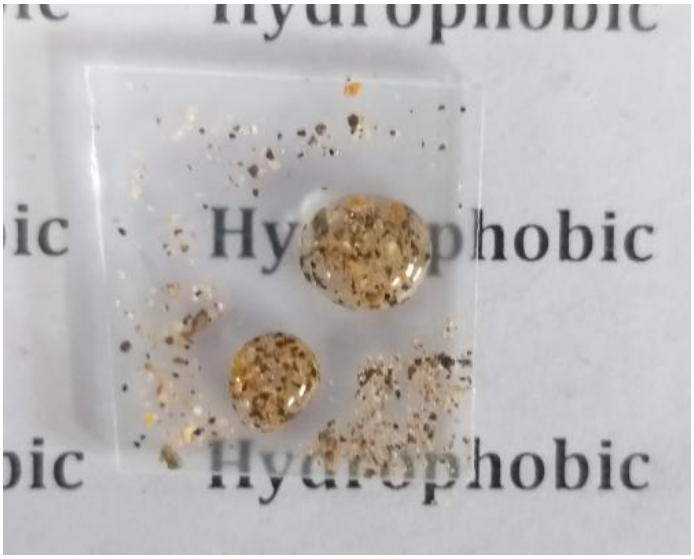

Fig.4.74 (c) TEOS/MTMS/PS coated substrate

4.3.5 SET – V [TEOS + PDMS + Polymer]

4.3.5.1 FTIR

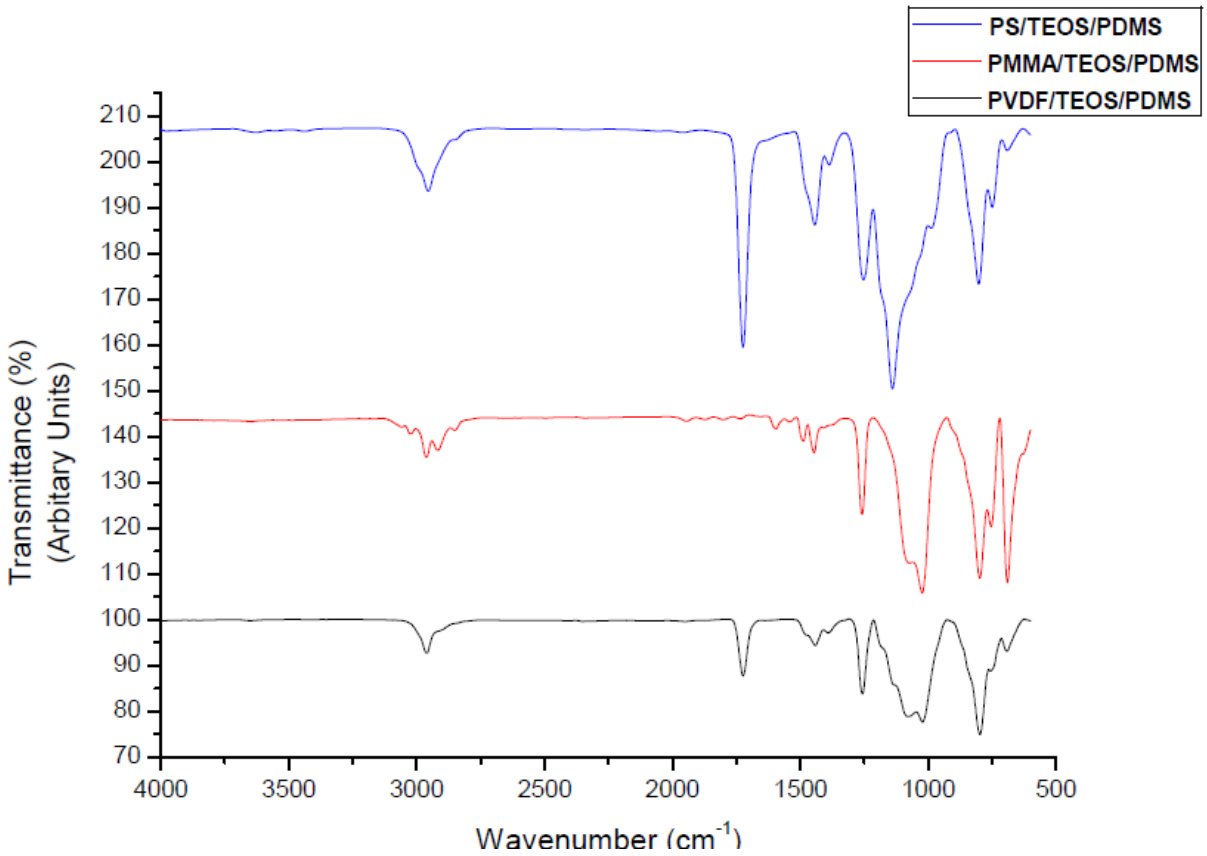

Fig.4.75 FTIR Spectrum of TEOS/PDMS/PVDF, TEOS/PDMS/PMMA and TEOS/PDMS/PS

The functional groups were elucidated using FTIR spectra. **Fig.4.75** shows the spectrum of TEOS/PDMS/PVDF, TEOS/PDMS/PMMA and TEOS/PDMS/PS . The peak at 1023cm^{-1} represents Si-O-Si stretching, due to the presence of silanes. The vibration of crystalline phase of PVDF is seen at 796 cm^{-1}. The peak at 1259cm^{-1} shows deformation of CH_3 bond.

The absorption peaks at 3439cm^{-1}, 1645cm^{-1} and 1087cm^{-1} represents –OH stretching,Si-H_2O bending vibration and Si-O-Si bond stretching respectively for

pristine Tetraethoxysilane (TEOS) **[Hui Tian et al., 2009 and Violeta Purcar et al., 2013]**, whereas for pristine Polyvinylidene fluoride(PVDF) ,C-F stretching vibration is seen at 1400cm^{-1} and 1175cm^{-1} **[F. Hamelmann et al., 2005]**.The band at 840cm^{-1} represents both β and ϒ phase, whereas the band at 796 cm^{-1} represents the α-phase **[Gaurav Mago et al., 2008]**.

4.3.5.2 Contact Angle

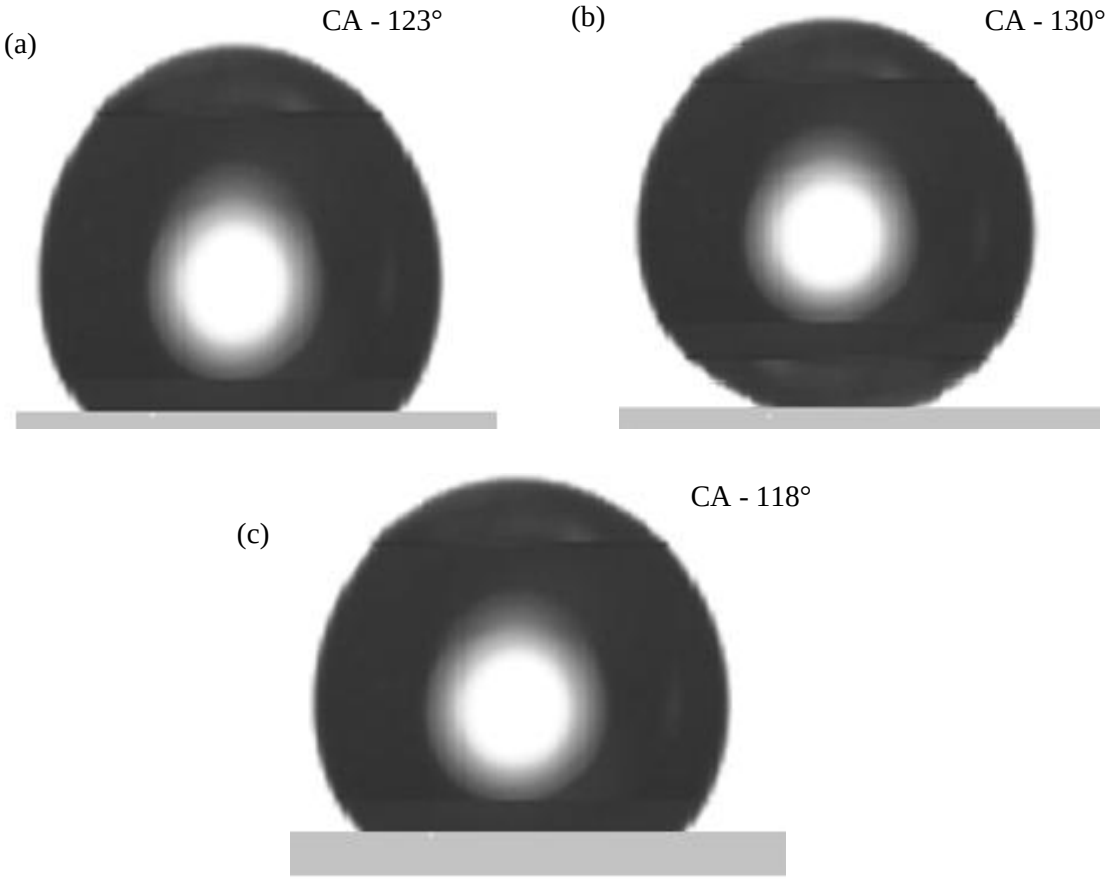

Fig. 4.76 Contact Angle for (a) TEOS/PDMS/PVDF, (b) TEOS/PDMS/PMMA and (c) TEOS/PDMS/PS

The static contact angle for TEOS/PDMS/Polymer was shown in the **Fig. 4.76**. Of all TEOS/PDMS/PMMA shows higher static contact angle of 130°,

which ensures that the liquid drop on the solid surface rolls off very perfectly, making the surface dust-free.

4.3.5.3 Surface Roughness and Surface Energy

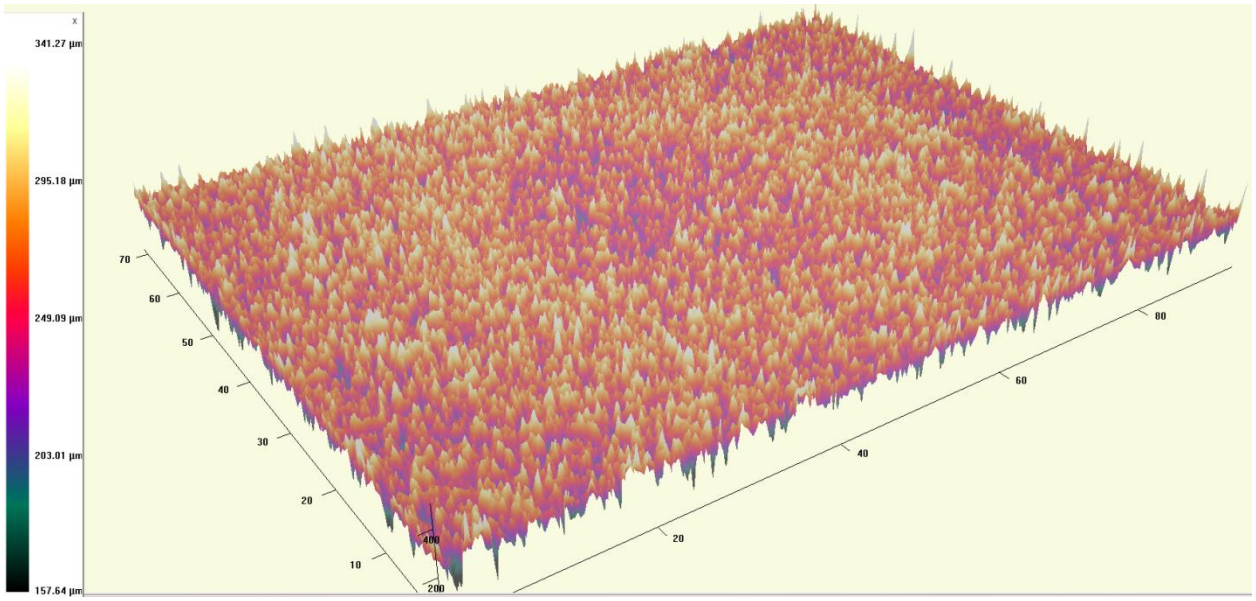

Fig. 4.77 Surface Roughness of TEOS/PDMS/PVDF

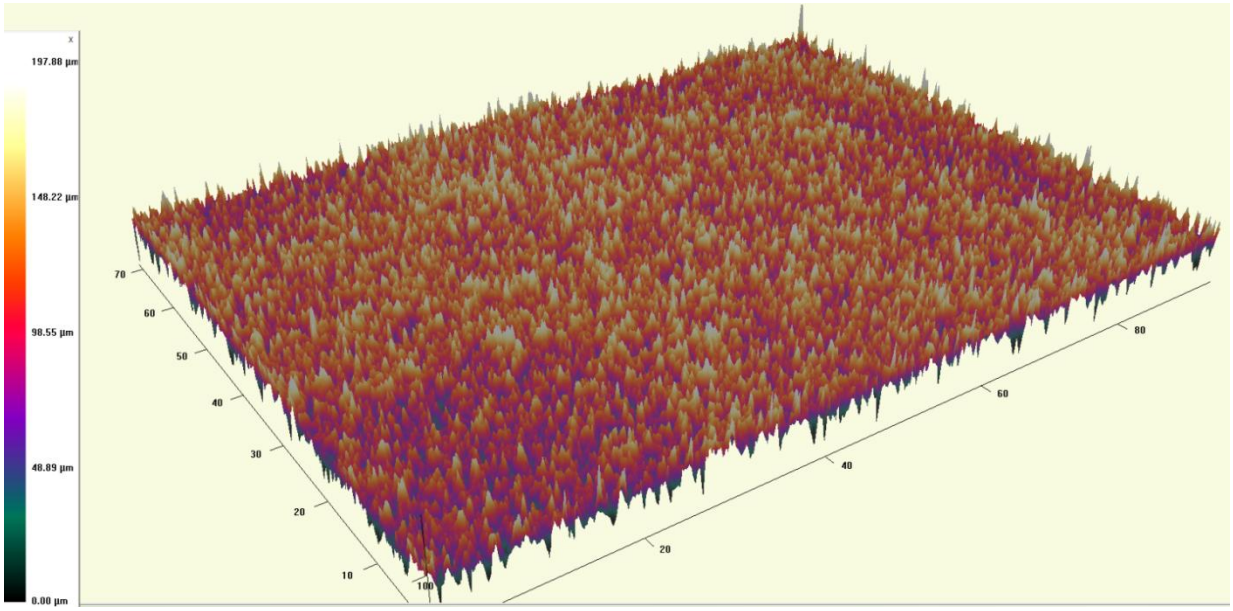

Fig. 4.78 Surface Roughness of TEOS/PDMS/PMMA

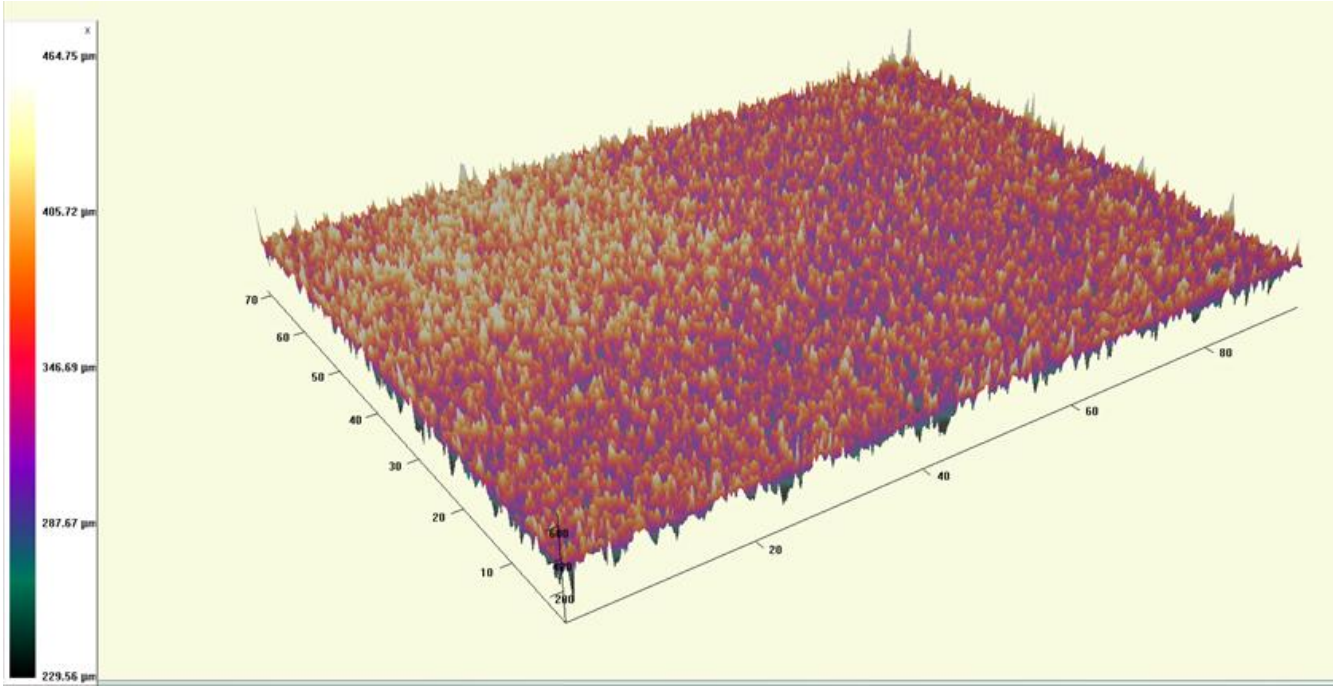

Fig. 4.79 Surface Roughness of TEOS/PDMS/PS

The surface roughness of the films were investigated with 3D-Zeta Profilometer **(Fig.4.77, 4.78 and 4.79)**. Surface roughness and surface energy are inter-related. As the roughness increases even in micro or nano scale, the hydrophobic nature of the surface/film also increases provided the surface energy decreases. The higher contact angle of 130° is exhibited by TEOS/PDMS/PMMA film which has roughness of 50.05 µm and energy of 19.24 Jm^{-1}/mNm^{-1} in the z-steps between 700µm to 1200µm. Surface roughness and computed surface energy with their corresponding Hamaker's constant are tabulated in **Table.4.9**. Due to increased surface roughness PMMA shows less transparency when PDMS is blended.

Table.4.9 - Surface Roughness and Thickness Measurement of the coated films

Sample	Hamaker Constant A_n (J x 10^{-21})	Surface Roughness, Ra (μm)	Surface energy, ϒ (Jm^{-1})	Contact Angle, CA (°)	Thickness (μm)
TEOS/PDMS/PMMA	1.94	50.05	19.24	130°	11.3
TEOS/PDMS/PVDF	2.14	47.28	22.16	123°	9.4
TEOS/PDMS/PS	3.21	43.56	21.47	119°	10.6

4.3.5.4 UV-Visible Spectroscopy

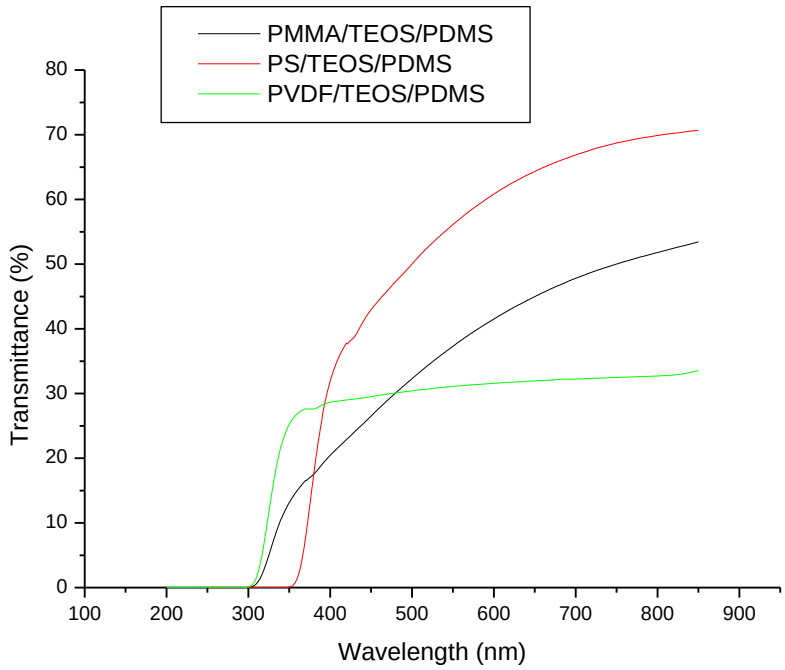

Fig.4.80 UV-Visible Spectrum for TEOS/PDMS/PVDF, TEOS/PDMS/PMMA and TEOS/PDMS/PS

The UV-Visible spectrum of TEOS/PDMS/Polymer was plotted in the **Fig.4.80**. From which it is shown that TEOS/PDMS/PMMA has the lowest cut-off

wavelength at 385nm, but beyond the cut-off wavelength, the transparency increases from 15% to 50%. Incase of TEOS/PDMS/PS, it varies between 40% to 65% and in TEOS/PDMS/PVDF film, the curve is stagnant at 354 nm with lesser transparency of 30%. With the methoxy group presence, even the optically active PMMA shows varied transparency range.

4.3.5.5 FESEM

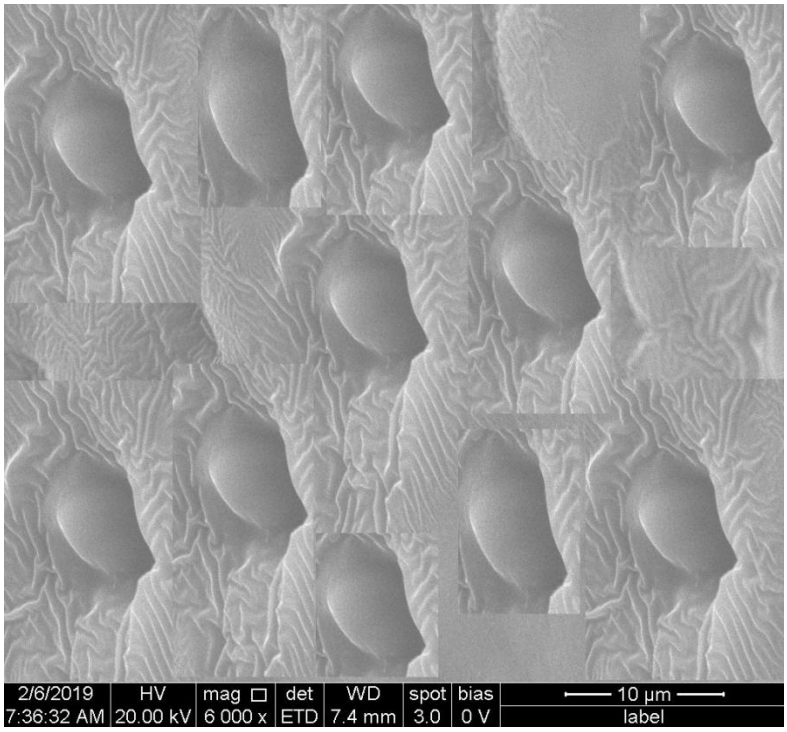

Fig.4.81 FE-SEM of TEOS/PDMS/PVDF

The surface morphology of TEOS/PDMS/PVDF shows a varied surface. The colloidal base surface denotes the Vinyledene fluoride's presence and the bumps on the surface is due to the presence of methoxy silane. These bumps are not crystals, but they form as a result of rougher surface, which plays

a better hydrophobic film holding the droplet on the solid surface. The EDX for the film has been shown in the **Fig.4.84**

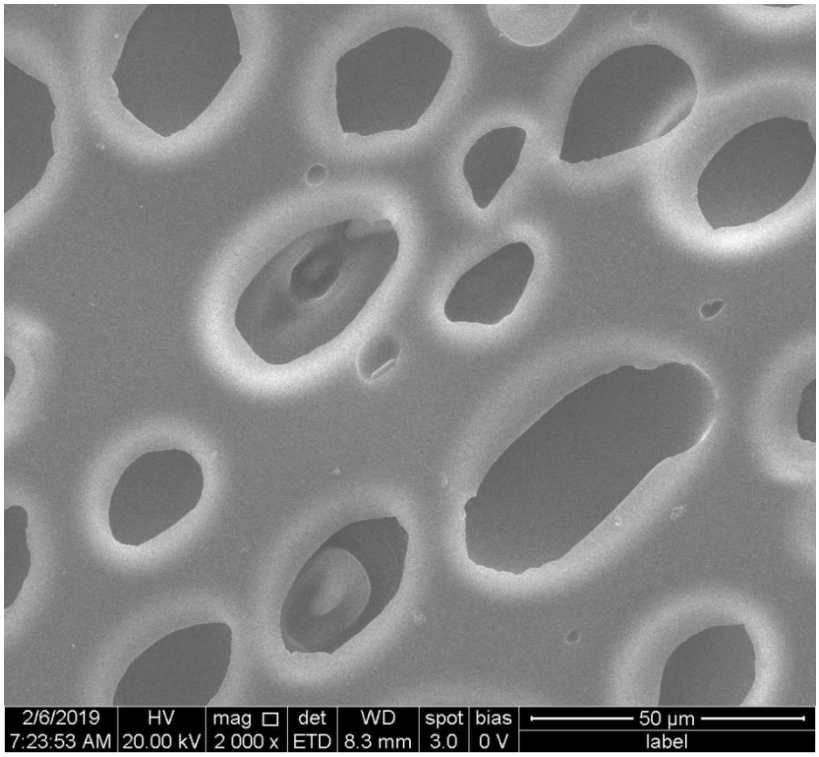

Fig.4.82 FE-SEM of TEOS/PDMS/PMMA

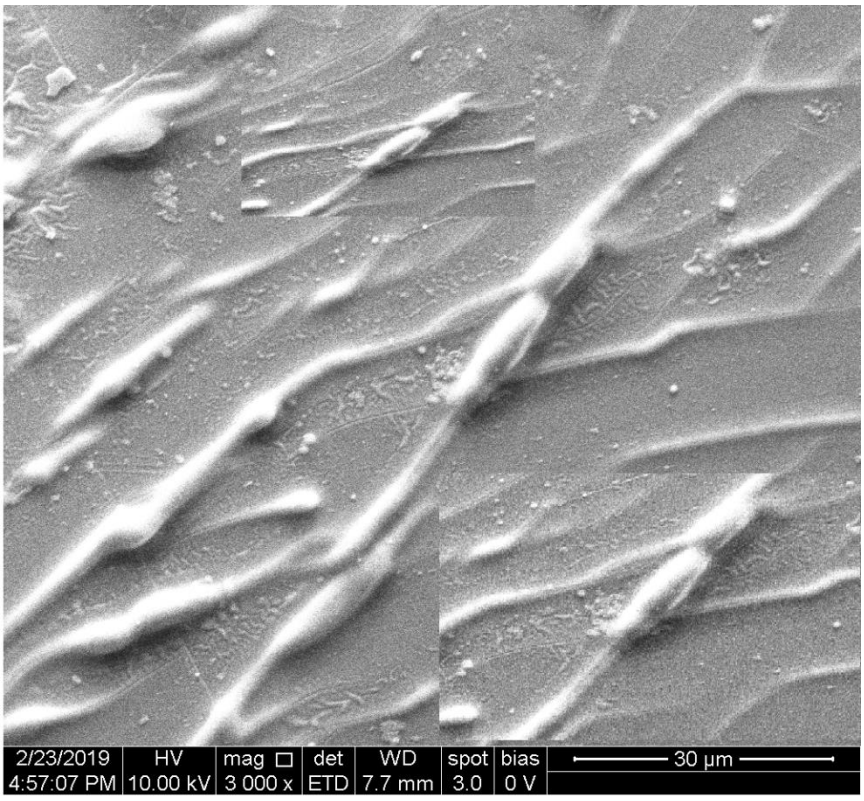

Fig.4.83 FE-SEM for TEOS/PDMS/PS

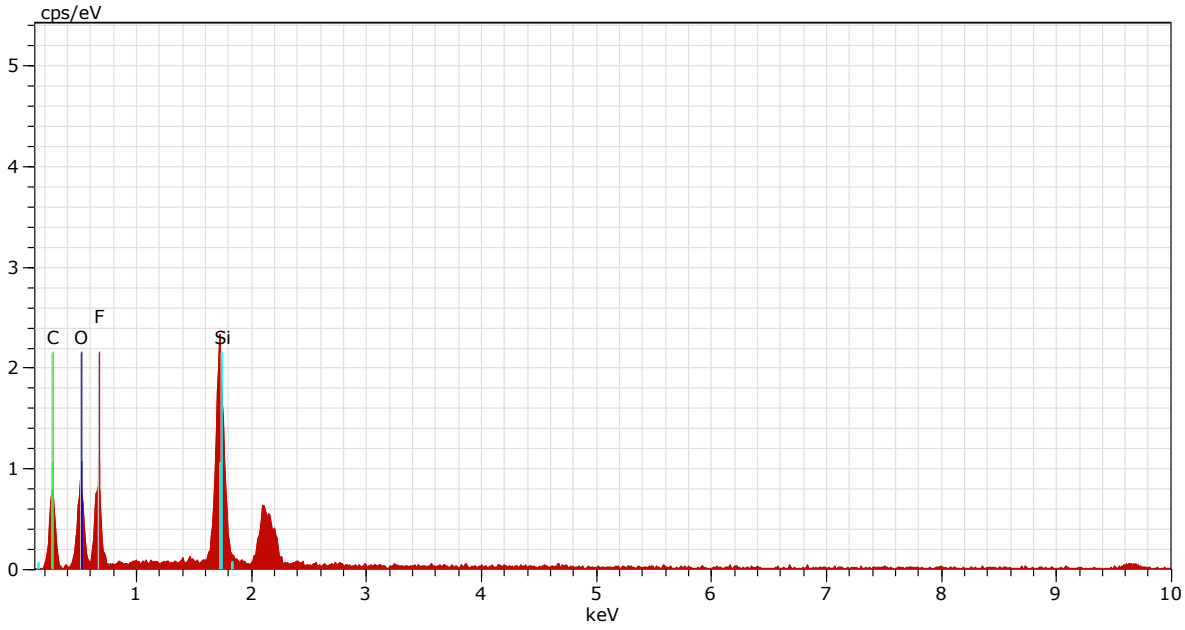

Fig.4.84 EDX of TEOS/PDMS/PVDF

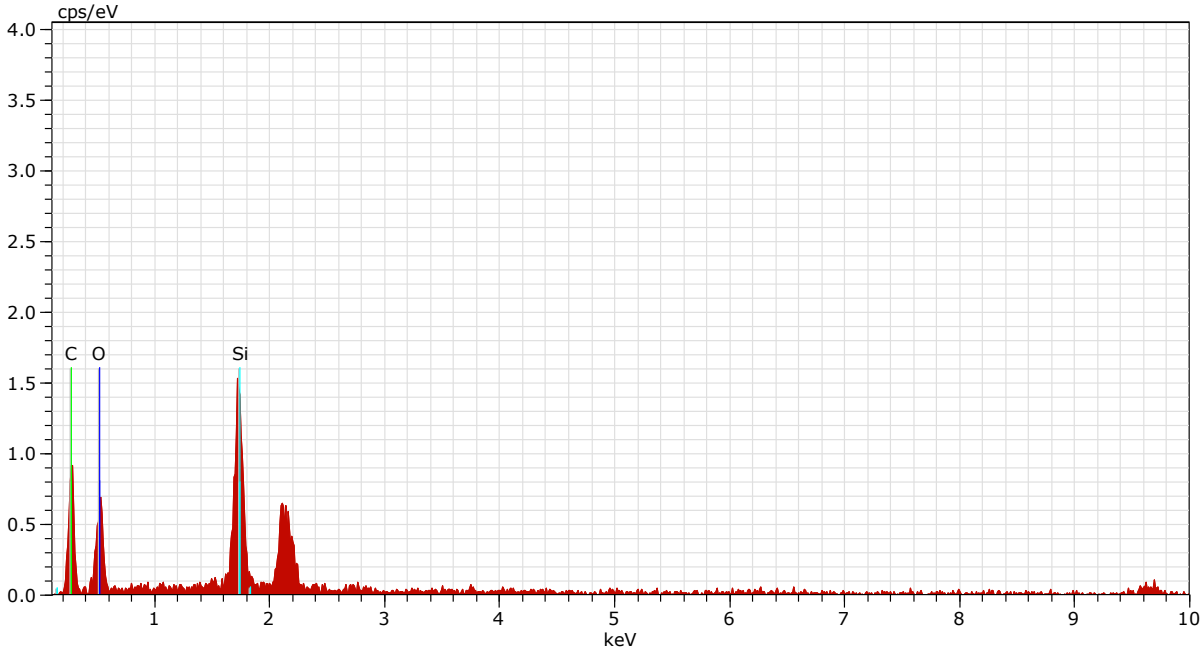

Fig.4.85 EDX of TEOS/PDMS/PMMA

The FE-SEM of TEOS/PDMS/PMMA and TEOS/PDMS/PS films were shown in the **Figs.4.82 and 4.83**. In case of Silane/Methyl methacrylate film, surface has shallow part with small bumps are seen inner to the shallow and for Silane/styrene film strong lines with rod like structure are seen. The EDX spectrum (**Figs.4.84,4.85 and 4.86**) represents the purity of the prepared films. It is found that the films are free from dirt. The particle size for all films with the help of histogram was observed between the z-steps of 750µm to 1250µm as shown in **Figs.4.87,4.88 and 4.89.**

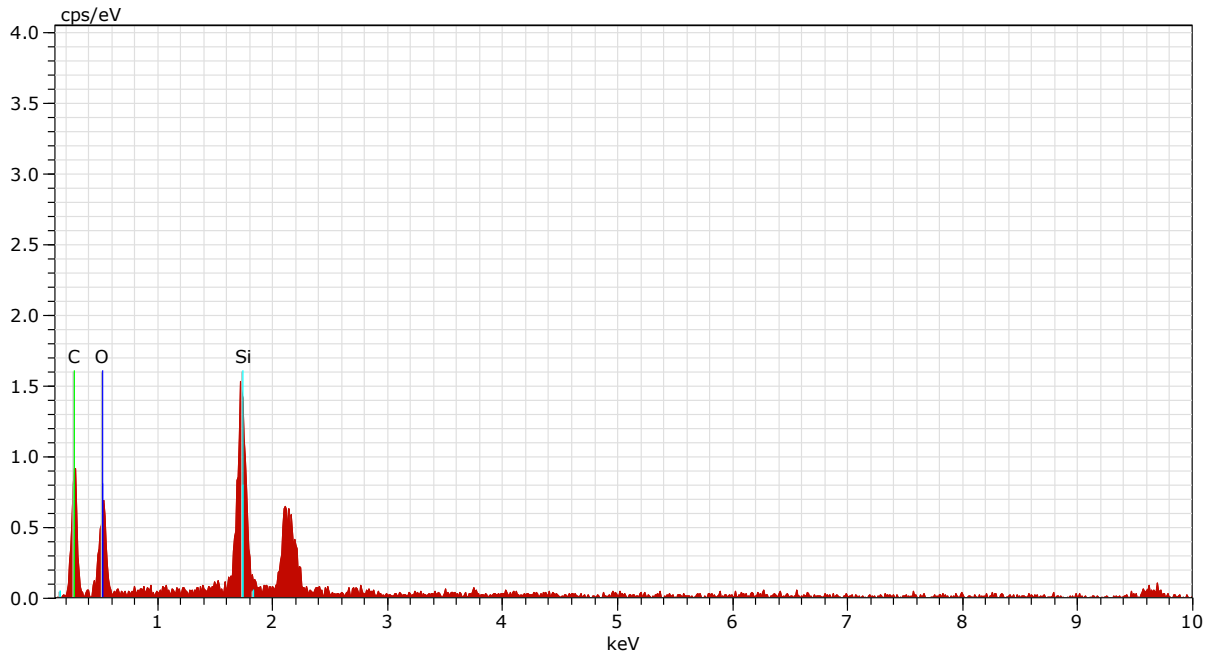

Fig.4.86 EDX for TEOS/PDMS/PS

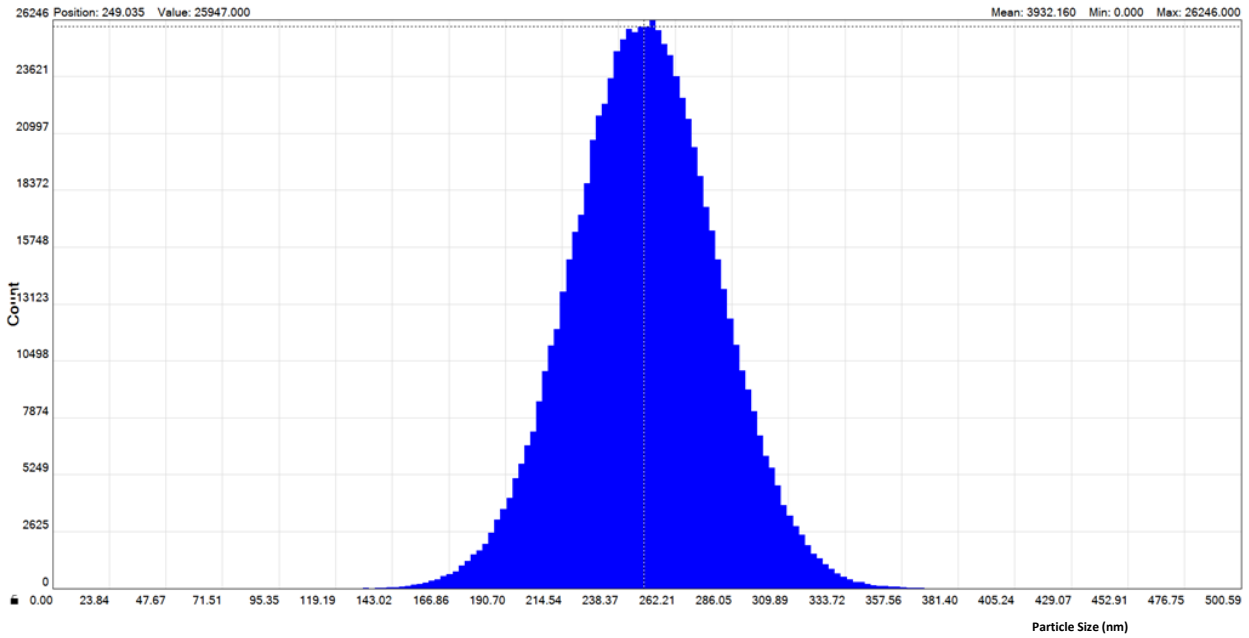

Fig. 4.87 Histogram for TEOS/PDMS/PVDF

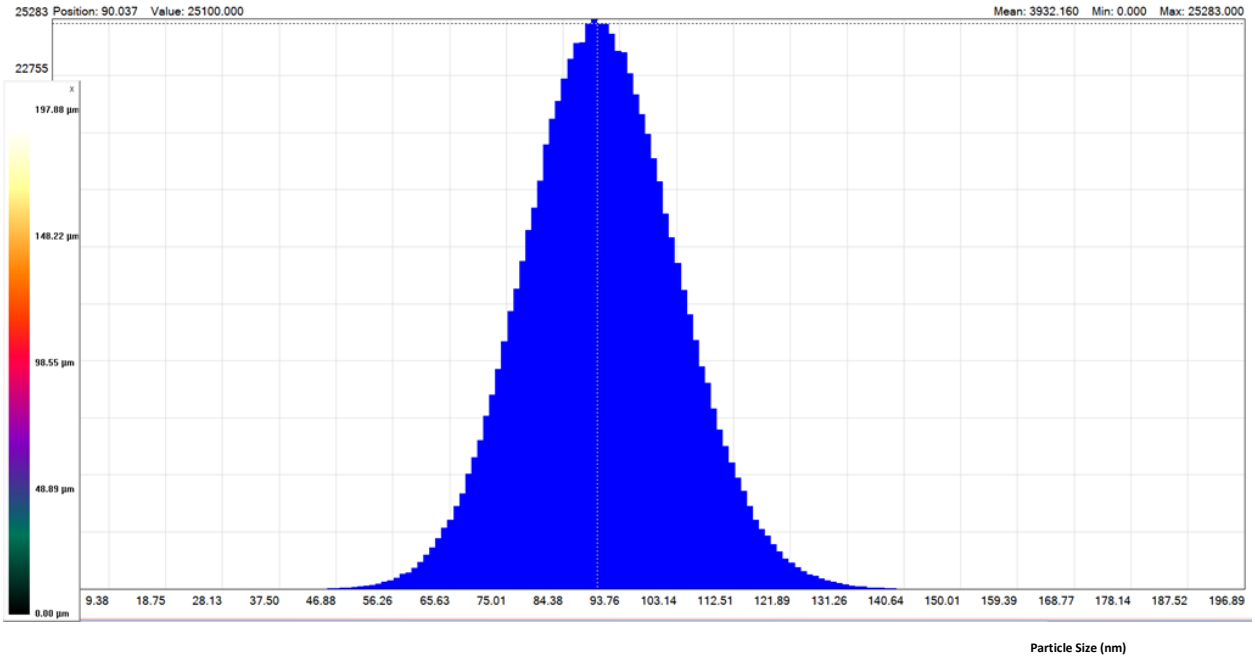

Fig.4.88 Histogram for TEOS/PDMS/PMMA

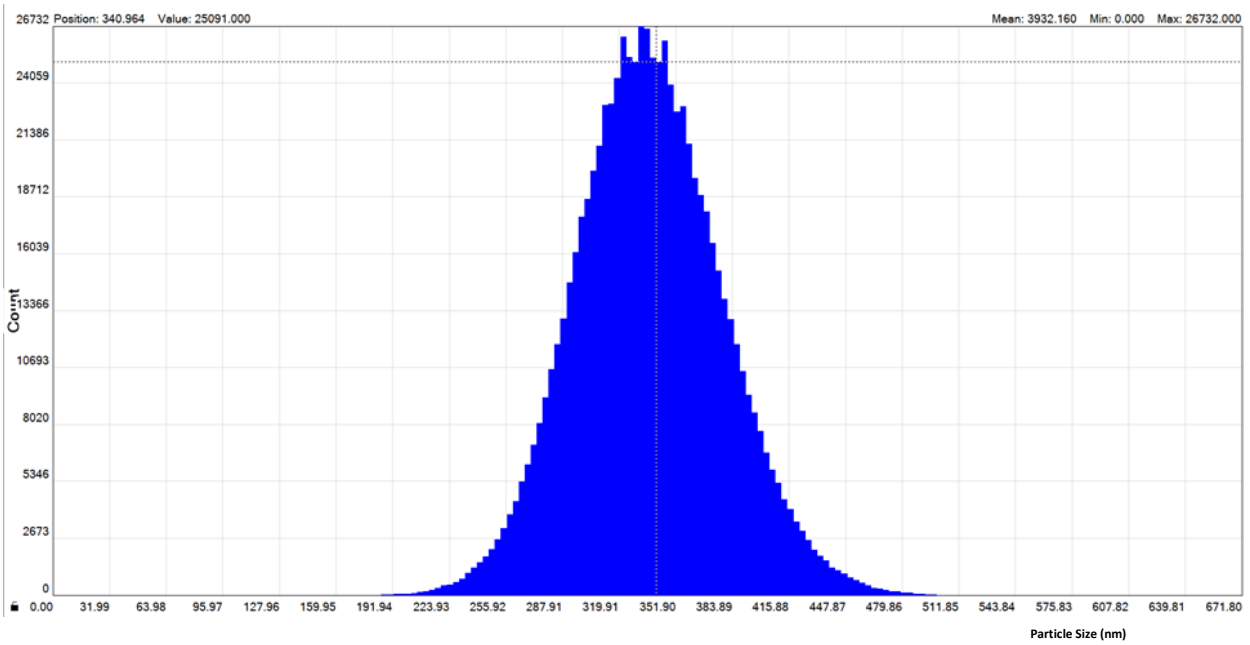

Fig.4.89 Histogram for TEOS/PDMS/PS

4.3.5.6 TG-DTA

The TG-DTA curve for TEOS/PDMS/Polymer is plotted in the **Figs.4.90,4.91 and 4.92** respectively. The thermal analysis for

TEOS/PDMS/PVDF shows a single stage decomposition with an exothermic peak at 500°C. Initially the material loss is less than 2% whereas, in case of TEOS/PDMS/PMMA, multi-stage decomposition is noted due to lack of intermediates. The exothermic peak at 300°C is due to the emission of volatile and alcoholic compounds. Polymeric decomposition is seen at 390°C, with the material loss of 16.48% in the second stage.

The DTA curve for TEOS/PDMS/PS, shows a bump initially at 180°C, which is the glass transition temperature (T_g). In general, styrene exhibit small bump around T_g. The polymeric compound gets decomposed at 410°C, weight loss of 8.2%. Overall, TEOS/PDMS/PVDF shows better thermal stability than the other two composite films.

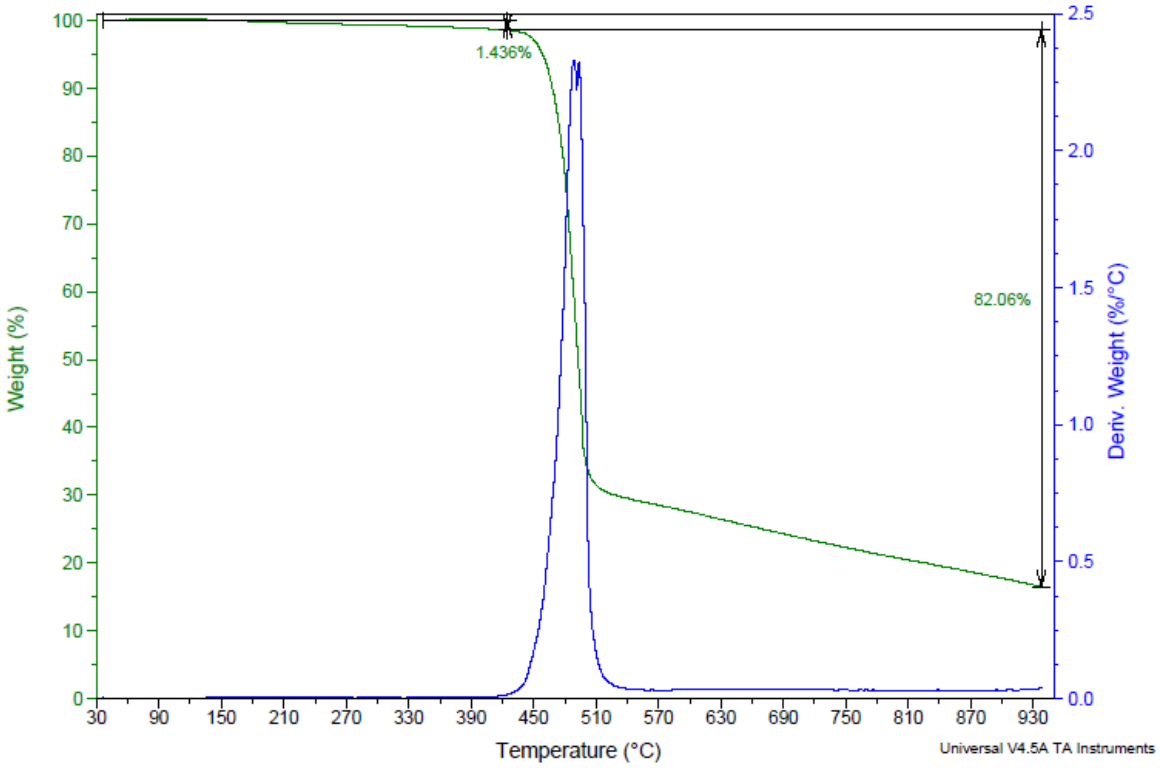

Fig.4.90 TG-DTA for TEOS/PDMS/PVDF

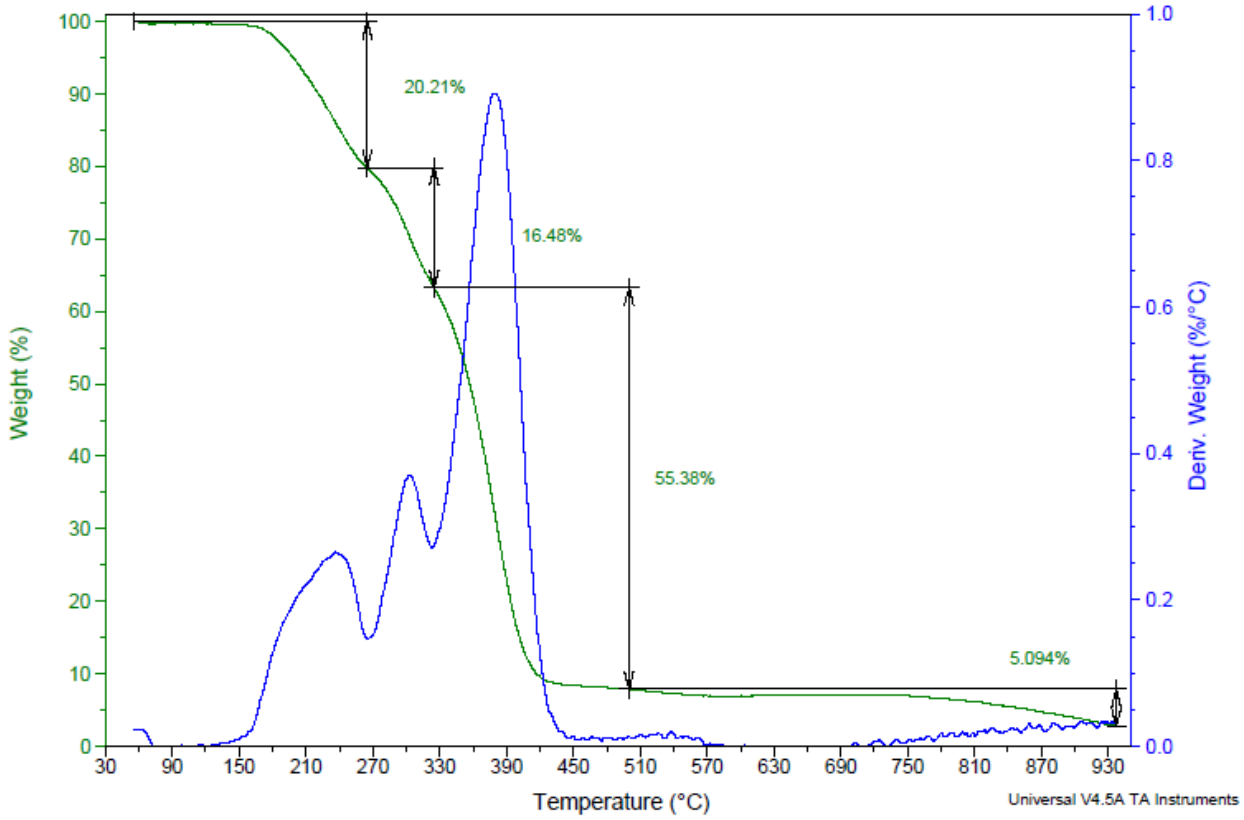

Fig.4.91 TG-DTA for TEOS/PDMS/PMMA

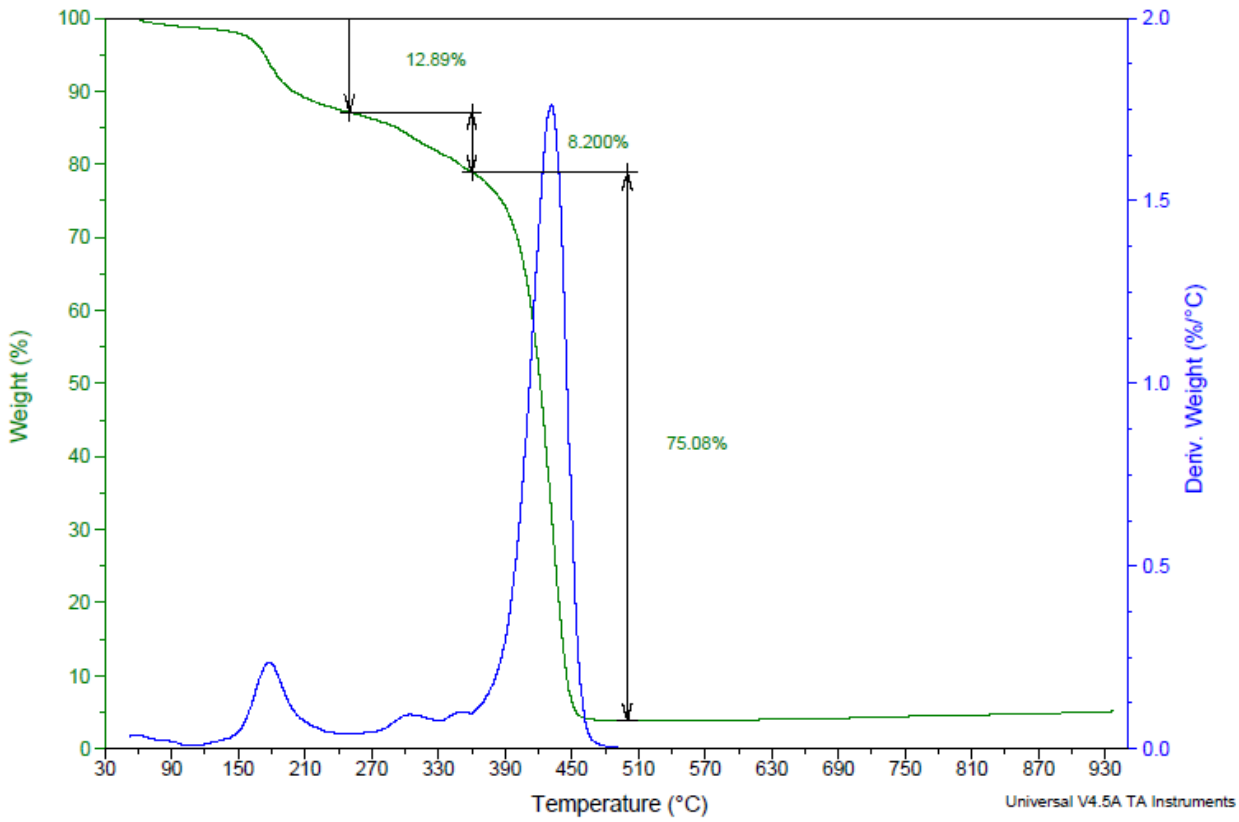

Fig.4.92 TG-DTA for TEOS/PDMS/PS

4.3.5.7 Application

Self-cleaning application was proved with TEOS/PDMS/Polymer (PVDF, PMMA and PS). The coated substrates were shown in the **Fig. 4.93 (a,b,c).** 3 grams of dust particles were placed on the coated substrates. 4µl of water was allowed on the same coated substrates. The dust particles gets beaded up along with the water droplet making the surface free from dust particles.

Fig. 4.93 (a) TEOS/PDMS/PVDF coated substrate

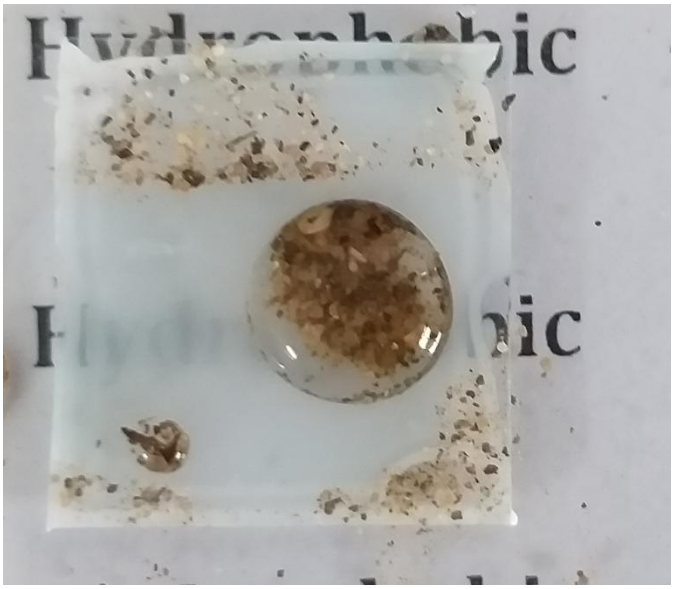

Fig. 4.93 (b) TEOS/PDMS/PMMA coated substrate

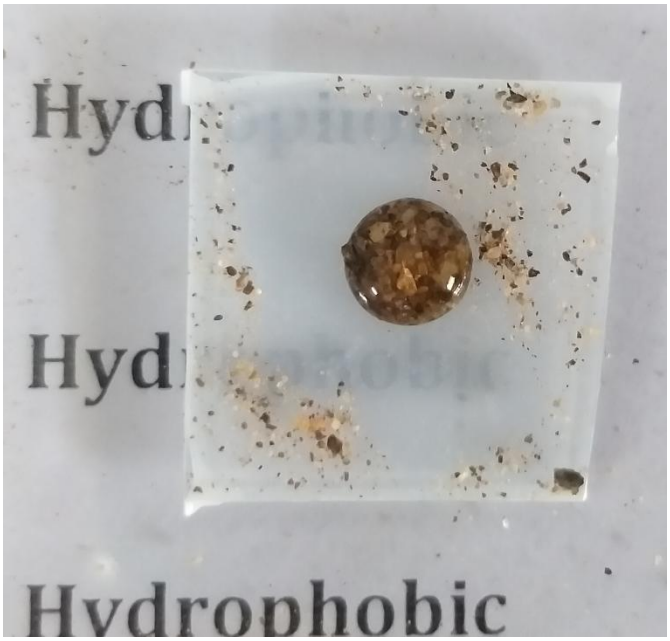

Fig. 4.93 (c) TEOS/PDMS/PS coated substrate

4.3.6 SET – VI [MTMS + PDMS +Polymer]

4.3.6.1 FTIR

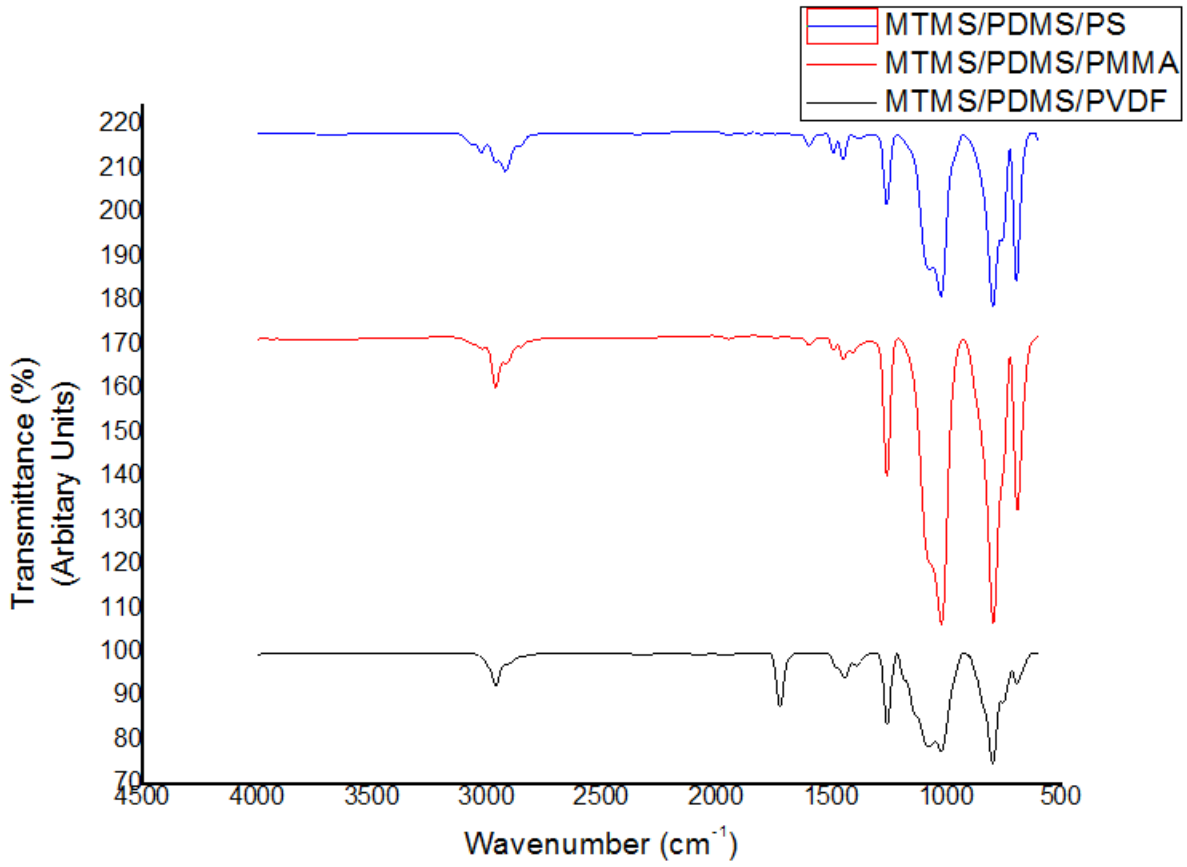

Fig. 4.94 FTIR spectrum of MTMS/PDMS/PVDF, MTMS/PDMS/PMMA and MTMS/PDMS/PS

The FTIR spectrum of MTMS/PDMS/PVDF, MTMS/PDMS/PMMA and MTMS/PDMS/PS is shown in the **Fig. 4.94**. The spectra of MTMS/PDMS/PVDF shows the presence of PVDF crystalline phase at 794cm^{-1}. CH_2 and CF_2 stretching vibrations is present at 1167cm^{-1} and 1402cm^{-1}. The presence of silane is seen at 1024cm^{-1} as Si-O-Si stretching.

In MTMS/PDMS/PMMA spectra, the peak at 1441 cm^{-1} and 755 cm^{-1} are due to the α-methylene group vibration **[S Sathya et al., 2016].** The band at 1022 cm^{-1}

represents the stretching mode of Si-O-Si. The peak at 2961cm^{-1} shows the presence of methyl group which were indicated with C-H stretching vibration modes of Si-CH_3. The peak at 1257 cm^{-1} indicates the deformation of CH_3 in PDMS. In case of MTMS/PDMS/PS, the absorption peak at 1446cm^{-1} represents bending modes of C-H bonds. The symmetric and asymmetric modes of C-H bond are seen at 2917 cm^{-1}. The peak shifted at 2852cm^{-1} in MTMS, denotes the inclusion of methenyl group.

4.3.6.2 Contact Angle

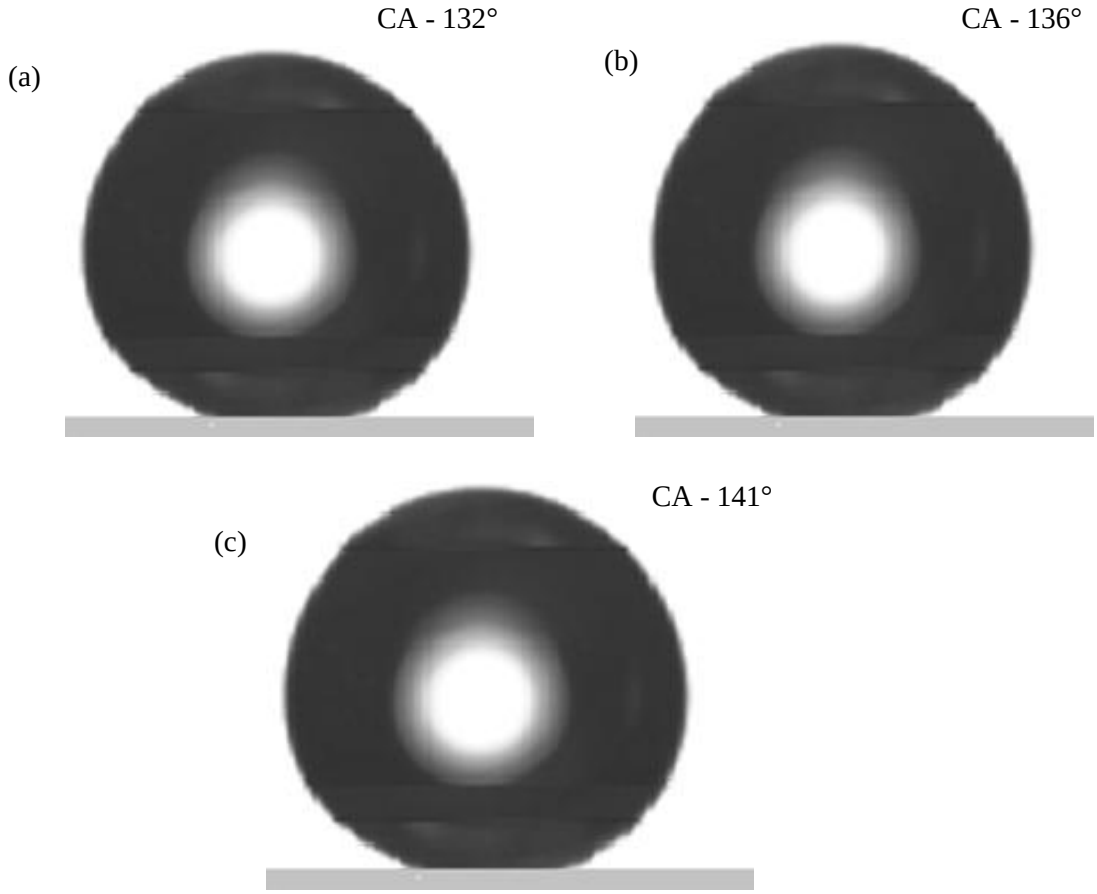

Fig.4.95 Static contact angle for (a) MTMS/PDMS/PVDF, (b) MTMS/PDMS/PMMA and (c) MTMS/PDMS/PS

The static contact angle for MTMS/PDMS blended with three polymers is shown in the **Fig.4.95 (a,b and c)**. These contact angles are found to be greater than 130°, hence the films exhibit super-hydrophobic nature. This is due to the addition of two methoxy-silane groups to the polymer. MTMS/PDMS/PS shows higher contact angle of 141°.

4.3.6.3 Surface Roughness and Surface Energy

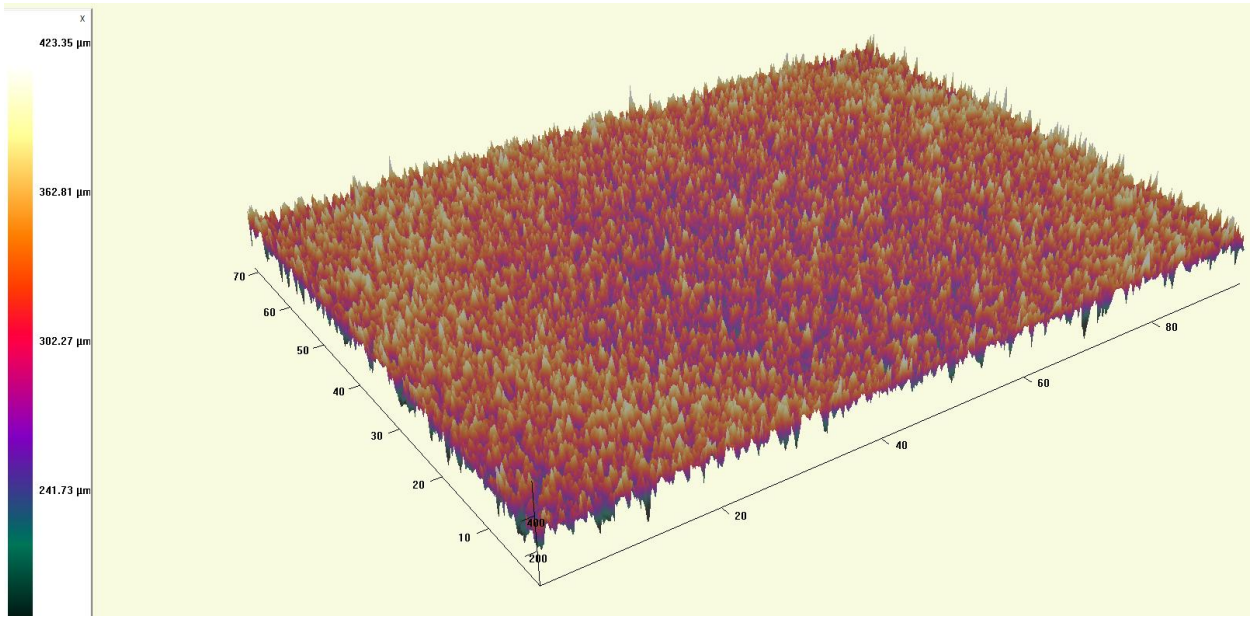

Fig.4.96 Surface Roughness of MTMS/PDMS/PVDF

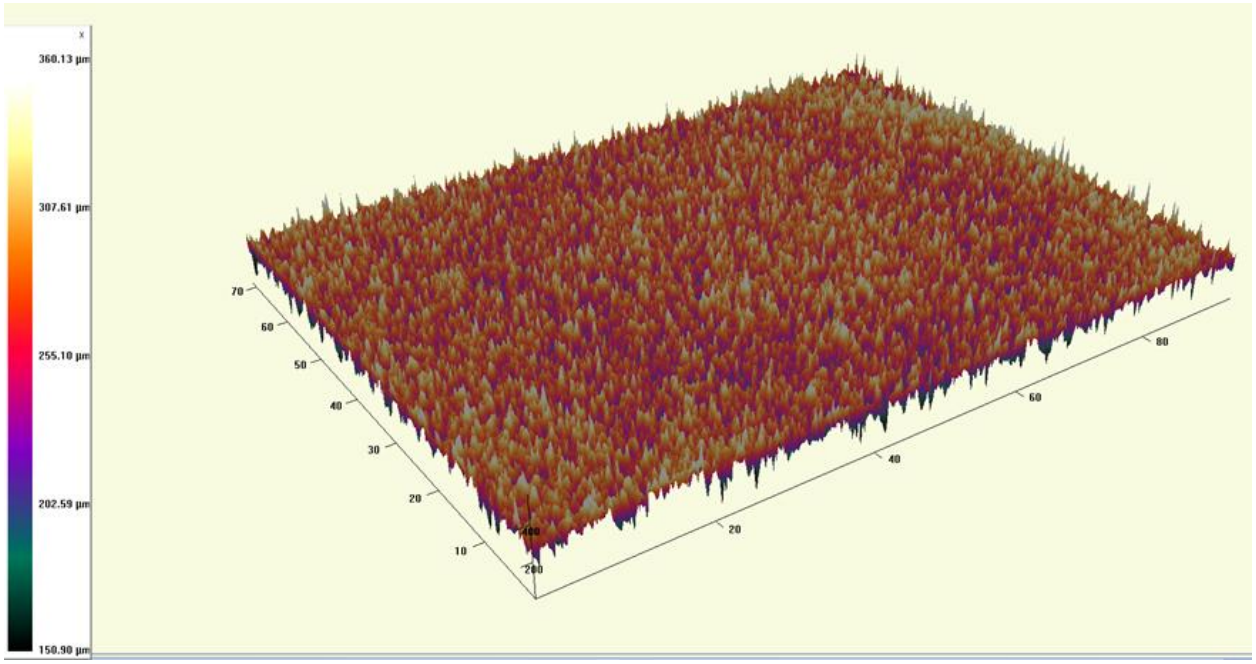

Fig.4.97 Surface Roughness of MTMS/PDMS/PMMA

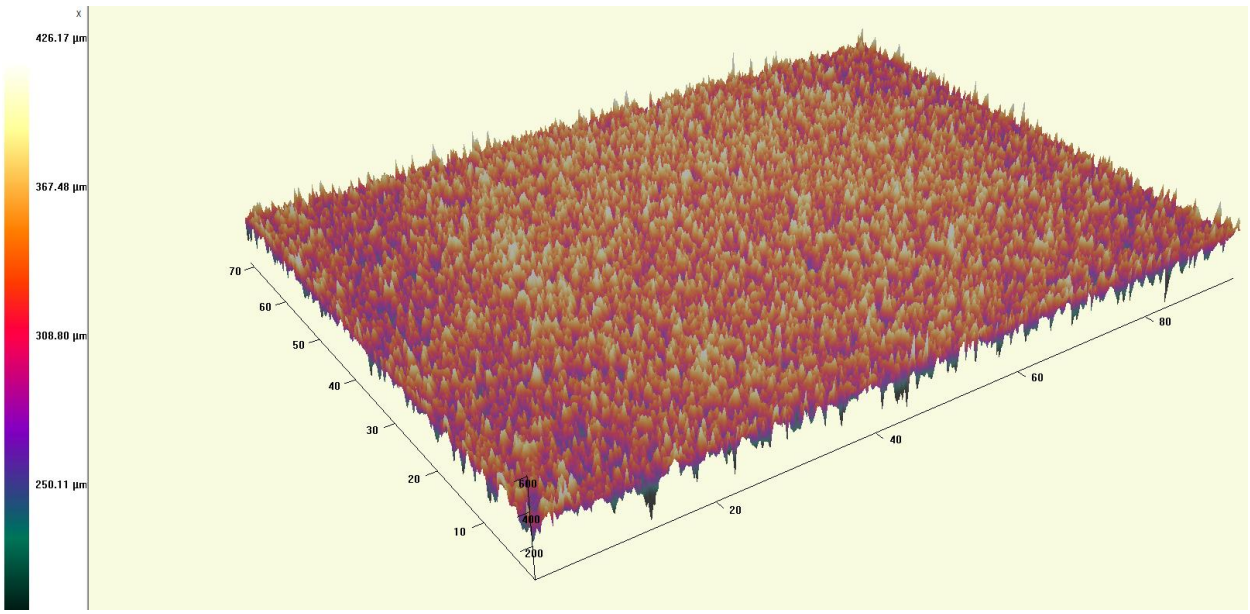

Fig.4.98 Surface Roughness of MTMS/PDMS/PS

The surface roughness of MTMS/PDMS/Polymer (PVDF, PMMA and PS) were shown in the **Figs. 4.96, 4.97, 4.98**. MTMS/PDMS/PS has higher surface roughness of 57.40µm with the peak height (Rp) of 300µm to 426.17µm. The surface energy for this composite film is 16.21µm, which is computed theorectically using the Hamaker constant. This is due to the attraction between two uncharged macroscopic surfaces across air or water and can be explained with Lifshitz theory of Van der Waals interaction **[Calcum J. Drummond et al., 1997].** The Surface roughness and energy for the composite films were tabulated in **Table. 4.10**.

Table.4.10 - Surface Roughness and Thickness Measurement of the coated films

Sample	Hamaker Constant A_n (J x 10^{-21})	Surface Roughness, Ra (µm)	Surface energy, Ɣ (Jm^{-1})	Contact Angle, CA (°)	Thickness (µm)
MTMS/PDMS/PS	2.03	57.40	16.21	141°	15.8
MTMS/PDMS/PMMA	1.97	53.21	18.46	136°	12.4
MTMS/PDMS/PVDF	1.24	49.27	20.83	132°	13.8

4.3.6.4 UV-Visible Spectroscopy

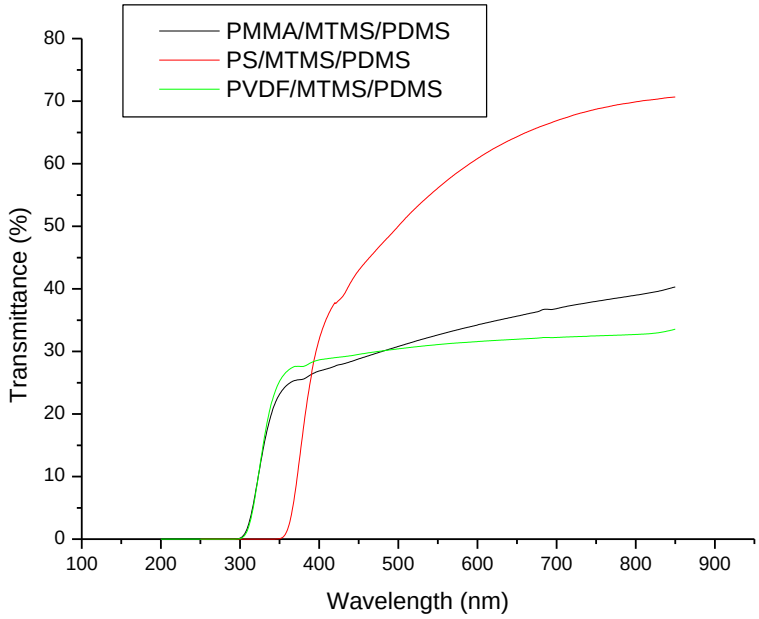

Fig.4.99 UV-Visible spectrum of MTMS/PDMS/Polymer

The **Fig,4.99** shows the UV-Visible spectrum of all the polymers blended with MTMS/PDMS. The point to be noted is PVDF, PMMA and PS were mixed separately to MTMS and PDMS (i.e) both the silanes has methoxy group, which makes the surface more hydrophobic. Hence, in this three prepared films, the surface roughness is higher and their corresponding contact angle also higher with reduced transparency. Both MTMS/PDMS/PMMA and MTMS/PDMS/PVDF has lesser transmittance percent of about 25% to 30%, whereas MTMS/PDMS/PS, the transmittance percent is little higher to 40%.

4.3.6.5 FESEM

The surface morphology of MTMS/PDMS/Polymer (PVDF, PMMA and PS) were shown in the **Figs.4.100, 4.101 and 4.102**. The presence of PDMS are seen like bumps and the polymeric material presence is like small voids, whereas in the case of MTMS/PDMS/PMMA has more crystallite like structure with the average particle size of more than 1µm is observed. The FE-SEM image of MTMS/PDMS/PS shows rougher surface with no bumps. But the surface has uneven missile like formation resulted due to rigid packing of molecules and hence making the surface more rougher.

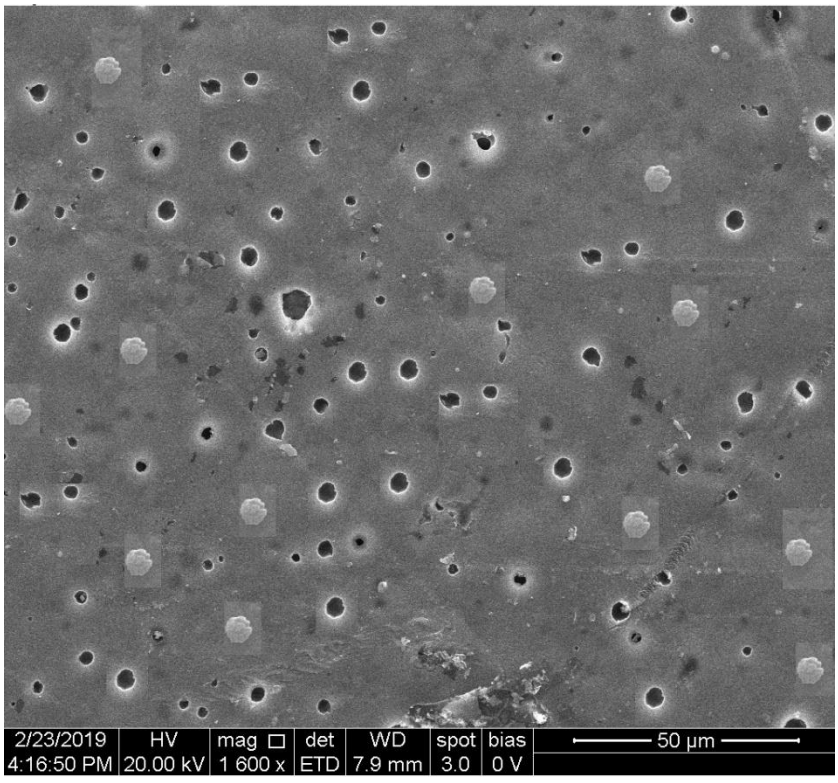

Fig.4.100 FE-SEM for MTMS/PDMS/PVDF

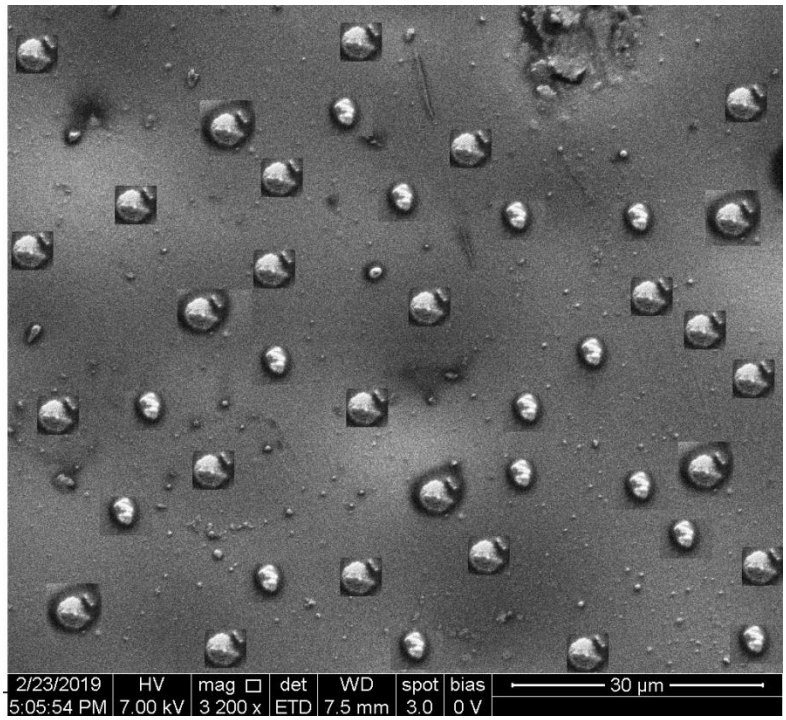

Fig.4.101 FE-SEM for MTMS/PDMS/PMMA

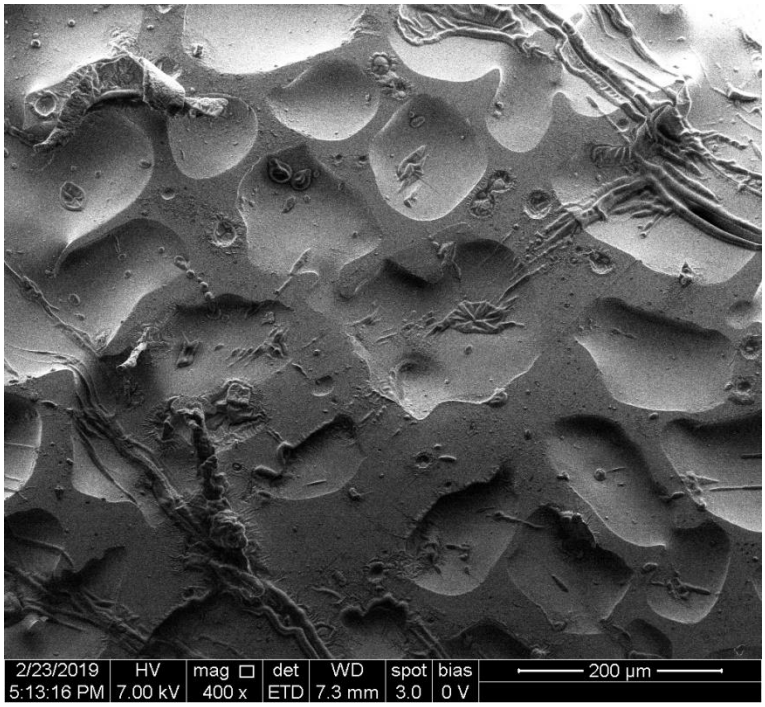

Fig.4.102 FE-SEM for MTMS/PDMS/PS

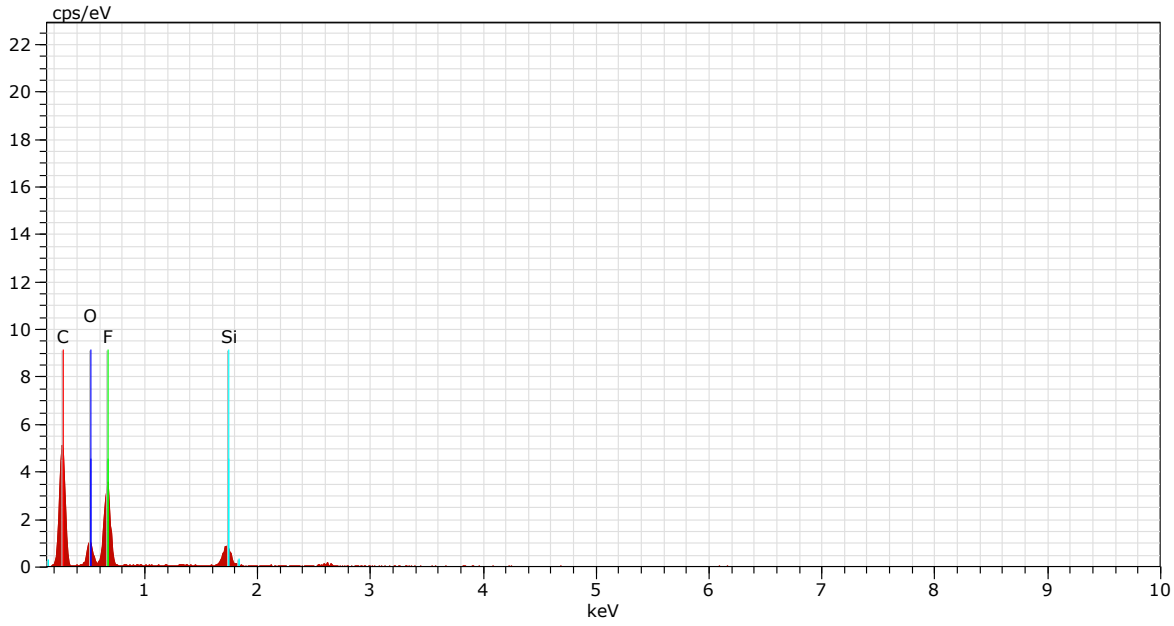

Fig.4.103 EDX for MTMS/PDMS/PVDF

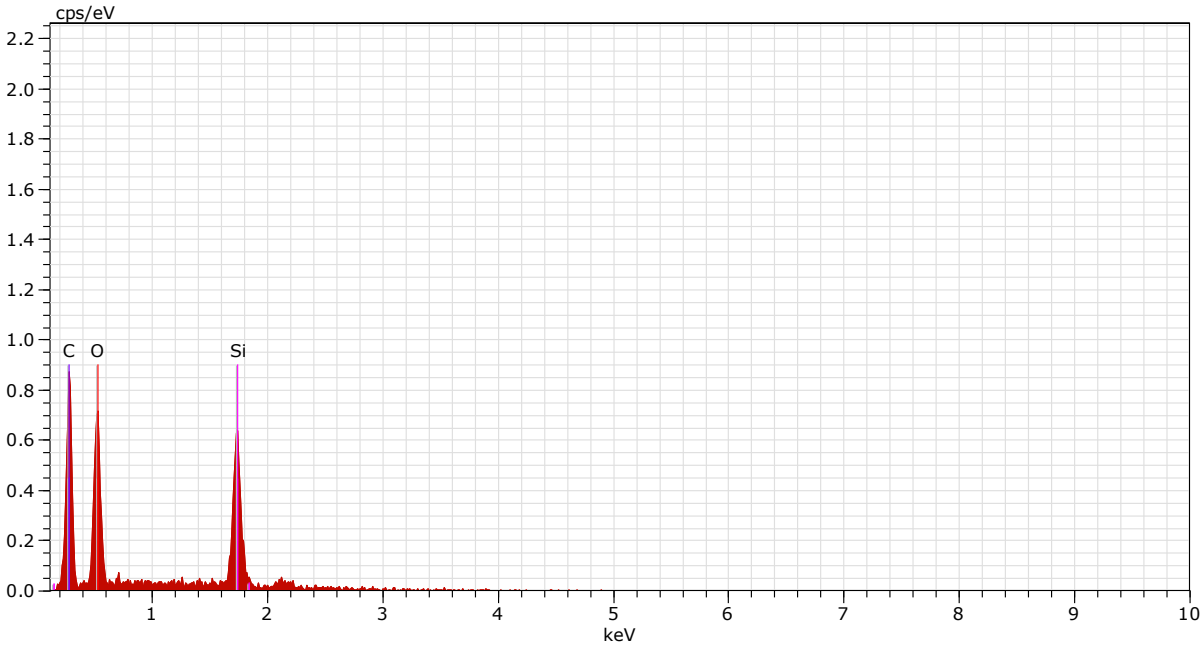

Fig.4.104 EDX for MTMS/PDMS/PMMA

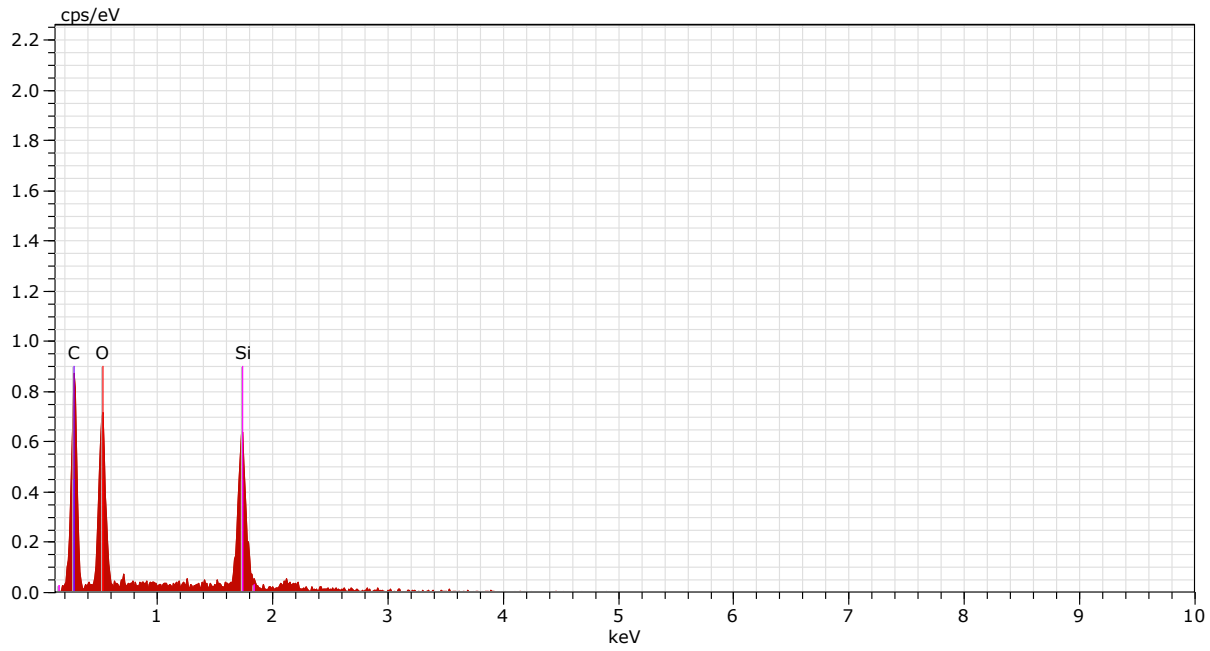

Fig.4.105 EDX for MTMS/PDMS/PS

With EDX (**Figs. 4.103,4.104 and 4.105**), the surface chemical analyzes was carried out and observed the following elements carbon (C), Oxygen(O), and Silica (Si) peaks for MTMS/PDMS/PVDF, MTMS/PDMS/PMMA and MTMS/PDMS/PS surface exhibits Carbon (C), Oxygen (O), and Silica (Si) peaks and Fluorine (F) in addition seen in MTMS/PDMS/PVDF surface as PVDF has fluorine. **Table 4.11** shows the atomic weight percentage of all the elements. This proves the deposition of dirt and impurities-free films by Sol-gel and spin-coating technique were prepared. The histogram of MTMS/PDMS/PVDF, MTMS/PDMS/PMMA and MTMS/PDMS/PS were shown in **Fig.4.106 (a,b and c)** using 3D Zeta profilometer with the average size of 200 nm to 400 nm between the z-steps of 700µm to 1200µm.

Table.4.11 Elemental composition obtained from EDX.

Sample	Atomic Weight (%)			
	C	O	Si	F
MTMS/PDMS/PVDF	53.26	12.24	3.98	30.52
MTMS/PDMS/PMMA	75.23	12.82	11.95	-
MTMS/PDMS/PS	77.85	11.65	10.5	-

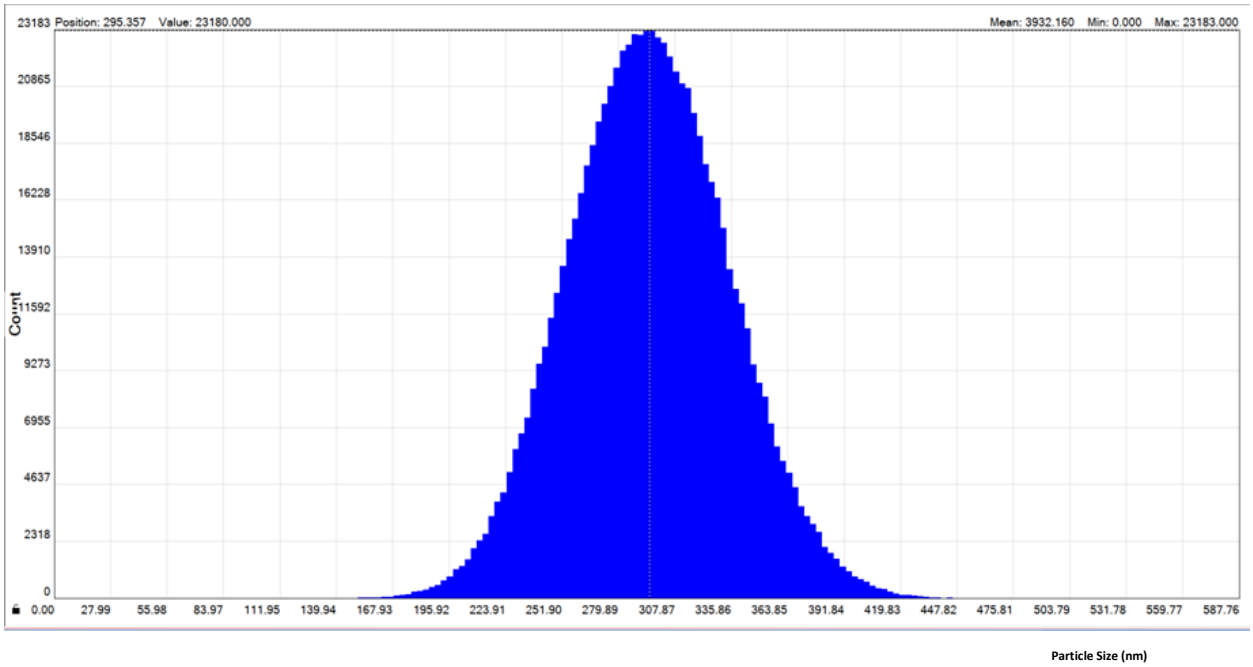

Fig. 4.106 (a) Histogram of MTMS/PDMS/PVDF

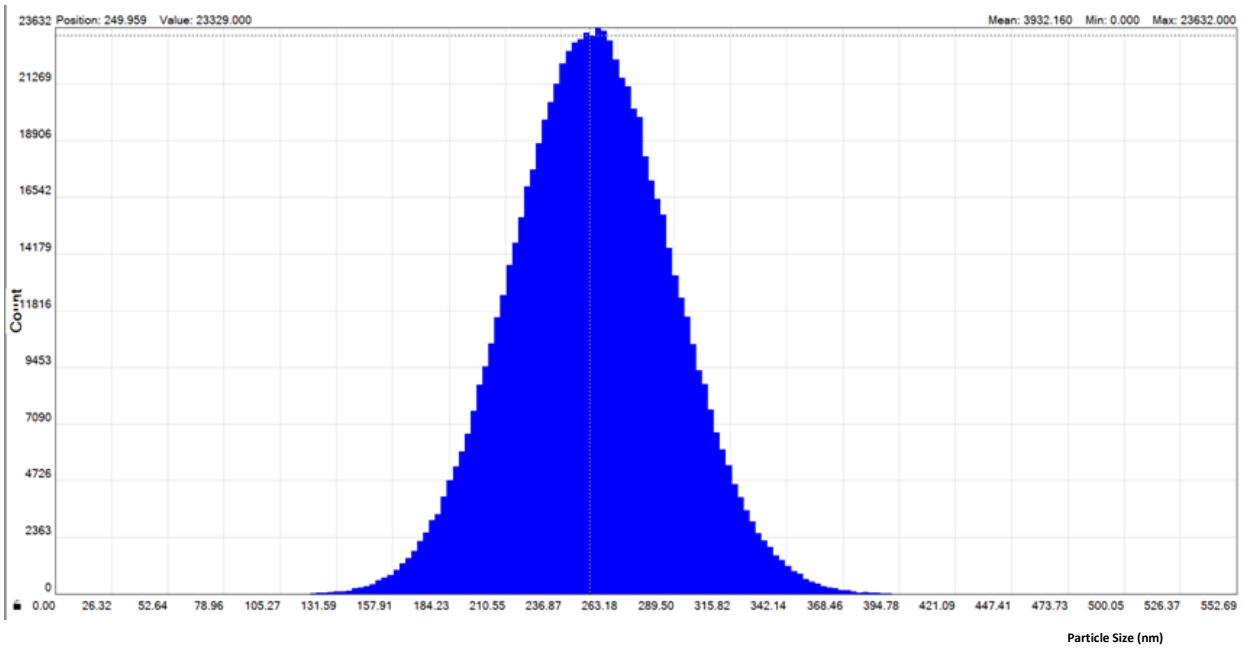

Fig. 4.106 (b) Histogram of MTMS/PDMS/PMMA

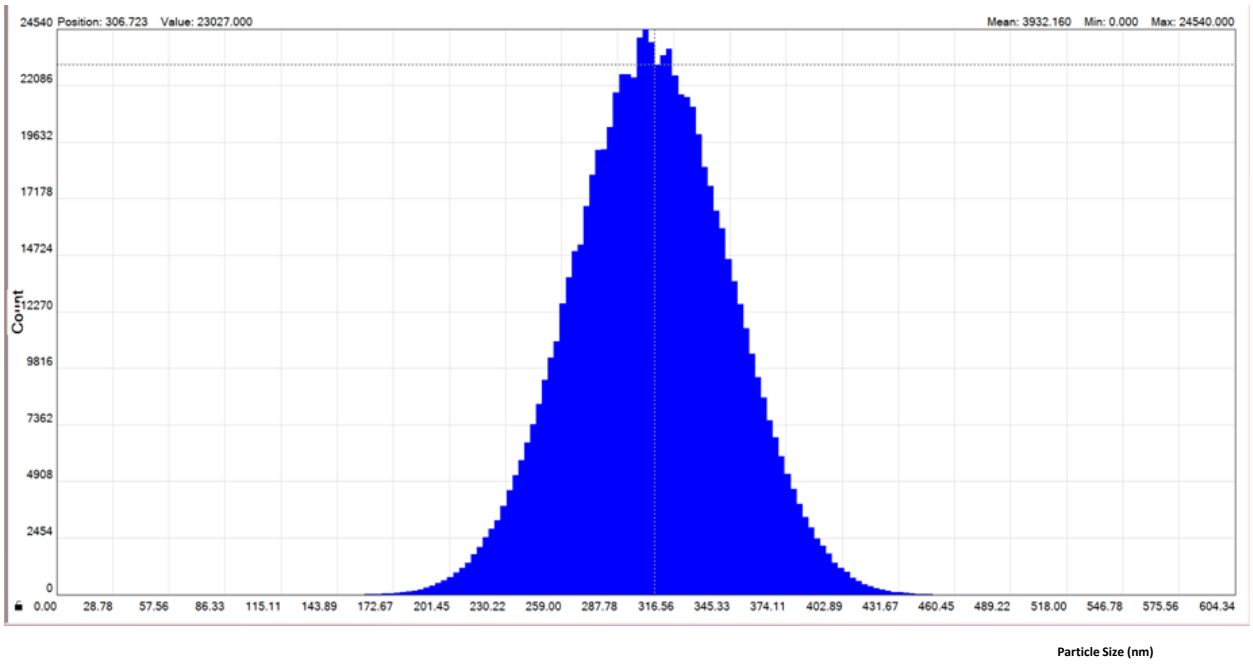

Fig. 4.106 (c) Histogram of MTMS/PDMS/PS

4.3.6.6 TG-DTA

The thermal analysis for MTMS/PDMS/PVDF shows a single stage decomposition with an exothermic peak at 500°C in **Fig.4.107**. Initially the

material loss is less than 5% whereas, in case of MTMS/PDMS/PMMA, multi-stage decomposition is noted due to lack of intermediates in **Fig.4.108**. The exothermic peak at 300°C is due to the emission of volatile and alcoholic compounds. The degradation of polymeric material is seen at 390°C, with the material loss of 18.52%.

The DTA curve for MTMS/PDMS/PS, **(Fig.4.109)** shows a small bump initially at 180°C, the glass transition temperature of PS. In general, polystyrene exhibit such a bump, to show its steric nature. The decomposition of polymeric material is seen at 410°C, with a loss of 10.202%.

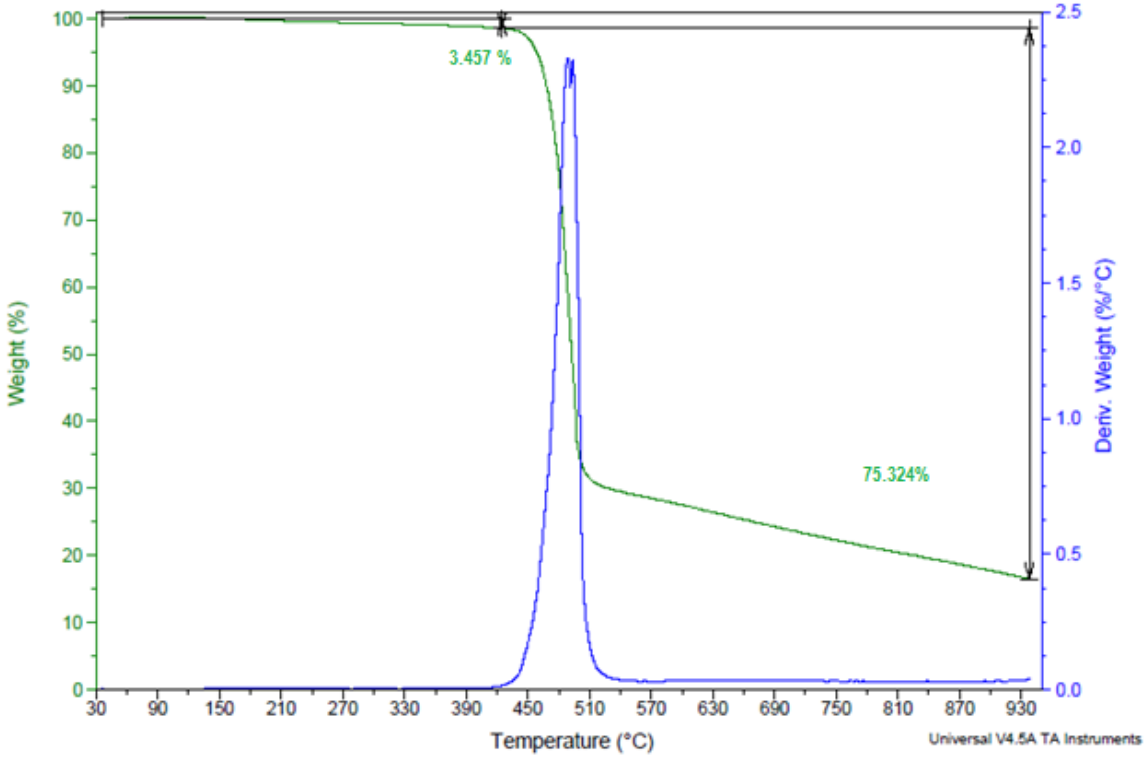

Fig.4.107 TG-DTA for MTMS/PDMS/PVDF

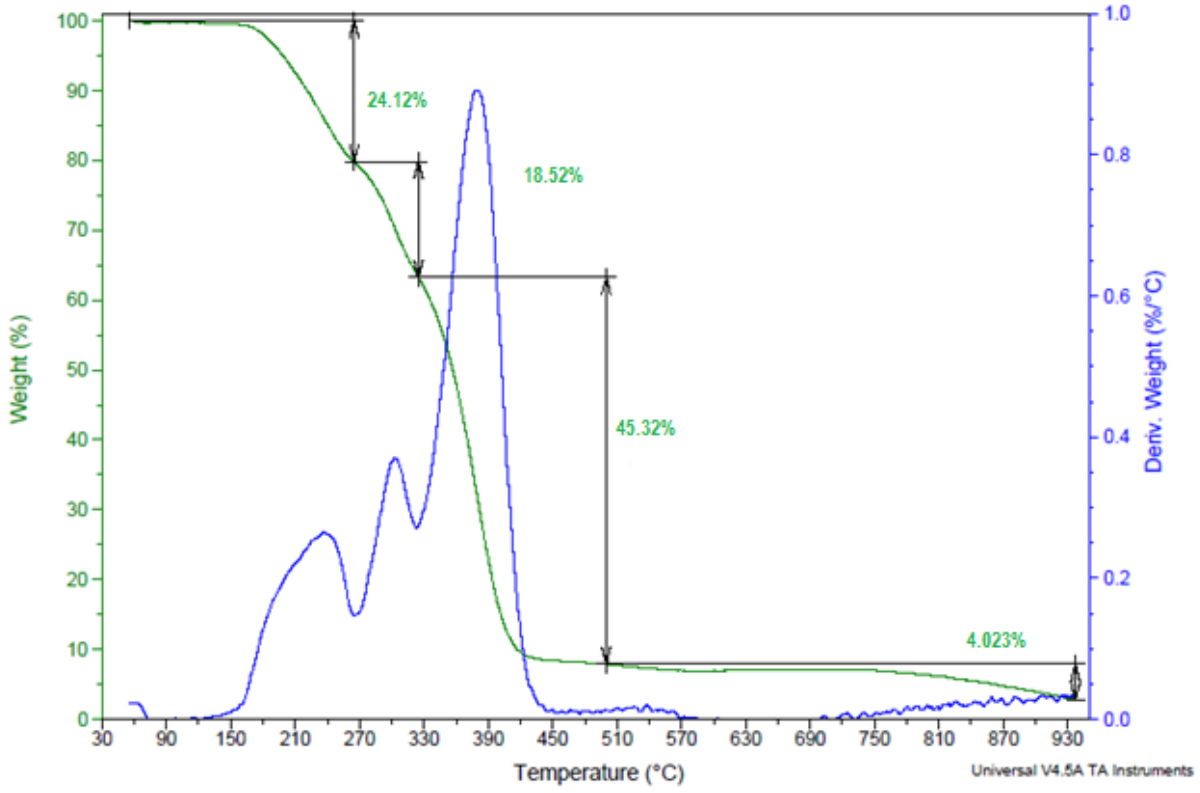

Fig.4.108 TG-DTA for MTMS/PDMS/PMMA

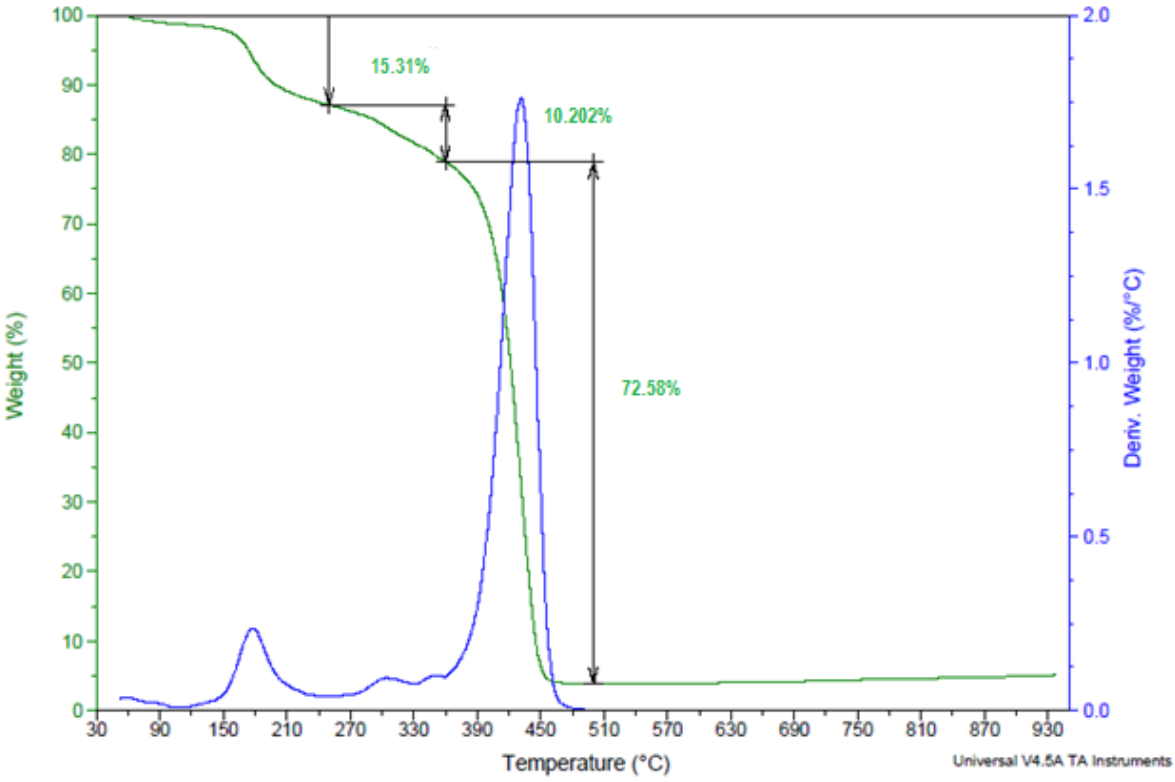

Fig.4.109 TG-DTA for MTMS/PDMS/PS

4.3.6.7 Application

The MTMS/PDMS/Polymer coated substrates were shown in the **Fig.4.110 (a),(b) and (c).** These substrates were proved for self cleaning application. 2 grams of dust particles were kept on the coated substrate. On allowing 4µl of water on this substrate, the dust particles got clinged to the water droplet and makes the substrate dirt free.

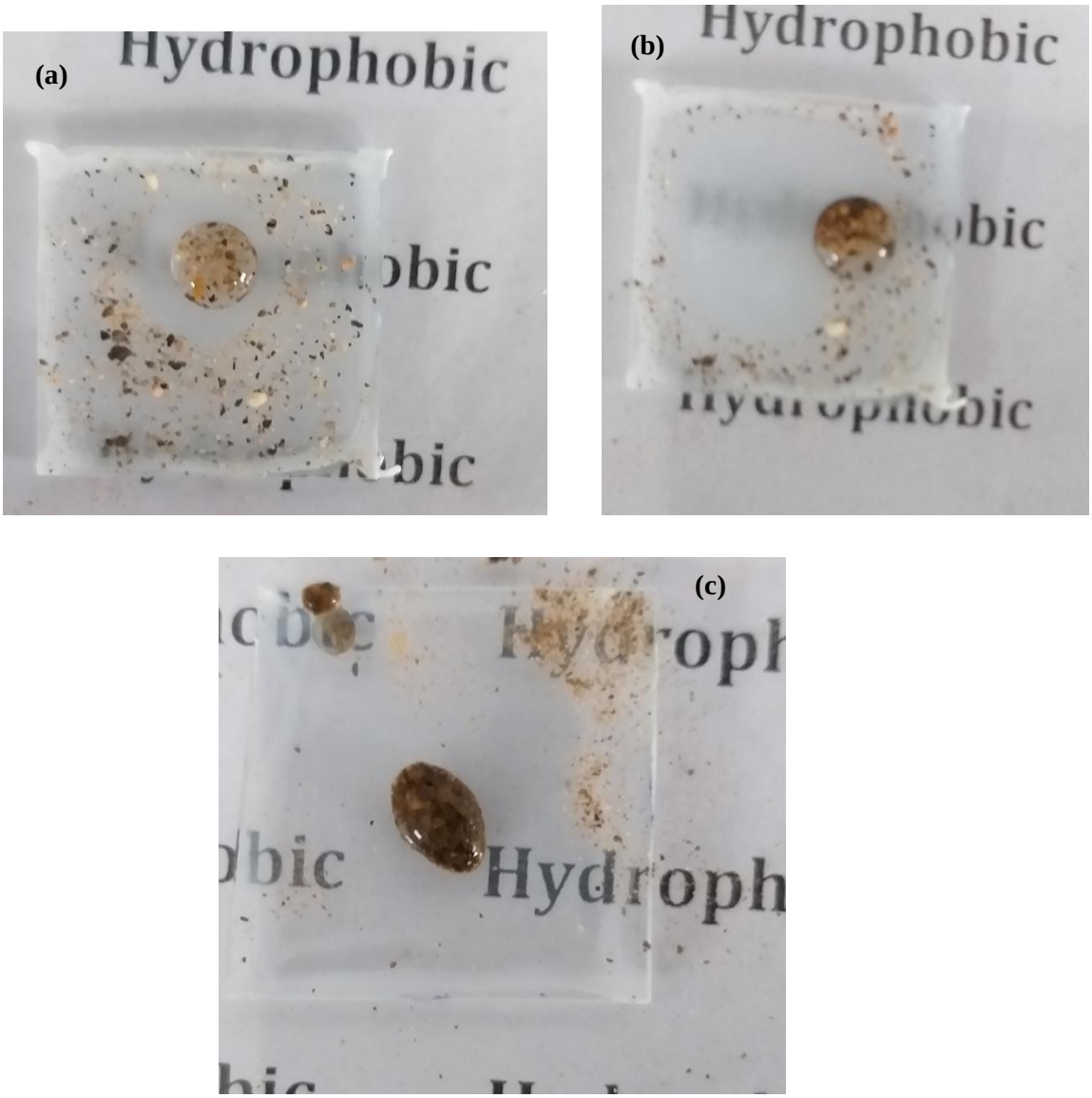

Fig. 4.110 (a)MTMS/PDMS/PVDF, (b) MTMS/PDMS/PMMA and (c) MTMS/PDMS/PS Coated substrates

4.3.7 SET – VII [TEOS + MTMS +PDMS +Polymer]

4.3.7.1 FTIR

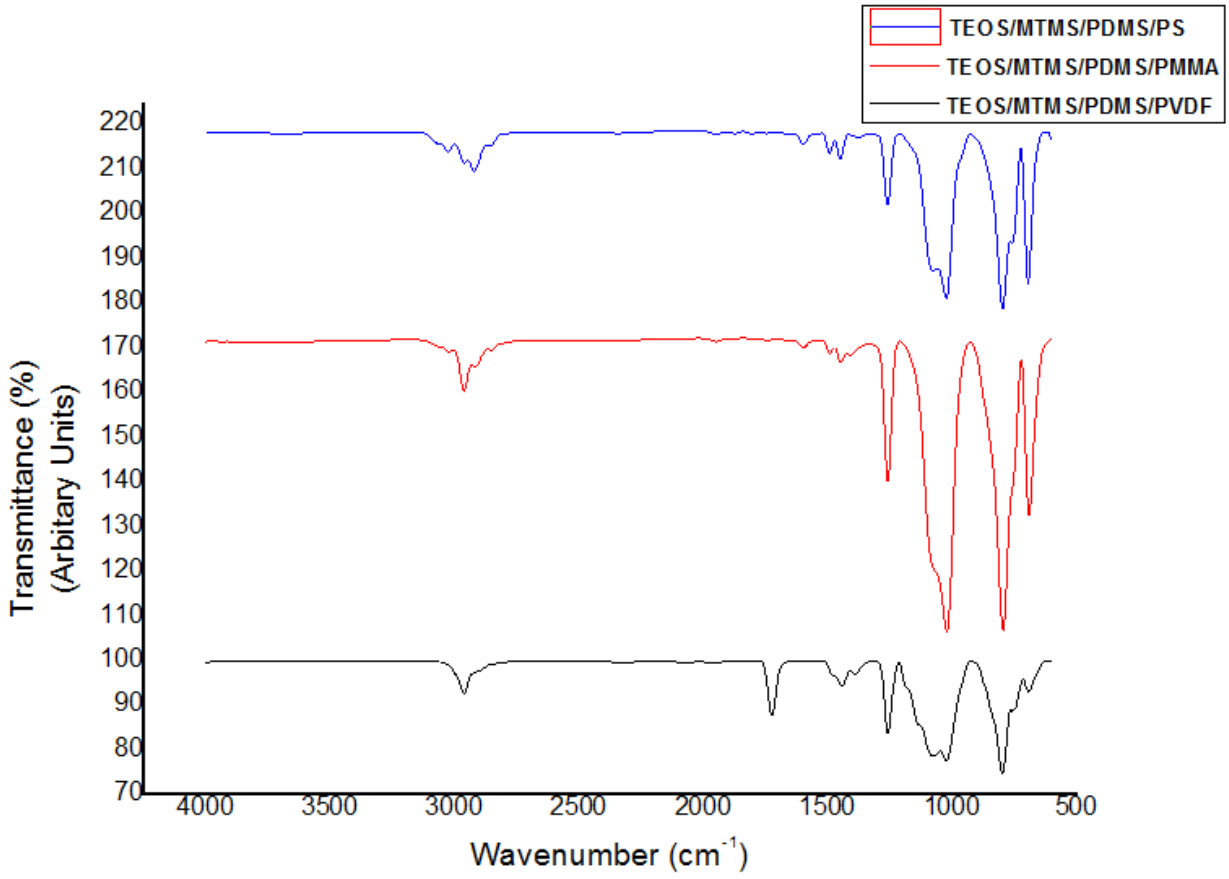

Fig. 4.111 FTIR spectrum of TEOS/MTMS/PDMS/PVDF, TEOS/MTMS/PDMS/PMMA and TEOS/MTMS/PDMS/PS

The **Fig. 4.111** shows the FTIR spectrum of TEOS/MTMS/PDMS/Polymer. This ensures the presence of functional group. Si-OH bond has been formed at 970 cm^{-1} and this ensures hydrolysis. Simultaneously, the peak at 1087cm^{-1} represents Si-O-Si stretching in the cyclic structure, which has been deformed to the linear structure at 1066cm^{-1} in TEOS/MTMS/PDMS/ PVDF composite. The band at 1168cm^{-1} has been noted as C-H rocking (CH_3) which decreases with the reaction time due to hydrolysis of TEOS.

In case of TEOS/MTMS/PDMS/PMMA, the absorption peaks at 1483 cm^{-1} and 1145 cm^{-1} represents deformation of CH_3 group whereas the peak at 905cm^{-1} notes the rocking mode **[Mas Rosemal et al., 2010].** The peaks at 1029 cm^{-1} and 1103 cm^{-1} are assigned to the stretching mode of Si-O-Si. The condensation of the hydrolyzed MTMS and the presence of methyl group were indicated with C-H stretching and bending vibration modes of Si-CH_3 at 2970 cm^{-1}, 1408 cm^{-1} and 1269 cm^{-1} . By Silylation process, the Si-OR group undergoes hydrolysis and condensation. If peak is seen above 3200 cm^{-1}, it would have referred to Si-OH hydrophilic groups due to hydrolysis. Here, due to condensation two peaks are obtained at 2949 cm^{-1} and 2992 cm^{-1} which tends to C-H symmetric and asymmetric stretching and this confirms the hydrophobic group **[Marielen Longhi et al., 2015].**

Incase of TEOS/MTMS/PDMS/PS composite film, the absorption peaks at 3024 cm^{-1} represents aromatic C-H stretching vibration. C-H deformation vibration is seen at 694 cm^{-1}. The intense peak at 1600 cm^{-1}, 1491 cm^{-1}, 1451cm^{-1} has been obtained due to aromatic C-H bond stretching vibration **[Xin Fan et al., 2012].** The absorbance peak at 905 cm^{-1} is strong and indicates the amorphous phase **[Hew-Der Wu et al., 2001]**. The peak at 2921.61 cm^{-1} represents the C-H stretching vibration mode.

4.3.7.2 Contact Angle

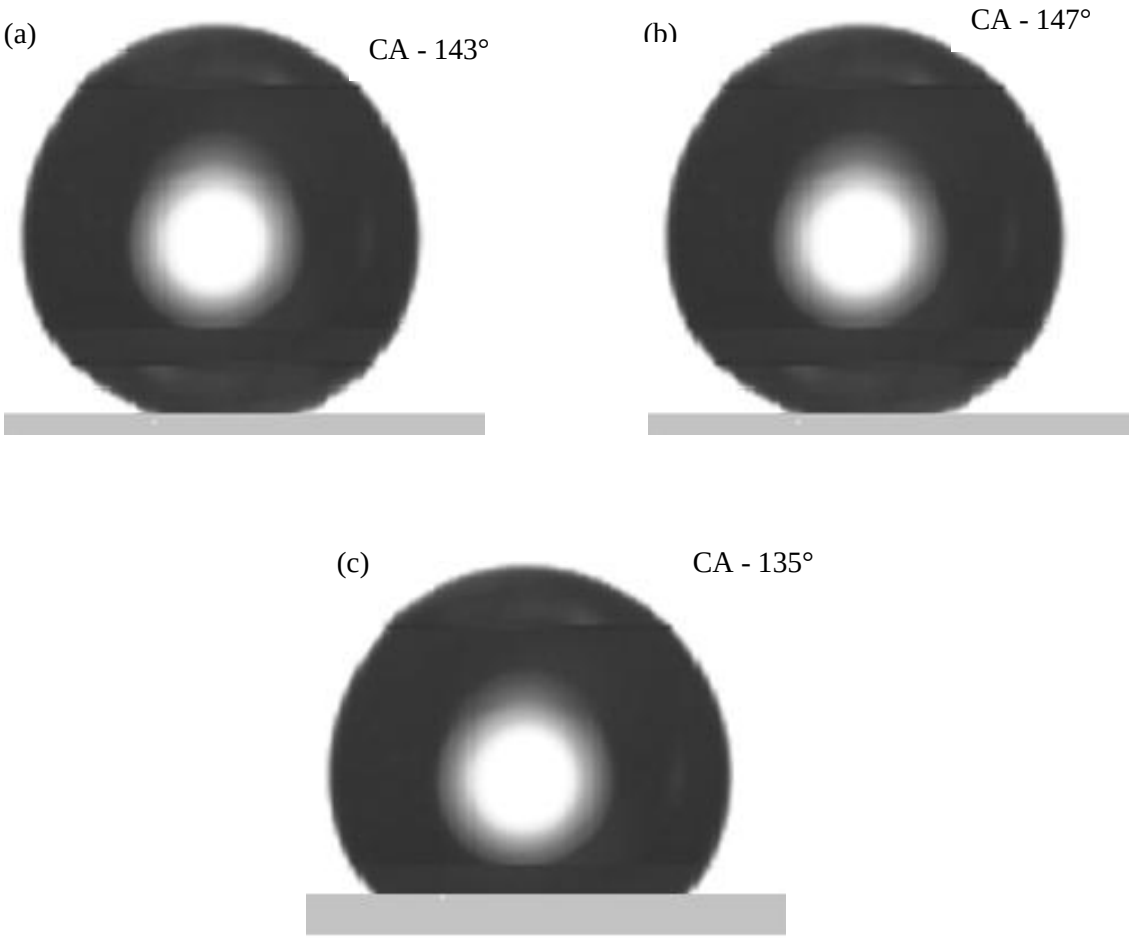

Fig 4.112 Contact angle for (a)TEOS/MTMS/PDMS/PVDF, (b)TEOS/MTMS/PDMS/PMMA and (c) TEOS/MTMS/PDMS/PS

The contact angle for TEOS/MTMS/PDMS/Polymer is shown in the **Fig.4.112** and found that all the composite films has contact angle greater than 130°, implanting the super-hydrophobic nature. The static contact angle proves the films non-wettable nature.

4.3.7.3 Surface Roughness and Surface Energy

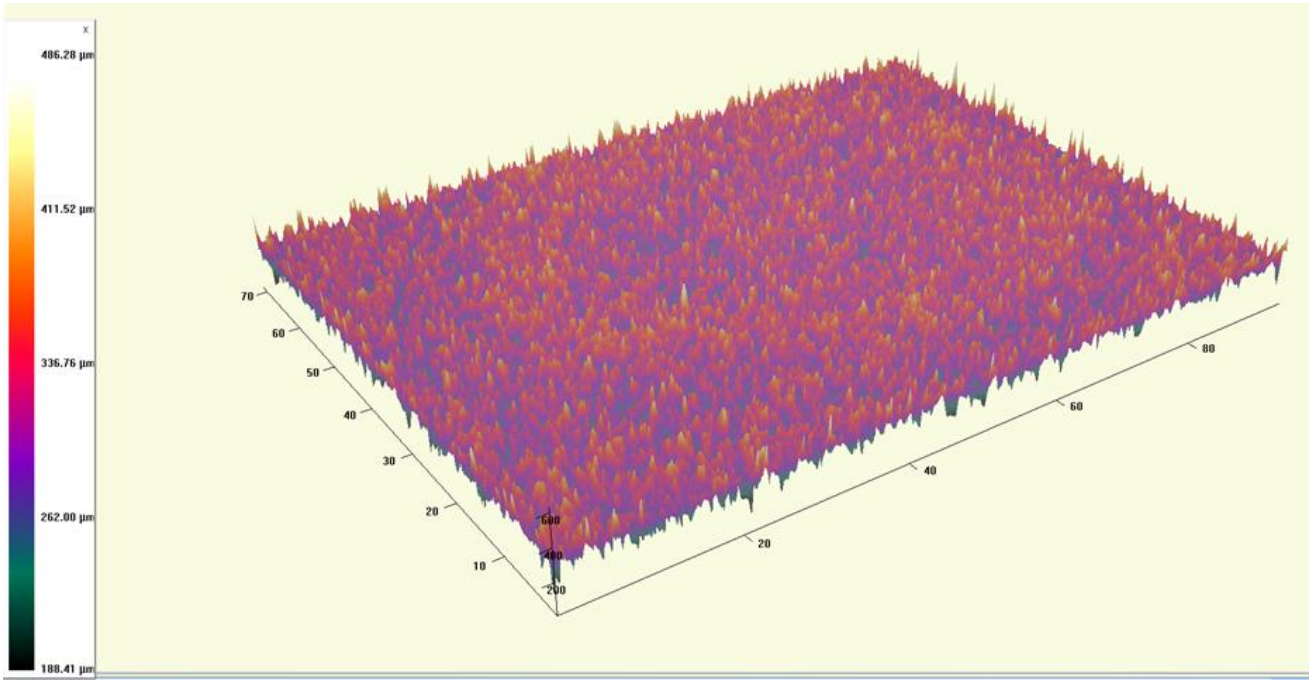

Fig. 4.113 Surface Roughness for TEOS/MTMS/PDMS/PVDF

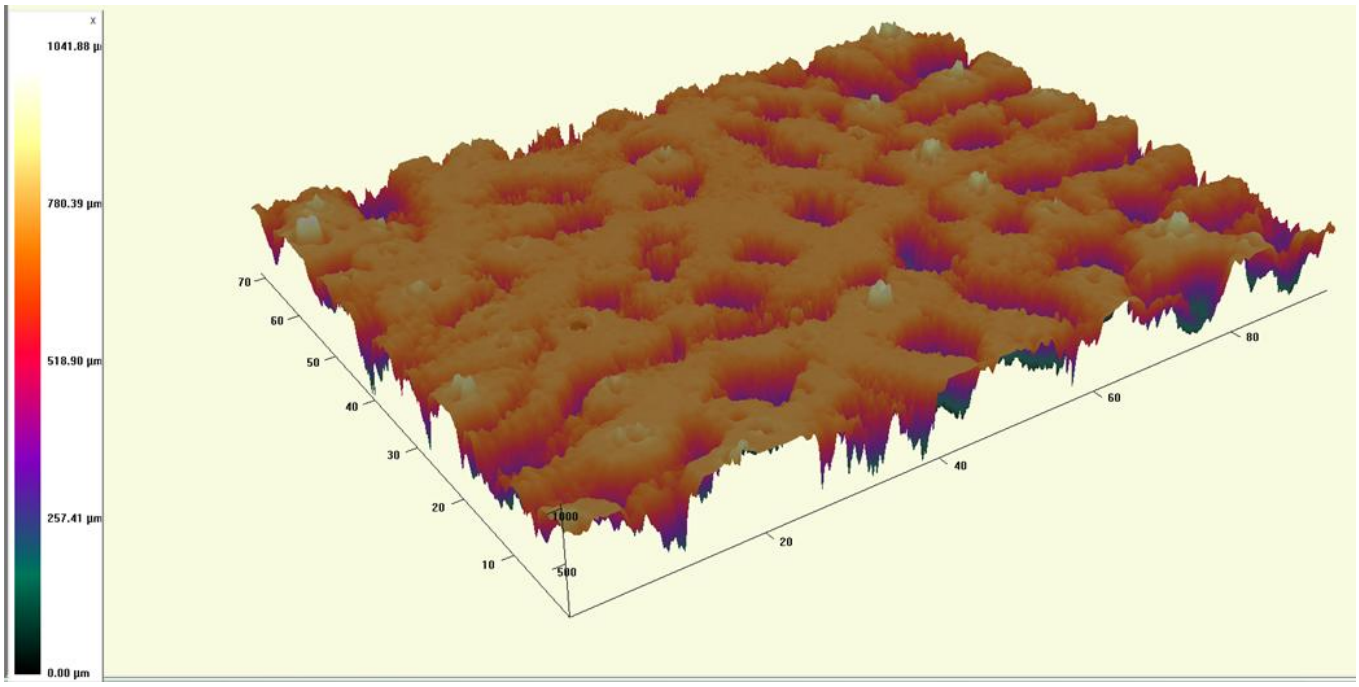

Fig. 4.114 Surface Roughness for TEOS/MTMS/PDMS/PMMA

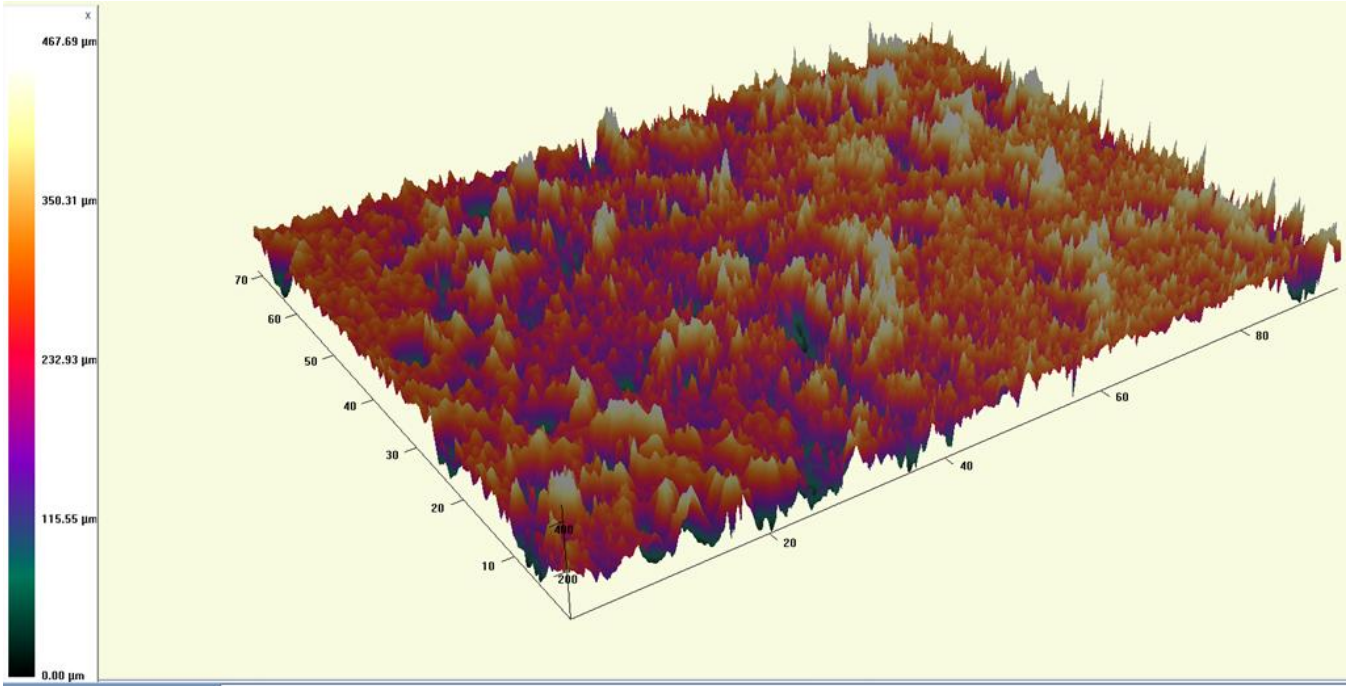

Fig. 4.115 Surface Roughness for TEOS/MTMS/PDMS/PS

The surface roughness and surface energy are inter-related. As the roughness increases, the surface energy decreases. With methoxy group presence, the hydrophobic nature can be enhanced. Hence, on adding all the three silanes (TEOS, MTMS and PDMS) with polymer makes the film more effective for non-wettable character. With the hamaker's constant , the surface energy can be computed. 3D Zeta profilometer (**Figs. 4.113,4.114 and 4.115**) was used to determine the surface roughness with the z-step between 700µm to 1200µm. **Table 4.12** shows the surface roughness and surface energy.

Table.4.12 - Surface Roughness and Thickness Measurement of the coated films

Sample	Hamaker Constant A_n (J x 10^{-21})	Surface Roughness, Ra (μm)	Surface energy, ϒ (Jm^{-1})	Contact Angle, CA (°)	Thickness (μm)
TEOS/MTMS/PDMS /PMMA	1.524	58.12	17.49	147°	14.6
TEOS/MTMS/PDMS /PVDF	2.086	54.35	18.57	143°	13.4
TEOS/MTMS/PDMS /PS	1.962	50.74	21.4	135°	11.2

4.3.7.4 UV-Visible Spectroscopy

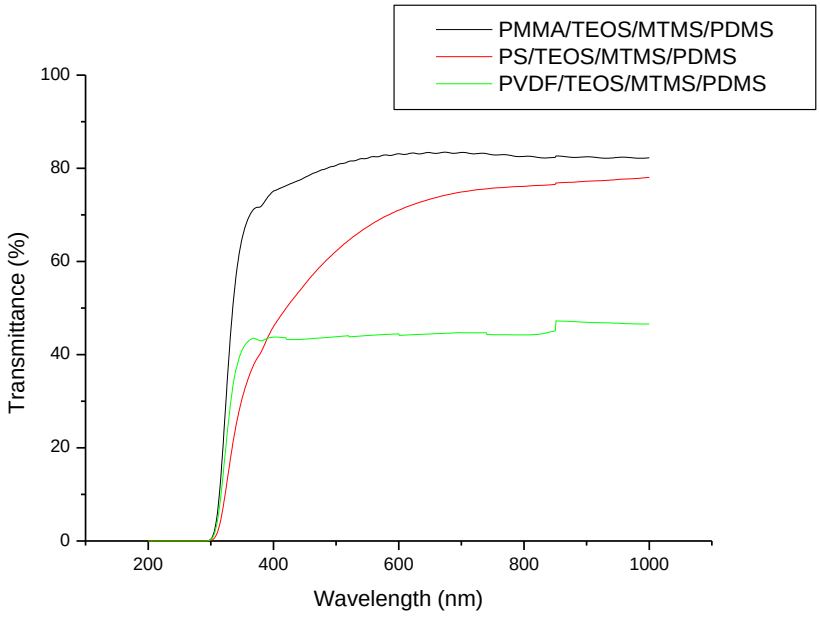

Figure 4.116 UV-Visible Spectrum for TEOS/MTMS/PDMS/Polymer

The **Fig.4.116** shows the UV-Visible spectrum of all the polymers blended with TEOS/MTMS/PDMS. All the three polymers were mixed with TEOS, MTMS and PDMS. The transparency for PVDF blended with TEOS/MTMS/PDMS was enhanced to 42%. The presence of ethoxy group of TEOS increases the % of transmittance for PMMA and PS films to 75% and 65% respectively. Hence, the prepared films were optically transparent and superhydrophobic in nature.

4.3.7.5 FESEM

The **Figs.4.117, 4.119, 4.121** represents TEOS/MTMS/PDMS/PVDF, TEOS/MTMS/PDMS/PMMA and TEOS/MTMS/PDMS/PS film structures. For TEOS/MTMS/PDMS/PVDF, the surface is not even. The surface has some spherical structure due to the presence of vinyledene. On closer interpretation, the spherical structure has nano bumps due to the presence of methoxy silane.. It has flaps as in case of non-wettable surfaces. The EDX spectrum (**Figs. 4.118, 4.120 and 4.122**) for all the films were determined to ensure the dirt free films. The Histogram of TEOS/MTMS/PDMS/Polymer is shown in the **Figs.4.123 (a,b,c)** with the z-steps between 750μm to 1350μm.

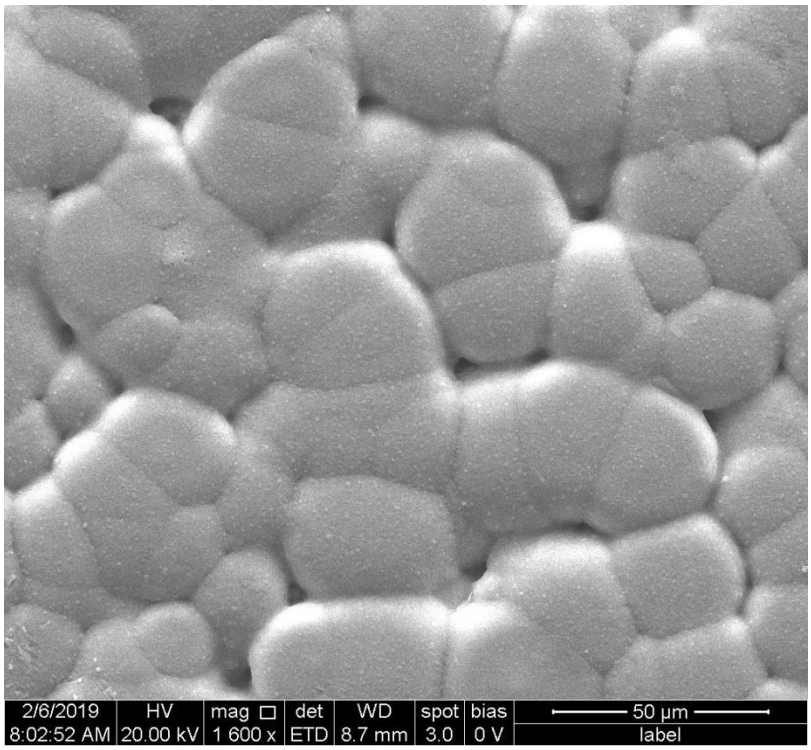

Figure.4.117 FE-SEM of TEOS/MTMS/PDMS/PVDF

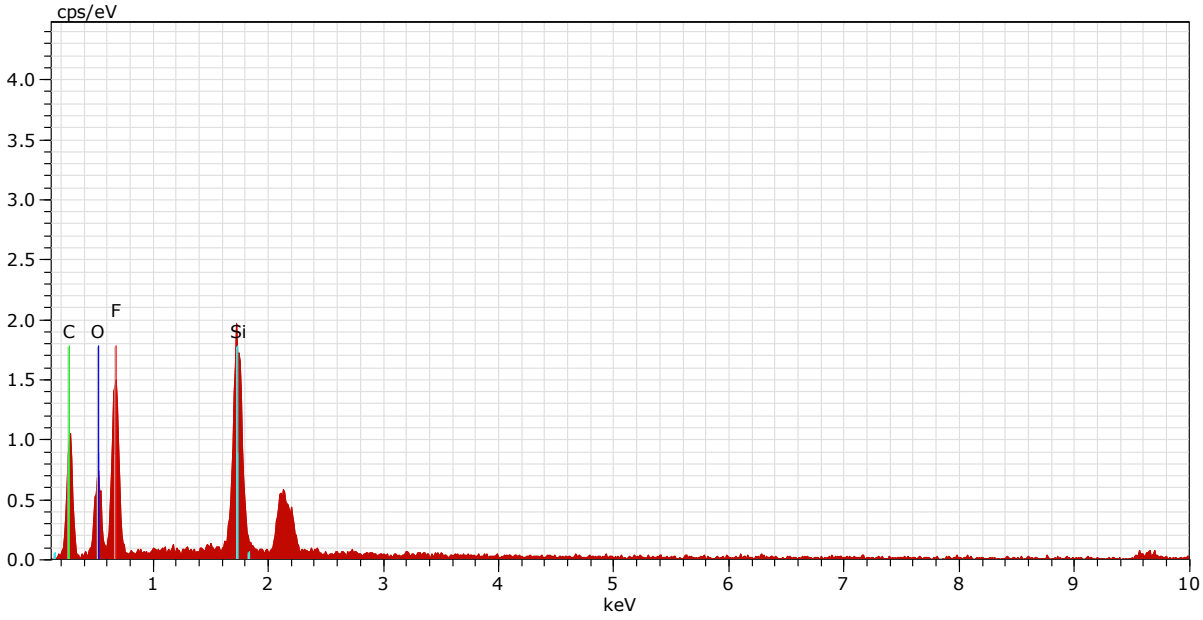

Figure.4.118 EDX for TEOS/MTMS/PDMS/PVDF

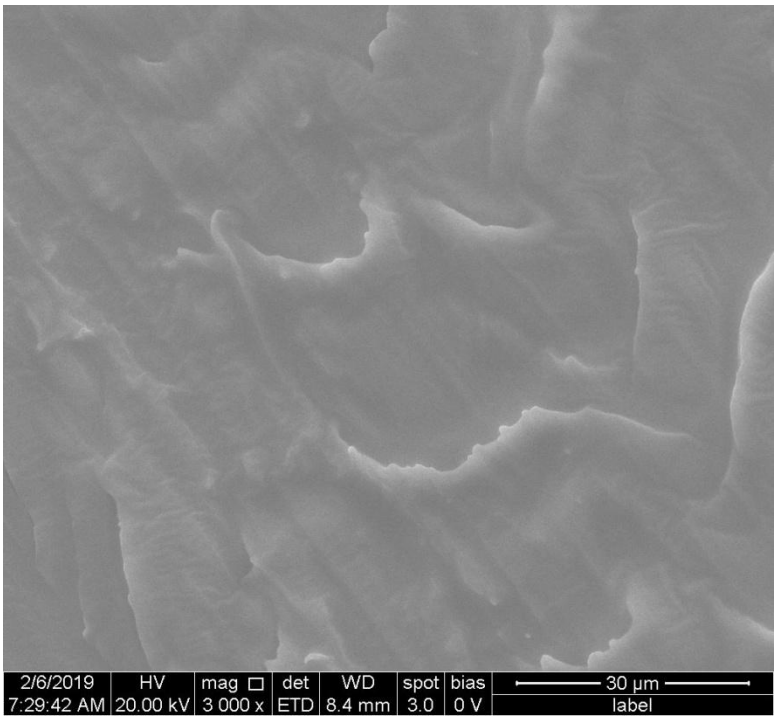

Figure.4.119 FE-SEM of TEOS/MTMS/PDMS/PMMA

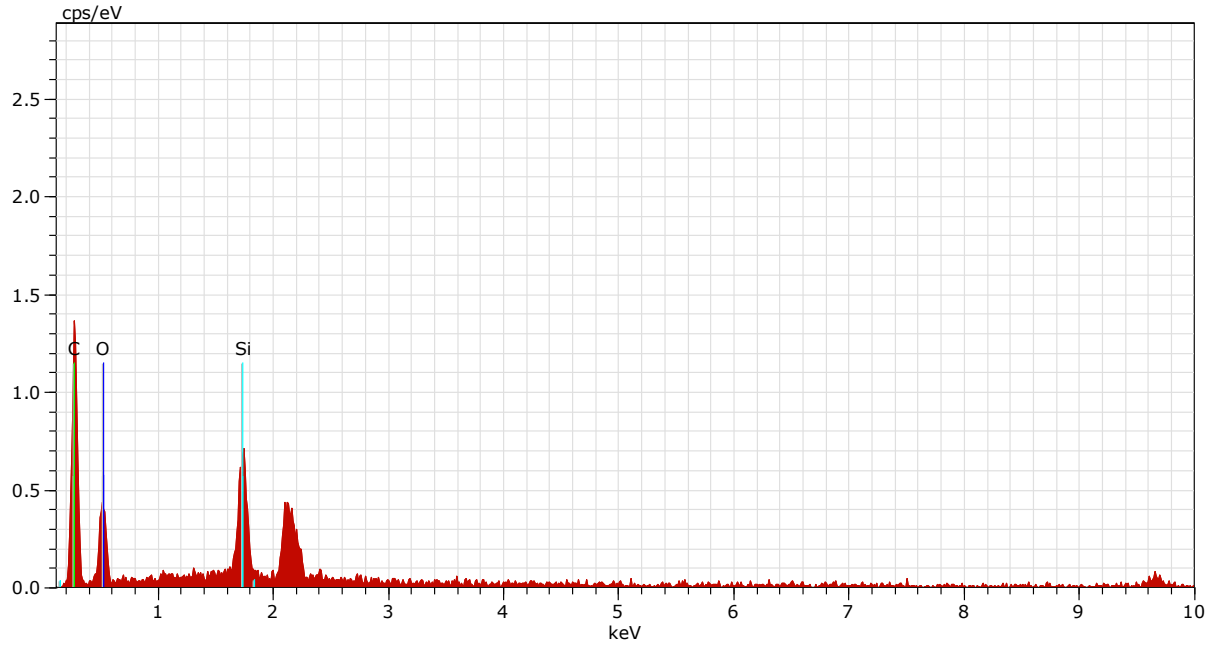

Figure4.120 EDX for TEOS/MTMS/PDMS/PMMA

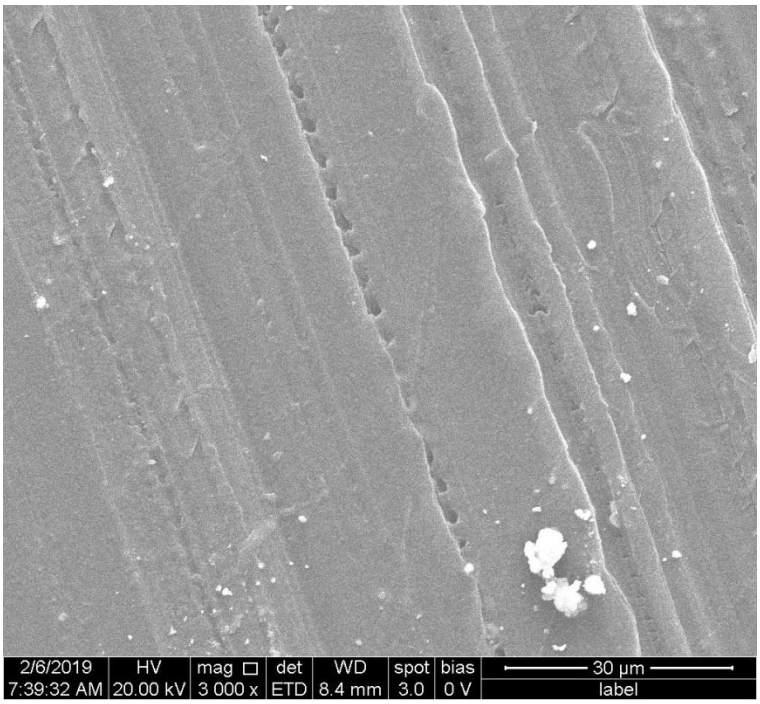

Figure.4.121 FE-SEM of TEOS/MTMS/PDMS/PS

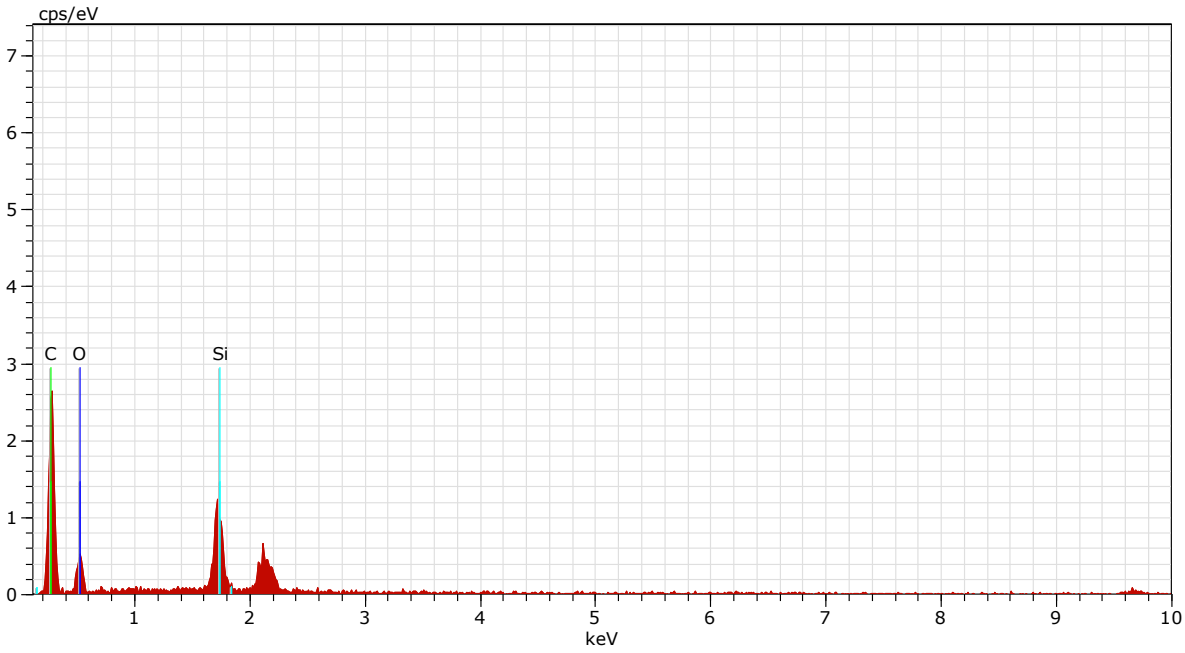

Figure. 4.122 EDX for TEOS/MTMS/PDMS/PS

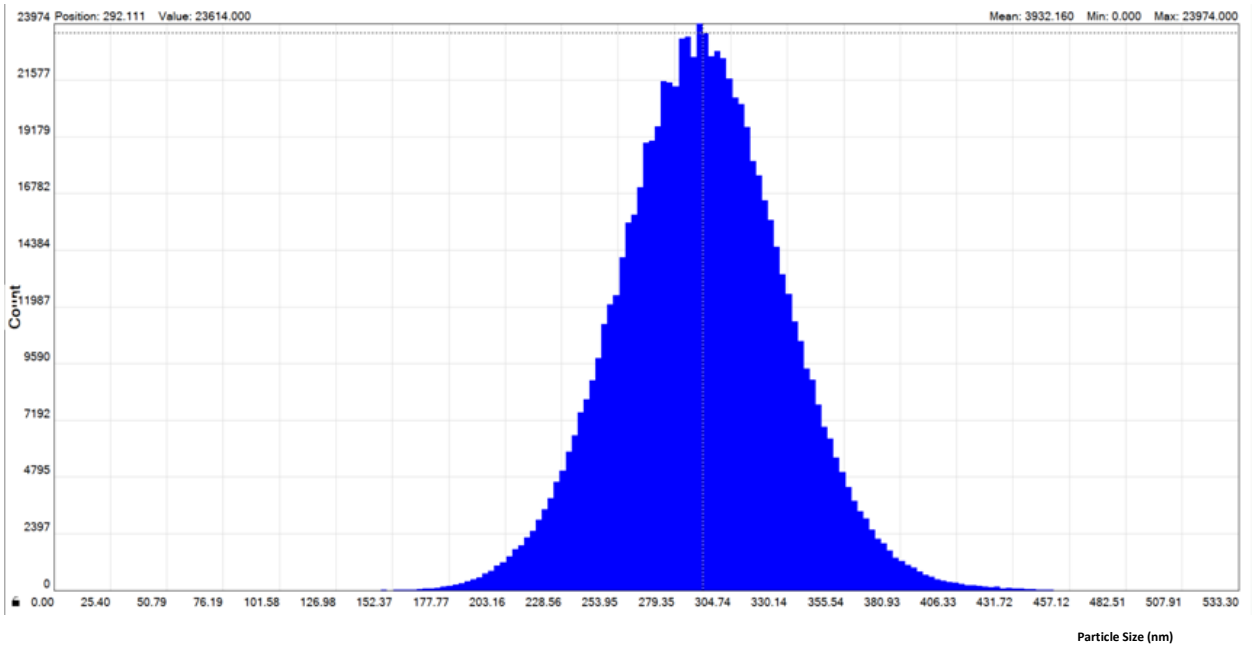

Figure. 4.123(a) Histogram for TEOS/MTMS/PDMS/PVDF

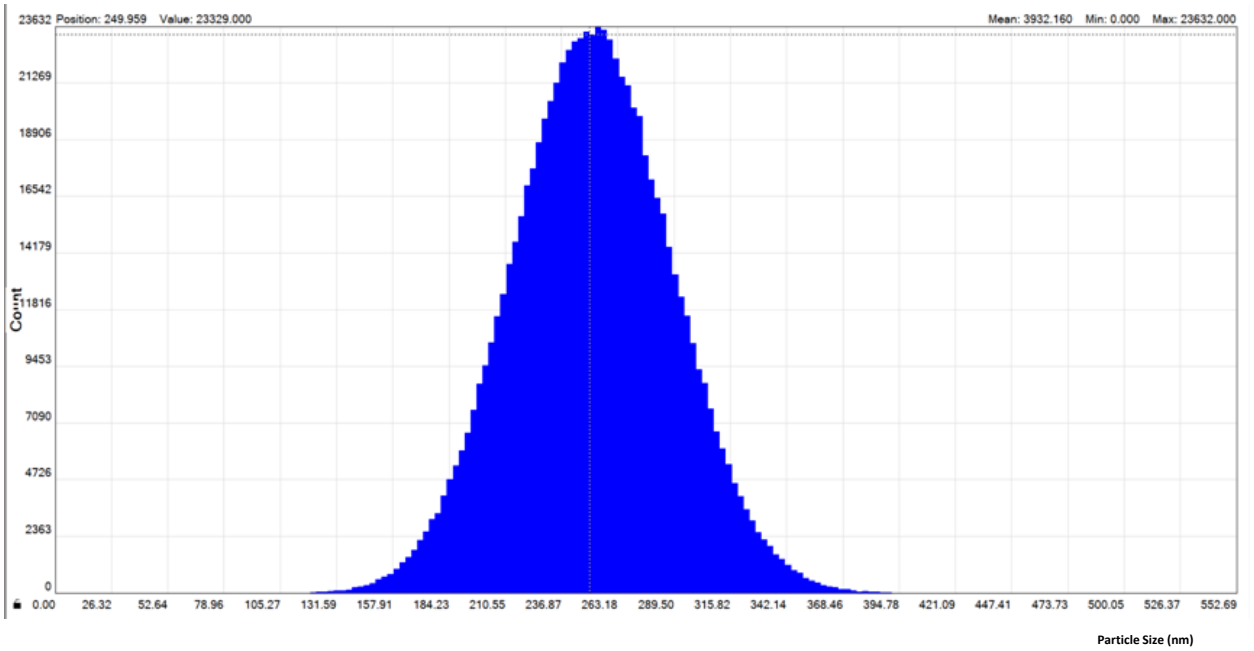

Figure. 4.123(b) Histogram for TEOS/MTMS/PDMS/PMMA

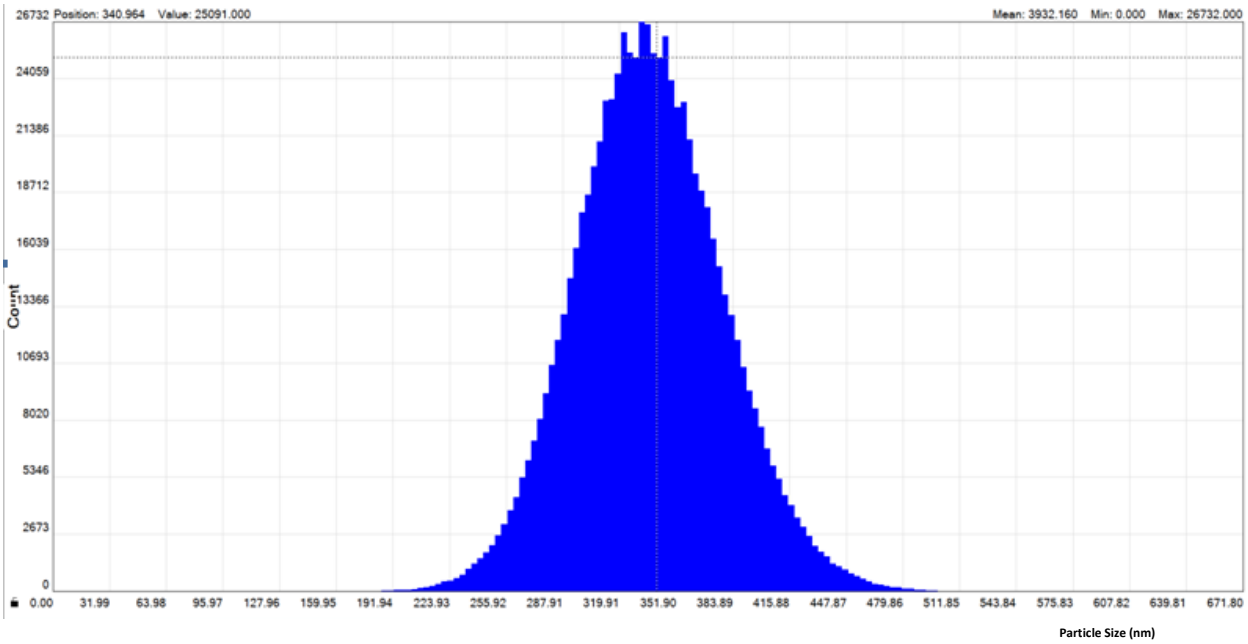

Figure. 4.123(c) Histogram for TEOS/MTMS/PDMS/PS

4.3.7.6 TG-DTA

The thermal analysis has been carried out for all the films **(Fig. 4.124,4.125 and 4.126).** Incase of TEOS/MTMS/PDMS/PVDF, the thermal stability is better. It undergoes single-stage decomposition with single exothermic peak at 490°C. Major weight loss was observed in the range 510-930ºC for the prepared sample. This could corresponds to structural decomposition of the polymer blend and their complexes. TEOS/MTMS/PDMS/PMMA shows two-stage decomposition with the material loss at 300°C and 390°C. This behaviour also indicates the random chain scission process of PMMA polymer that undergoes during degradation Even,the styrene film shows better thermal stability. There is single-stage decomposition of the polymeric material at 410°C.

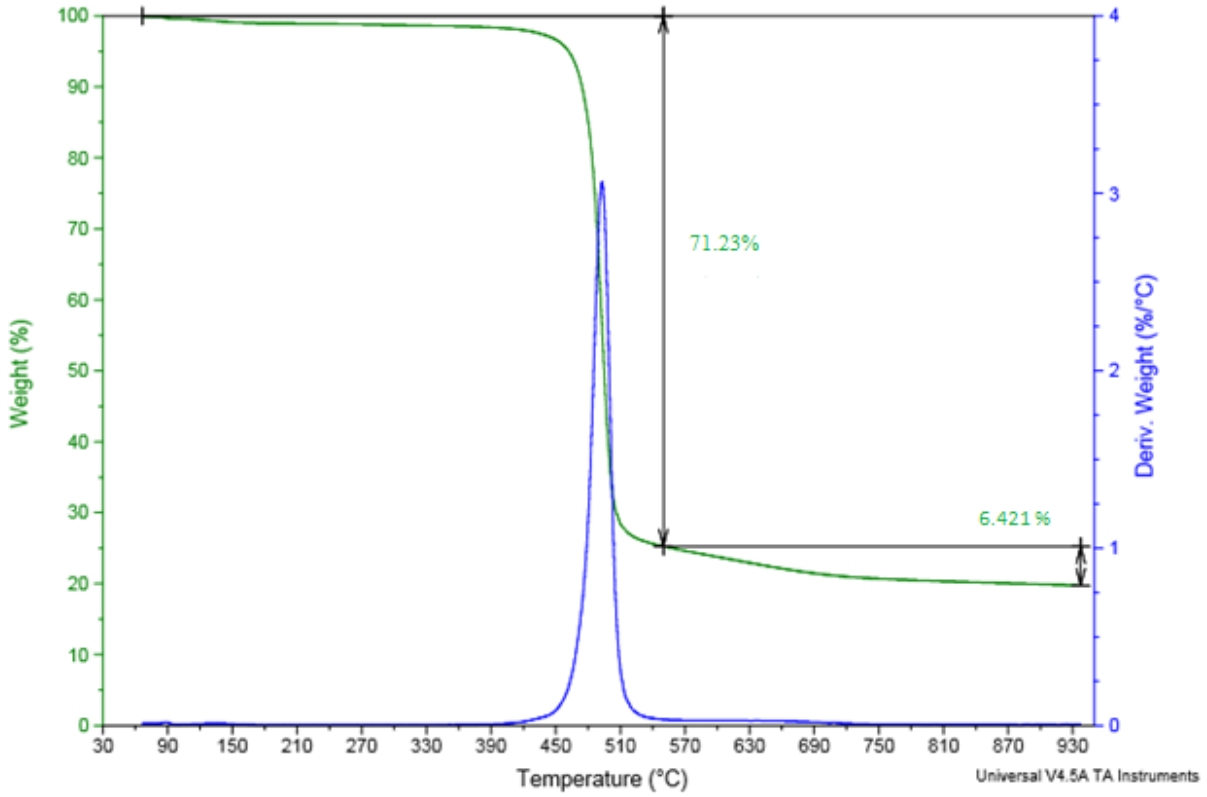

Figure.4.124 TG-DTA for TEOS/MTMS/PDMS/PVDF

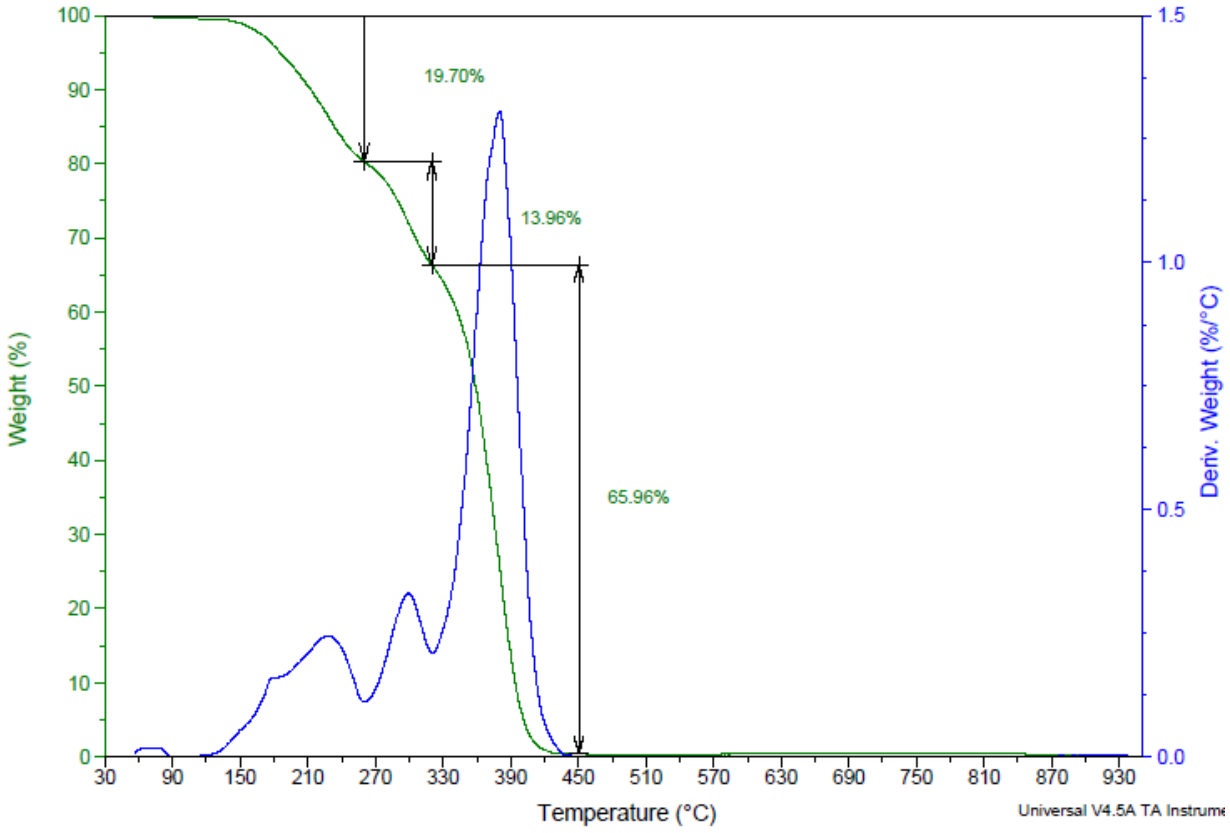

Figure4.125 TG-DTA for TEOS/MTMS/PDMS/PMMA

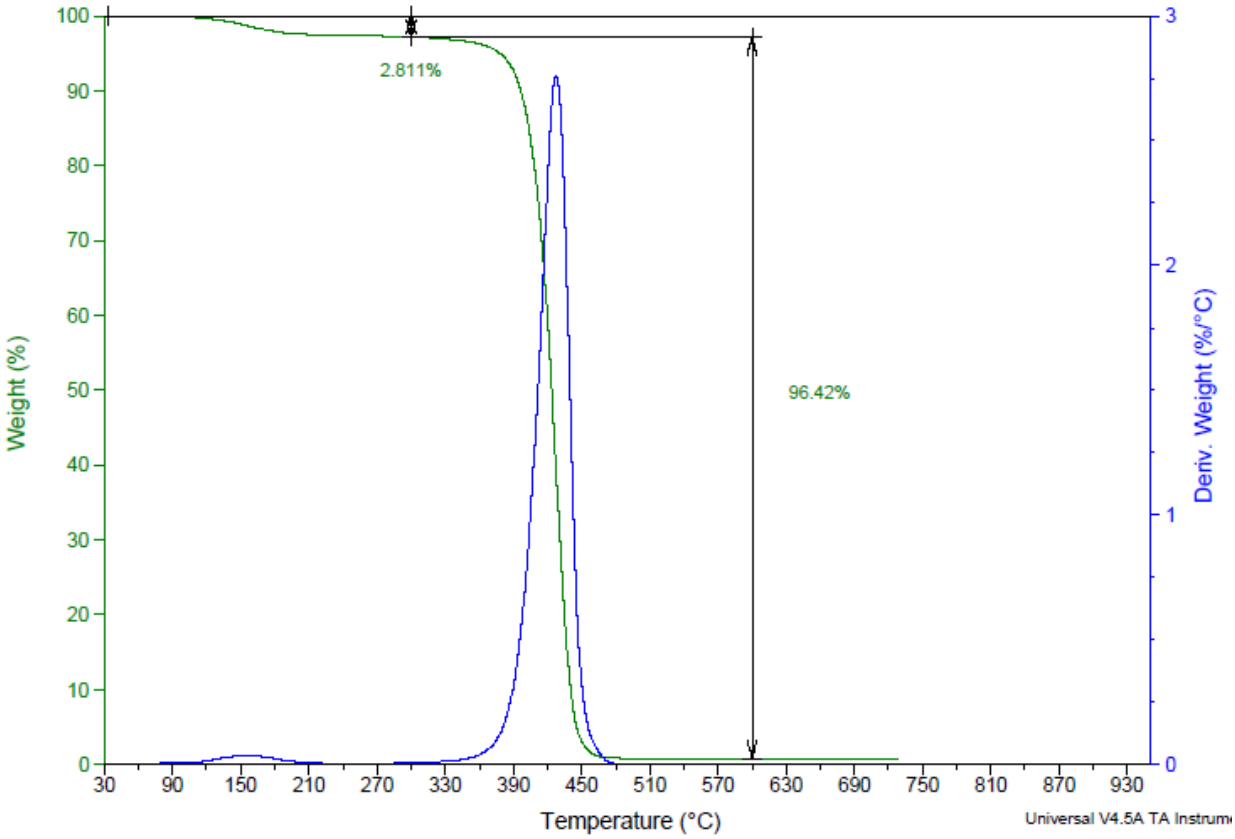

Figure.4.126 TG-DTA for TEOS/MTMS/PDMS/PS

4.3.7.7 Application

Self-cleaning and oil-water separation application have been proved. 2 gram of dust particles were placed on the coated substrates. 2µl of water was allowed on the coated substrates. Water droplet gets beaded up along with the dust particles as shown in the **Fig.4.127 (a,b and c).** Filter paper was used to separate oil and water. Filter paper was coated with TEOS/MTMS/PDMS/PVDF, TEOS/MTMS/PDMS/PMMA and TEOS/MTMS/PDMS/PS solutions. 30 ml of water and 10 ml of oil (Kerosene) were mixed together. The mixture was filtered using the coated filter paper. 24.6 ml of water was filtered and collected using TEOS/MTMS/PDMS/PMMA coated filter paper as shown in the **Fig.4.128**.

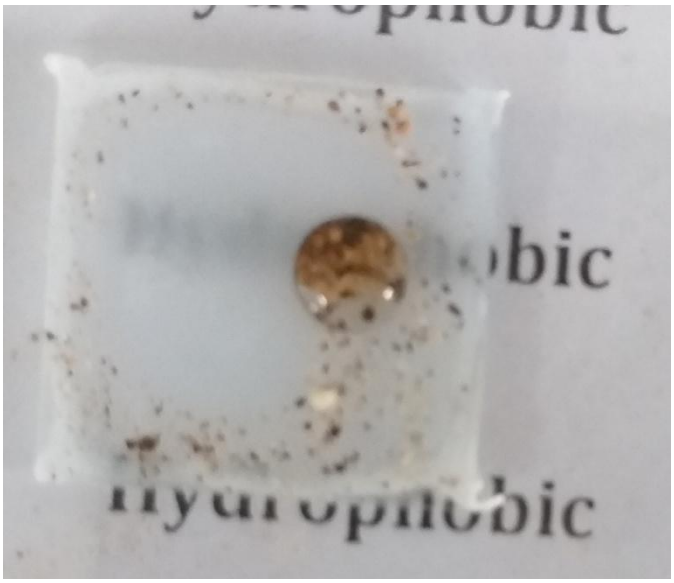

Fig. 4.127 (a) TEOS/MTMS/PDMS/PVDF coated substrate

Fig. 4.127 (b) TEOS/MTMS/PDMS/PMMA coated substrate

Fig. 4.127 (c) TEOS/MTMS/PDMS/PS coated substrate

Step- I

(Mixture of Kerosene oil& Water)

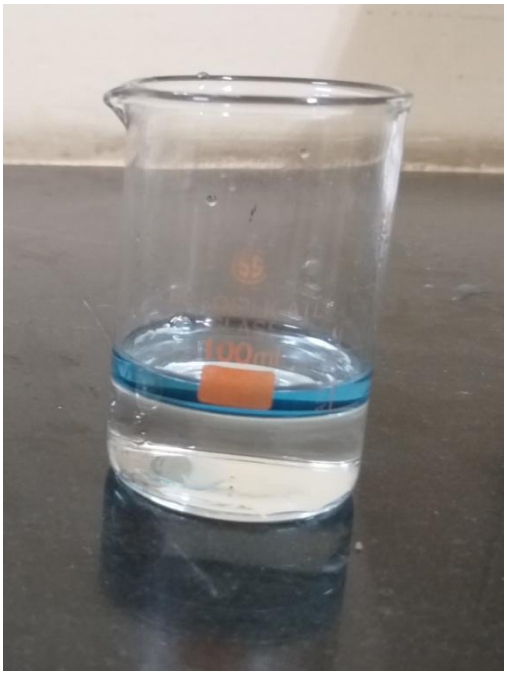

Step- II

(a)TEOS/MTMS/PDMS /PVDF

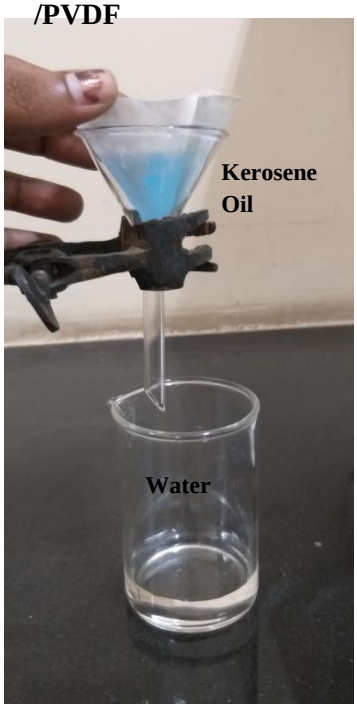

(b)TEOS/MTMS/PDMS/ PMMA

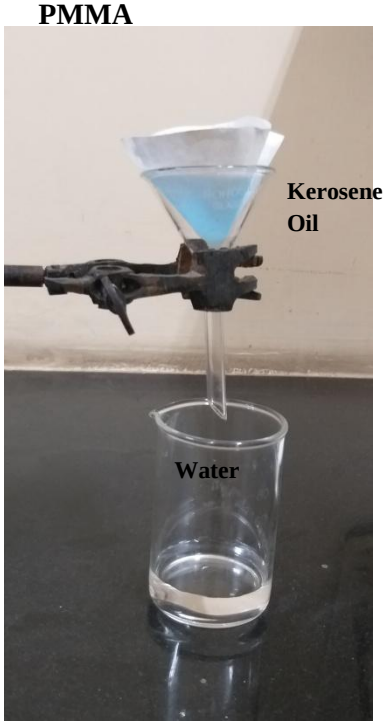

(c)TEOS/MTMS/PDMS/ PS

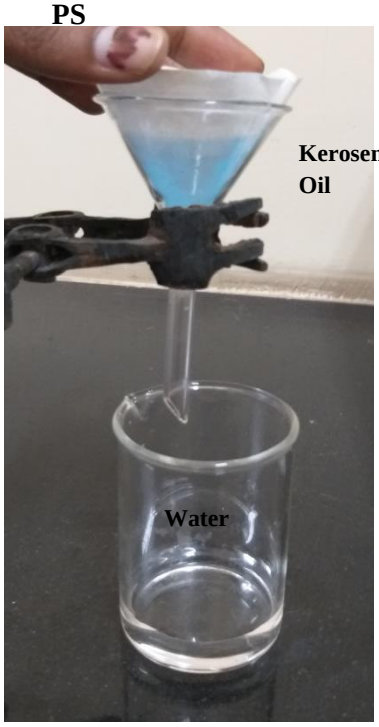

Step- III

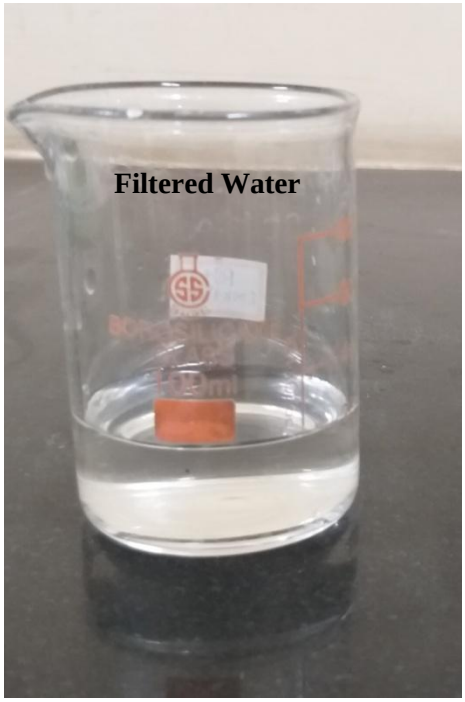

Fig. 4.128 Step I-III shows the oil-water separation

4.3.8 CONCLUSION

Polymer-silane composite films were developed by spin-coating and sol-gel technique. Surface energy calculated with Hamaker's constant was found to be lesser and supports the non-wettable character. The transmittance decreases in those films which possess higher surface roughness (Ra). The prepared films were tested for self cleaning performance. Set-III (Polymer-PDMS), and Set-VII (Polymer-TEOS/MTMS/PDMS) films exhibited superhydrophobic nature and oil-water separation phenomena was also observed.